Supplement to Volume 15 ■ Number 5 ■ September 2021

By Popular Demand
Retinal Cases & Brief Reports
Now 6 Times a Year

RETINAL CASES & BRIEF REPORTS®

Wolters Kluwer

Full Text OVID

Lippincott Williams & Wilkins

ISSN 1935-1089

Essential Titles in VISION CARE

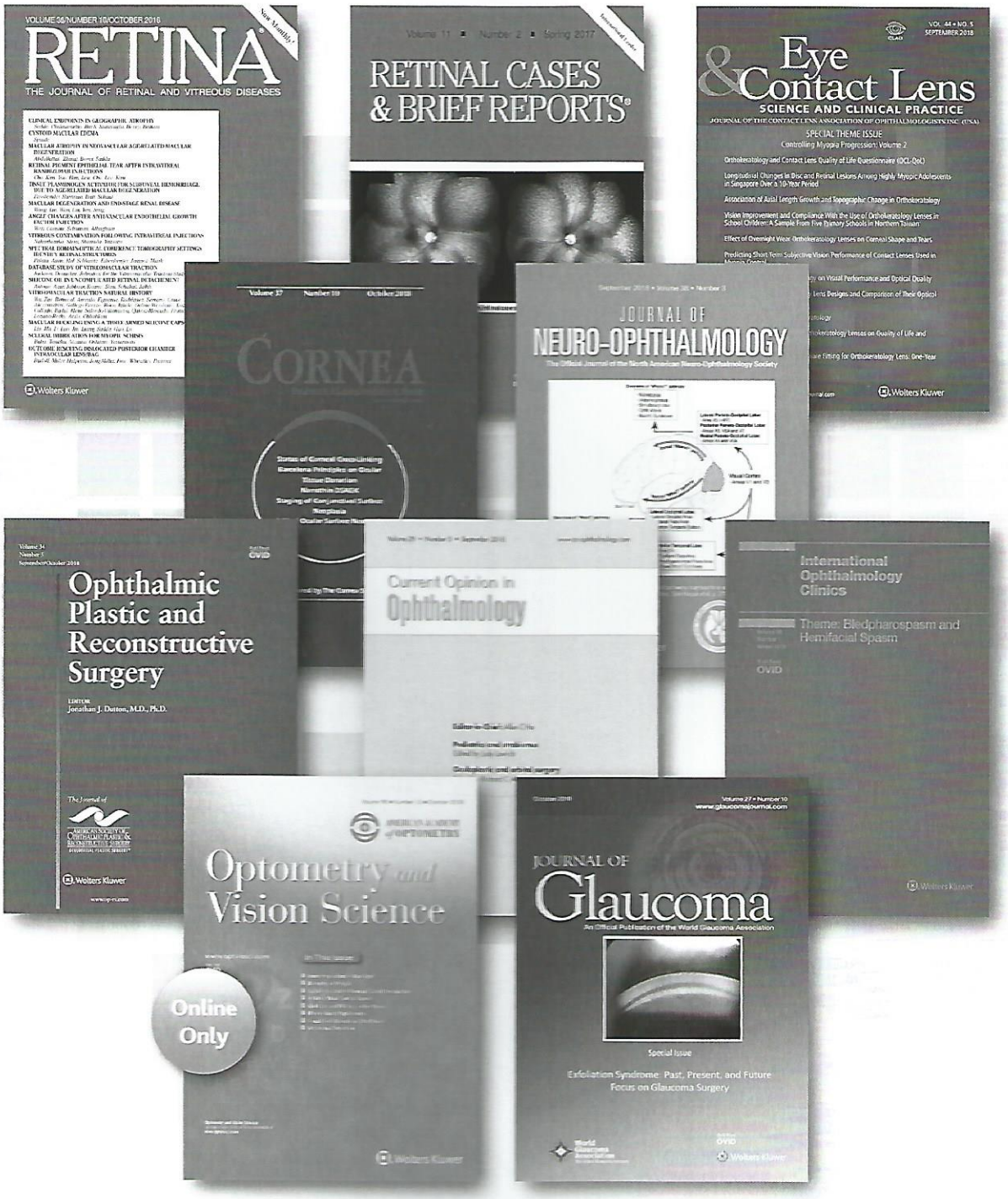

SUBSCRIBE online at shop.lww.com.

Wolters Kluwer

8-R152

RETINAL CASES & BRIEF REPORTS®

RETINAL CASES & BRIEF REPORTS® (ISSN 1935-1089) is published four times a year for the Ophthalmic Communications Society, Inc., by Wolters Kluwer Health, Inc. at 14700 Citicorp Dr. Bldg #3, Hagerstown, MD 21742. Business offices are located at Two Commerce Square, 2001 Market St., Philadelphia, PA 19103. Production offices are located at 351 W. Camden Street, Baltimore, MD 21201-2436. Mails Standard class at Hagerstown & other additional offices.

Address for subscription information, orders, or changes of address (except Japan): Wolters Kluwer Health, Inc. at 14700 Citicorp Drive, Bldg 3, Hagerstown, MD 21742; phone: 800-638-3030; fax: 301-223-2400; in Maryland, call collect, 301-223-2300. In Japan, contact Wolters Kluwer Health Japan Co., Ltd., Forecast Mita Building, 5th floor, 1-3-31 Mita Minato-ku, Tokyo, Japan 108-0073; Tel: 81 3 5427 1969. Annual subscription rates worldwide: $189.00 Individual Domestic, $193.00 Individual International, $584.00 Institutional Domestic, $609.00 Institutional International, $135.00 Residents Domestic, $135.00 Residents International. All prices include a handling charge. United States residents of AL, CO, DC, FL, GA, HI, IA, ID, IN, KS, KY, LA, MD, MO, ND, NM, NV, PR, RI, SC, SD, UT, VT, WA, WV add state sales tax. (The Canadian GST tax of 7% will be added to the subscription price of all orders shipped to Canada. Lippincott Williams & Wilkins' GST Identification Number is 895524239. Publications Mail Agreement #864927.) Subscriptions outside the United States must be prepaid. Subscriptions outside North America must add $17.00 for airfreight delivery. Single copies, when available, may be ordered from the publisher. Single copies $153.00. Prices subject to change without notice. Copies will be replaced without charge if the publisher receives a request within 90 days of the mailing date, both in the U.S. and worldwide. Visit us on-line at www.retinalcases.com.
Web site: www.retinalcases.com

Individual and in-training subscription rates include print and access to the online version. Institutional rates are for print only; online subscriptions are available via Ovid. Institutions can choose to purchase a print and online subscription together for a discounted rate. Institutions that wish to purchase a print subscription, please contact Wolters Kluwer Health, Inc. at 14700 Citicorp Drive, Bldg 3, Hagerstown, MD 21742; phone 800-638-3030 (outside the United States 301-223-2300); fax 301-223-2400. Institutions that wish to purchase an online subscription or online with print, please contact the Ovid Regional Sales Office near you or visit www.ovid.com/site/index.jsp and select Contact and Locations.

POSTMASTER: Send address changes to RETINAL CASES & BRIEF REPORTS®, P.O. Box 1610, Hagerstown, MD 21740. For advertising inquiries: Ryan Magee, Senior National Account Manager, Plastic Surgery & Ophthalmology, Wolters Kluwer Health, Two Commerce Square, 2001 Market Street, Philadelphia, PA 19103; telephone: 215-521-8804; email: Ryan.magee@wolterskluwer.com. Text printed on acid-free paper.

RETINAL CASES & BRIEF REPORTS®

SUPPLEMENT TO SEPTEMBER 2021 VOLUME 15, NUMBER 5

MYSTERY MACULA BRAZIL

Please visit the Journal's website at: www.retinalcases.com

Instructions for Authors can be found in the Author and Reviewer Information section of the website and manuscripts can be submitted online through Editorial Manager.

Get the research you need in the palm of your hand.

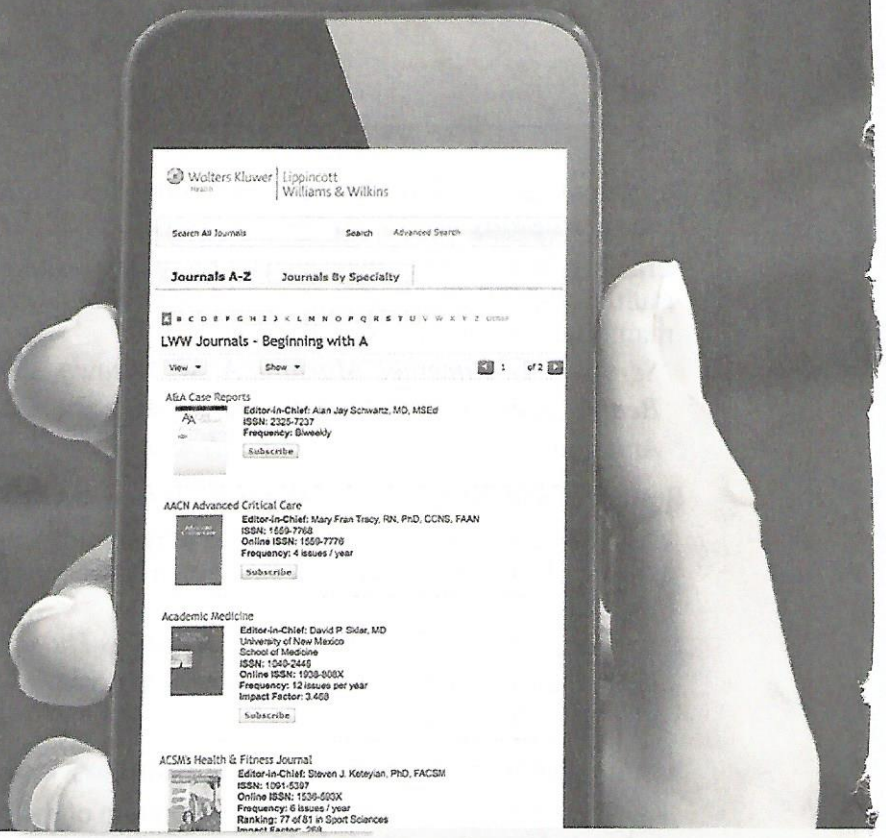

Mobile view from LWW

Stay in the know when you're on the go.

Mobile access is easy!
Then navigate your mobile Web browser to the journal website of your choice.

All the features you want are on mobile view:

- Search
- Current TOC
- Full-text view
- Image handling
- Abstracts
- Featured articles
- And more

Are you a society member?
If you access a journal through your society's portal as a member, please navigate your mobile browser to your society portal and login there for full-text access.

On the train ... between patients ... get the research and clinical information you need, when and where you need it.

With mobile view, you can read journal articles on most Internet-enabled mobile devices.

journals.lww.com

See what you might be missing.

Wolters Kluwer

5-Q357

UNDERSTANDING THE MYSTERY MACULA, A SUPPLEMENT OF *RETINAL CASES AND BRIEF REPORTS*

Mauricio Maia, MD, PhD,* Raul N. Vianna, MD, PhD,† Marcio B. Nehemy, MD, PhD,‡ Marcos P. Avila, MD, PhD,§ Michel E. Farah, MD, PhD*

*From the *Department of Ophthalmology, Federal University of São Paulo (EPM/UNIFESP); †Department of Ophthalmology, Federal Fluminense University (UFF); ‡Department of Ophthalmology, Federal University of Minas Gerais (UFMG); and §Department of Ophthalmology, Federal University of Goiás (UFG).*

The Brazilian Society of Retina and Vitreous (BRAVS), founded in 1977, was the birth child of several previous meetings of colleagues who increasingly became more interested in this very challenging subspecialty with scarce therapeutic resources during the 1970s. The courses on retinal detachment surgery and the first reports on fluorescein angiography motivated these colleagues to meet more often and envision the possibility of reducing the blindness rates. The BRAVS had a crucial role in the development of the retina subspecialty in Brazil, housing all specialists and postgraduate professors from all over the country with more than 1.200 members nowadays. Presently, BRAVS makes possible the exchange and dissemination of scientific retinal knowledge to the society's members and offers updates on the most important subjects, with the participation of national and international leaders in the field.

On July 29, 2020, BRAVS hosted a virtual meeting, Mystery Macula, organized by our colleagues Drs. Raul N. Vianna, Eduardo Cunha, Rodrigo Meirelles, and Luiz Lima who invited coordinators Drs. Márcio Nehemy, Marcos Ávila, and Michel Farah, and that included Drs. Anita Agarwal, David Sarraf, Jose Pulido, and Lawrence Yannuzzi, as international guest discussants. There were 10 very interesting and novel cases that were presented by Brazilian vitreoretinal specialists. These cases were discussed by our international guests. Because of the uniqueness of the presented cases in the Mystery Macula section, and the commentary added by our guest discussants, the organizing committee decided to submit these cases along with the commentary for possible publication as a supplement in *Retinal Cases and Brief Reports*. The idea was presented and promptly accepted by the Editor of the journal, Dr. Alexander Brucker.

All cases were subjected to the strict peer review procedures of the journal and are now presented as a supplement to the journal, *Retinal Cases and Brief Reports.*

We wish to acknowledge and thank the participation of the international discussants and Dr. Chandrakumar Balaratnasingam, who organized the manuscripts uniformly in the Mystery Macula section, and their help in the publication process of this supplement of *Retinal Cases and Brief Reports*.

We are also thankful to all organizers; coordinators; discussants; manuscript authors; the Editor of *Retinal Cases and Brief Reports*, Dr. Alexander Brucker; and our vitreoretinal fellows from the Federal University of Sao Paulo, Brazil, Dr. Dante Akira and Dr. Luciana Arrais (who helped in this publication). We would also like to extend a special thanks to the sponsors of BRAVS website and CME activities: Allergan Brazil, Bayer Brazil, Novartis Brazil, and Roche Brazil.

We believe that the Mystery Macula supplement will be of general interest to the *Retinal Cases and Brief Reports* readers. We also hope the articles in this supplement will stimulate further investigation of the medical retina diseases reported in this supplement.

None of the authors has any financial/conflicting interests to disclose.

BACILLARY DETACHMENT IN AN IDIOPATHIC CHORIORETINITIC DISORDER

Carolina R. Hilgert, MD,* Ricardo M. Japiassú, MD,† Álvaro H. Hilgert, MD,* Luiz H. Lima, MD,‡ Chandrakumar Balaratnasingam, MD,§¶ Lawrence A. Yannuzzi, MD, PhD,** Raul N. G. Vianna, MD, PhD††

*From the *Instituto da Visão de Mato Groso do Sul, Campo Grande, Brazil; †Hospital da Gamboa, Rio de Janeiro, Brazil; ‡Department of Ophthalmology, Federal University of São Paulo (UNIFESP), São Paulo, Brazil; §Center for Ophthalmology and Visual Science, University of Western Australia, Perth, Australia; ¶Department of Ophthalmology, Sir Charles Gairdner Hospital, Western Australia, Australia; **Vitreous-Retina-Macula Consultants of New York, New York, New York; and ††Department of Ophthalmology, Universidade Federal Fluminense, Niterói/RJ, Brazil.*

A 40-year-old otherwise healthy woman presented with a 10-day history of visual disturbance in the right eye and pain of 24-hour duration in the left eye. The medical and family histories were unremarkable. The best-corrected visual acuity in the right and left eyes was 20/400 and 20/50, respectively. Slit-lamp examination was unremarkable. Funduscopy showed creamy-white deep multifocal plaques bilaterally, predominantly in the right eye, and no vitreous cells. Fluorescein angiography showed initial hypofluorescent plaques with a hyperfluorescent aspect in the later phases. Spectral-domain optical coherence tomography (SD-OCT) showed increased choroidal thickness bilaterally, a subfoveal bacillary detachment in the right eye, with hyperreflectivity to the outer retinal layers (Figure 1).

Question: What is the most likely diagnosis?

Response: Serpiginous choroidopathy, multifocal choroiditis, Vogt–Koyanagi–Harada disease, syphilis, and acute posterior multifocal placoid pigment epitheliopathy (APMPPE).

None of the authors has any financial/conflicting interests to disclose.

Reprint requests: Ricardo M. Japiassú, MD, R. da Gamboa, 303, Santo Cristo, 20220-324 Rio de Janeiro, Brazil; e-mail: japimed@yahoo.com.br

Question: Does the presence of a bacillary detachment aid in differentiating this presentation?

Response: A bacillary detachment is believed to represent a split in the photoreceptor band at the level of the myoid. Conditions that manifest bacillary detachments include toxoplasmosis chorioretinitis, blunt eye trauma, bilateral diffuse uveal melanocytic proliferation, Vogt–Koyanagi–Harada disease, posterior scleritis due to antiphosopholipid syndrome, central serous chorioretinopathy in systemic lupus erythematosus, panuveitis secondary to anti-v-raf murine sarcoma viral oncogene homolog B1/anti-mitogen-activeted protein kinase kinase toxicity, choroidal osteoma complicated by choroidal neovascularization, and choroidal metastases.[1]

Question: Would you perform any further ancillary imaging or systemic tests? How would that assist your management of this case?

Response: Optical coherence tomography angiography would help further delineate if the disease process involves the choroidal and outer retinal layers. Blood tests for infectious and infective etiologies would also be appropriate.

Optical coherence tomography angiography multimodal imaging showed some plaques with a decreased signal in the outer retina and choriocapillaris; *en face* imaging showed lesions with hypersignaling in the outer retina and choriocapillaris (Figure 2). The laboratory screening results were negative for any known infectious or autoimmune etiology, including syphilis. After 1 week, during the investigation, the patient complained of acute and severe headaches.

Question: What is the most likely diagnosis and what would you do next?

Response: The ophthalmoscopic, dye angiography and OCT features of the case are consistent with a diagnosis of APMPPE. The onset of headache is concerning for cerebral vasculitis, and an urgent

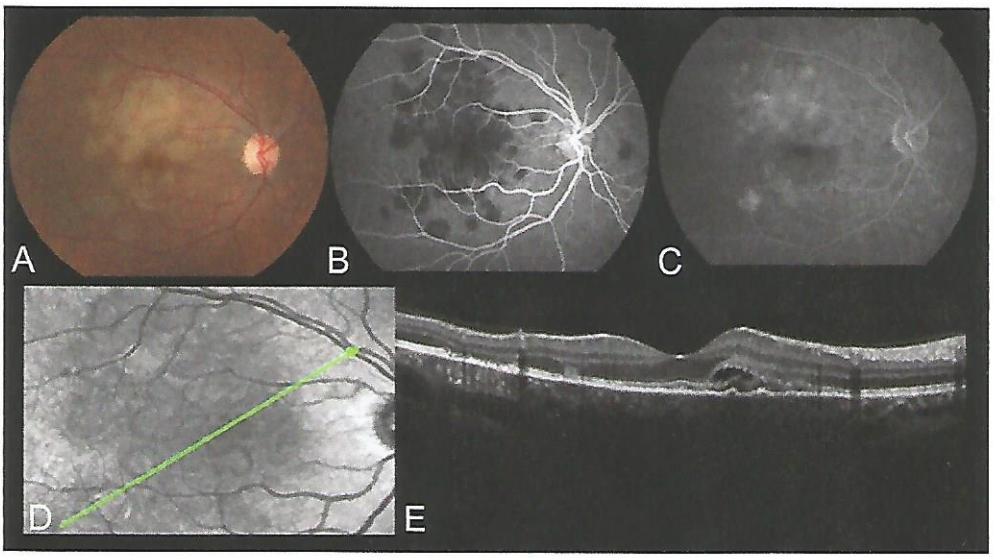

Fig. 1. A. Color fundus photograph shows creamy-white deep multifocal plaques in the right eye and no vitreous cells. **B** and **C.** Fluorescein angiography demonstrates initial hypofluorescent plaques with a hyperfluorescent spot in the later phases. **D** and **E.** Spectral-domain OCT and near-infrared images depict increased choroidal thickness and outer retinal layer hyperreflective findings compatible with APMPPE and a subfoveal bacillary detachment in the right eye.

MRI of the brain is warranted. MRI of the brain was normal with no evidence of inflammation.

Question: Is there a role for immunosuppression in this case?

Response: Yes, given the severe reduction in visual acuity and the involvement of the macula in this case requires immunosuppression.

The patient started IV methylprednisolone 1 mg/kg for 3 days and oral prednisone 60 mg 4 times daily for 2 weeks, with improvement of the best-corrected visual acuity to 20/30 and 20/20 in the right and left eyes, respectively, and complete resolution of placoid lesions as seen on multimodal imaging. Immunosuppression also resulted in the resolution of headaches. At the 1-month follow-up, OCT showed resolution of the bacillary detachments (BDs) and thinning of the outer retina, particularly the outer nuclear layer (mainly in the right eye), and no signs of inflammatory activity on fluorescein angiography (Figure 3). Optical coherence tomography angiography showed a decreased signal from the lesions at the outer retina and choriocapillaris, mainly on the infrared images (Figure 4).

Discussion

Although the exact pathogenesis of APMPPE is debatable, it is currently believed to be secondary to choroidal perfusion vasculitis, resulting in hypoperfusion of the terminal choroidal lobules in the posterior pole with secondary impairment of the RPE and retinal outer layer.[2] Based on a patient with severe APMPPE who presented with granulomas just beneath the RPE, de Vries et al postulated that APMPPE might be caused by choroidal granulomas and be a part of a generalized granulomatous disease.[3]

The clinical spectrum and evolution of BDs are poorly defined. Cicinelli et al[4] hypothesized that the hyperacute circumstances of BDs may force the fluid to penetrate the neuroretina, causing a splitting within the photoreceptors layer related to the shear stress caused by vigorous and sudden exudation. Some authors have reported that cone photoreceptor deterioration reinforces the pathogenic process, specific for BD cases.[5,6] More recently, intraretinal fibrin has been postulated to account for the separation of retinal layers seen in bacillary detachments although it is possible that this separation is a variant of schisis with mechanical separation.[5,6] Histopathological studies of eyes with bacillary detachment will be required to reconcile the exact pathogenesis.

This is the first case to provide a multimodal imaging correlation between OCT angiography and en face OCT in a case of bacillary detachment due to APMPPE. We show that bacillary detachment is a sign of active disease and resolves on treatment; hence, expanding our understanding of the pathophysiologic mechanisms underlying this disease.

Comment

it has been one of my convictions that detachment of the whole-layer inner segment myoids without the effect of the other inner layers of the retina was simply a histopathological artifact. Now, there is a race to associate numerous acute and chronic diseases of the macula with such a separation. In this case, it was acute posterior multifocal pigment epitheliopathy

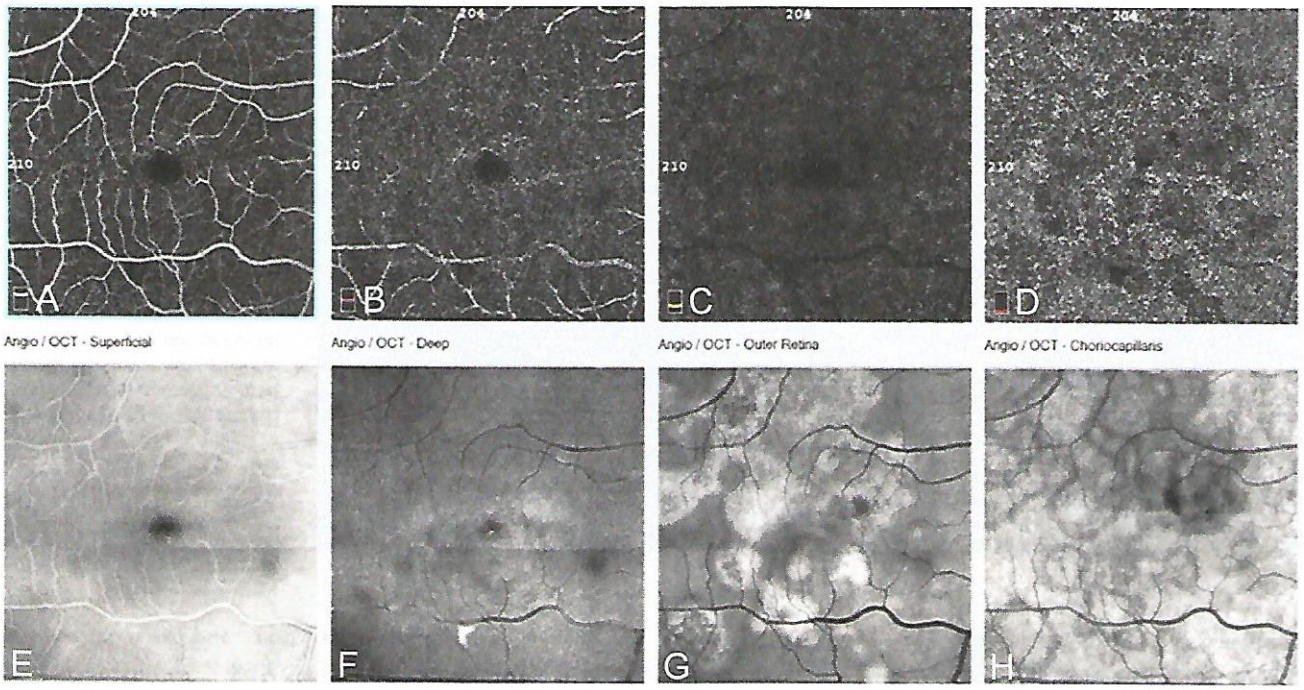

Fig. 2. A–D. Optical coherence tomography angiography shows a decreased signal in the outer retina and choriocapillaris. **E–H.** *En face* imaging demonstrates hyperreflective lesions in the outer retina and choriocapillaris.

or APMPPE. This is not the first report linking macular detachment with APMPPE. Gass originally reported such a detachment in APMPPE, but in a personal communication with me, he later agreed that his unifocal, unilateral case was actually unilateral acute idiopathic maculopathy or UAIM, which had not yet been described or published. Gass was also helpful to me by eventually describing bilateral involvement in AIM, necessitating a name change from UAIM to AIM or acute idiopathic maculopathy. Such a gradual learning process in the macula is not unusual when there is a lacking in clinical histopathological correlations. Progressive knowledge from accumulative case studies can and does unveil a better understanding of newly recognized clinical manifestations. This experience is needed for BD which is now associated with an increasing number of maculopathies, principally inflammatory and infectious diseases but also oncologically, degenerative, and even immune-mediated disorders. Hence, melanocytes, inflammations, and infectious diseases are the most common disorders that predispose to this

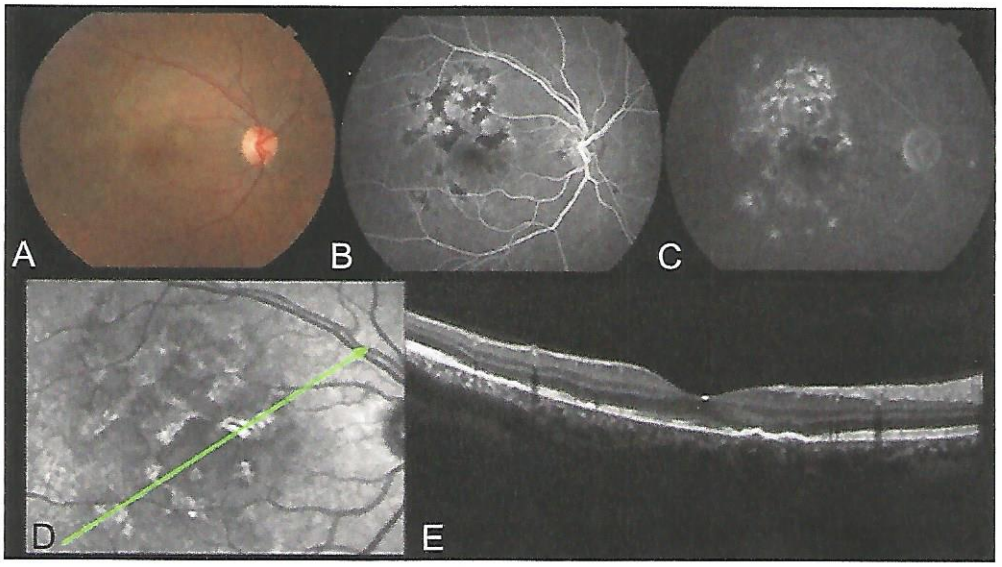

Fig. 3. A. After 1 month of treatment, fundus color photography of the right eye shows grayish cicatricial lesions in the retina. **B** and **C.** No signs of inflammatory activity are seen on the fluorescein angiogram. **D** and **E.** En face reflectance imaging and OCT show resolution of the bacillary layer detachment and thinning of the outer retina, particularly in the outer nuclear layer.

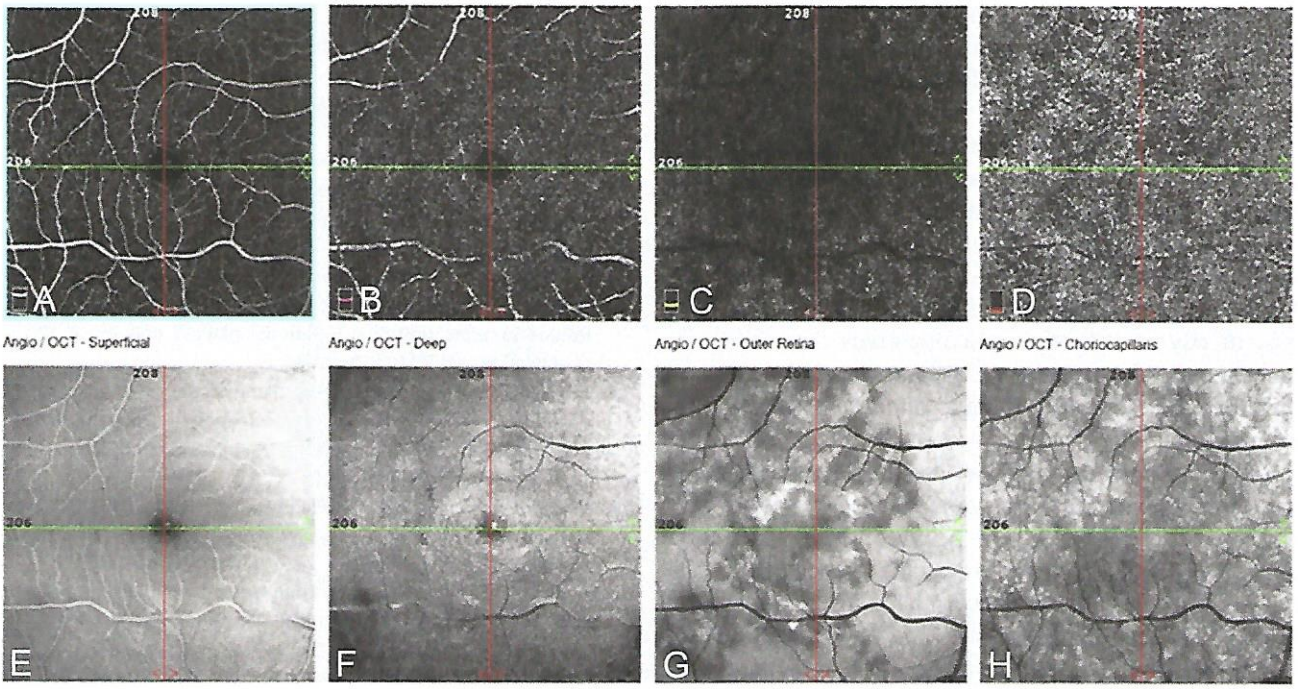

Fig. 4. A–D. After 1 month of treatment, OCT angiography of the right eye shows a decrease in flow signal at the site of the lesions in the outer retina and choriocapillaris. **E–H.** *En face* OCT angiography images also highlight these lesions.

unusual but well-documented disturbance in the macula.

The parade of authors who have recognized and described this complex manifestation is impressive. Their conclusions have emphasized the marked variability of this complex exudative manifestation of the disorder of the retina, beginning with a cleavage of the outer retina, most probably at the myoid of the photoreceptor layer, the retinal pigment epithelium. This layer is likely the remains of the outer retina combined with proteinaceous debris, fibrin, inflammatory cells, and degenerating/regenerating photoreceptors. Within these barriers, there may be serous fluid and zones of homogeneous OCT reflectance from a mixture of these cellular and amorphous components. In some cases, in the absence of histopathological correlations, it is not surprising that unanimity does not exist in this conclusion. Focal defects in the ellipsoid, and even in the otherwise continuous external limiting membrane, have been described based on high-definition OCT imaging. A thin to thick reflective surface is plastered against the retinal pigment epithelium. Within these barriers, there may be serous fluid, cellular debris, proteinaceous exudate, and zones of homogeneous OCT reflectance or any combination of these mixed changes. In some eyes, I would add that the ellipsoid appears to extend from the edges throughout the dome of the lesion without interruption. In other cases, the ellipsoid is difficult to detect and trace. The lesion itself is bordered by unremarkable changes. The same is true for the dome of the elevation. More commonly, however, it is the presence of identifiable changes, including micro and macro cysts, sensory retinal detachments, and prominent schisis cavities. There is no blood or lipid exudation to my knowledge.

There is a remarkable metamorphosis after the administration of low-dose steroids that apparently melts the lesion down without residual anatomical and functional damage. To date, there is no specificity linking a bacillary detachment with a particular maculopathy. There are other features to a bacillary detachment that have not received much attention to date in the ophthalmic literature. The first is that it is not a true detachment. It is a cystic space within the retina, a large schisis cavity with an inner and outer retinal anatomical barrier. It is more like a macular cyst than a macular detachment. Furthermore, with fluorescein angiography, there is no permeability or leakage, such as cystic degeneration or a macular cyst or in this case a retinal schisis. In addition, these lesions are usually associated with fibrin deposition from the inflammatory or infectious process. The fibrin molecule is sticky in nature. This characteristic accounts for the multiple cystoid elevations seen in chronic central serous chorioretinopathy or Vogt–Koyanagi–Harada disease when there is fibrin in the exudative environment. The presence of fibrin in conjunction with the inflammatory process may be

enough to explain, at least in part, the bacillary lesion in APMPPE and other similar maculopathies where there is a bacillary cystoid abnormality. Another feature to this peculiar lesion is the remarkable metamorphosis which occurs after the use of steroids that apparently melts the bacillary lesion down without residual anatomical or functional damage. About APMPPE and the presence of a "bacillary detachment or schisis," there is no specificity, to my knowledge. Nor is there any particular bacillary lesion characteristic of any of the other maculopathies described as associations. Its presence in an otherwise typical APMPPE case does not seem to alter the prognosis or eventual outcome.

The prompt and complete resolution coincidental with the use of steroids warrants consideration by physicians managing these patients in the clinical setting. To date, there is no specific characteristic of the bacillary lesion which correlated to a particular maculopathy. Its presence seems to be incidental but suggestive of the use of a pulse of steroid therapy. Hopefully, the bacillary lesion in the presence of inflammation and possibly fibrin will serve as a marker for related disease of the macula and their management.

Key words: bacillary detachment, chorioretinitis, placoid disease, multimodal imaging.

References

1. Breazzano M, Bacci T, Wang H, et al. Bacillary layer detachment in bilateral diffuse uveal melanocytic proliferation masquerading as neovascular AMD. Ophthalmic Surg Lasers Imaging Retina 2020;51:413–417.
2. Burke TR, Chu CJ, Salvatore S, et al. Application of OCT-angiography to characterise the evolution of chorioretinal lesions in acute posterior multifocal placoid pigment epitheliopathy. Eye 2017;31:1399–1408.
3. De Vries JJ, Den Dunnen WF, Timmerman EA, et al. Acute posterior multifocal placoid pigment epitheliopathy with cerebral vasculitis: a multisystem g ranulomatous disease. Arch Ophthalmol 2006;124:910–913.
4. Cicinelli MV, Giuffré C, Marchese A, et al. The bacillary detachment in posterior segment ocular diseases. Ophthalmol Retina 2020;4:454–456.
5. Mehta N, Chong J, Tsui E, et al. Presumed foveal bacillary layer detachment in a patient with toxoplasmosis chorioretinitisans-pachychoroid disease. Retin Cases Brief Rep 2018;15:391–398.
6. Goldenberg D, Habot-Wilner Z, Loewenstein A, Goldstein M. Spectral domain optical coherence tomography classification of acute posterior multifocal placoid pigment epitheliopathy. Retina 2012;32:1403–1410.

ASYMPTOMATIC RETINAL NERVE FIBER LAYER THICKENING IN A PATIENT WITH ATAXIA

Juliana M. F. Sallum, MD,* Flavio M. R. Filho, MD,† José L. Pedroso, MD,† Mauro Goldbaum, MD,‡ Orlando G. P. Barsottini, MD,† Luiz H. Lima, MD,‡ Chandrakumar Balaratnasingam, MD,§¶ Jose S. Pulido, MD, MS, MPH, MBA,** Eduardo Cunha de Souza, MD*

*From the *Department of Ophthalmology, Federal University of São Paulo, São Paulo, Brazil; Departments of †, and ‡Ophthalmology, University of São Paulo, São Paulo, Brazil; §Center for Ophthalmology and Visual Science, University of Western Australia, Perth, Australia; ¶Department of Ophthalmology, Sir Charles Gairdner Hospital, Western Australia, Australia; and **Wills Eye Hospital, Thomas Jefferson University, Philadelphia, Pennsylvania.*

An 18-year-old man experiencing increasing ataxia since early childhood underwent ophthalmic assessment as part of his neurologic evaluation. Despite having normal visual acuity and being visually asymptomatic, he was noted to have prominent nerve fiber layers bilaterally (Figure 1). A retinal crest was also seen in the papillomacular bundle in the right eye (Figure 2).

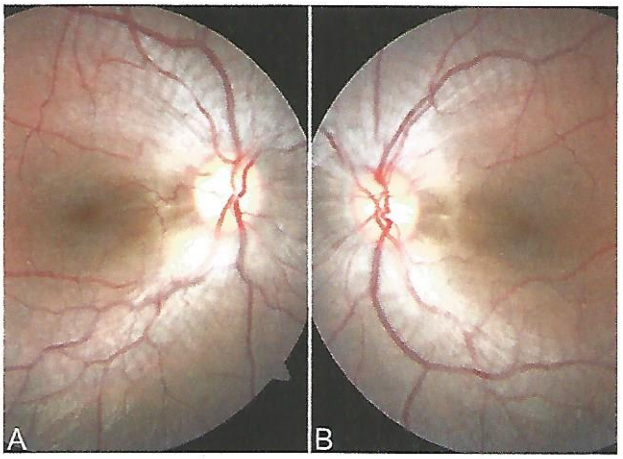

Fig. 1. Fundus photograph of both eyes demonstrating symmetrical increased visibility of retinal nerve fiber layer.

Question

What conditions are associated with prominent or thickened nerve fiber layers?

Response

Acute papillitis due to optic neuritis is an important cause of nerve fiber layer thickening. Other causes of acute papillitis such as sarcoidosis, toxoplasmosis, bartonella, tuberculosis, and ischemic optic neuropathy can also lead to nerve fiber layer thickening. Systemic or intracranial hypertension resulting in papilledema can also result in thickening. Inherited conditions that have been associated with nerve fiber layer thickening include

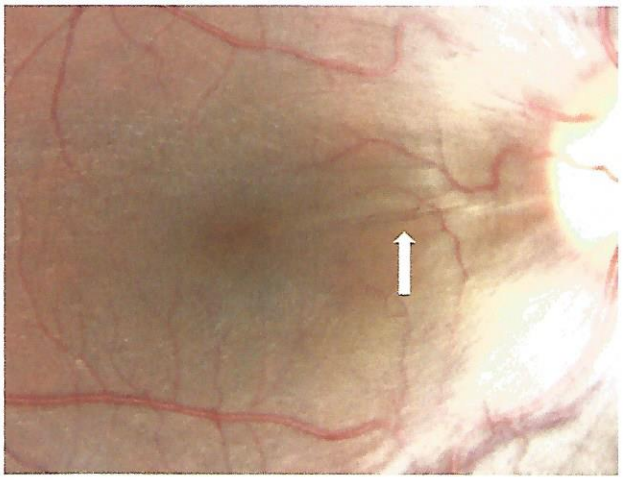

Fig. 2. Fundus photograph in higher magnification depicting a retinal crest (arrow) between fovea and optic disk in the papillomacular area of the right eye.

None of the authors has any financial/conflicting interests to disclose.

Reprint requests: Mauro Goldbaum, MD, University of São Paulo (USP), Av. Dr. Enéas Carvalho de Aguiar, 255, 6o andar, Sala 6119, São Paulo, SP 05403-900, Brazil; e-mail: mgoldbaum@hotmail.com

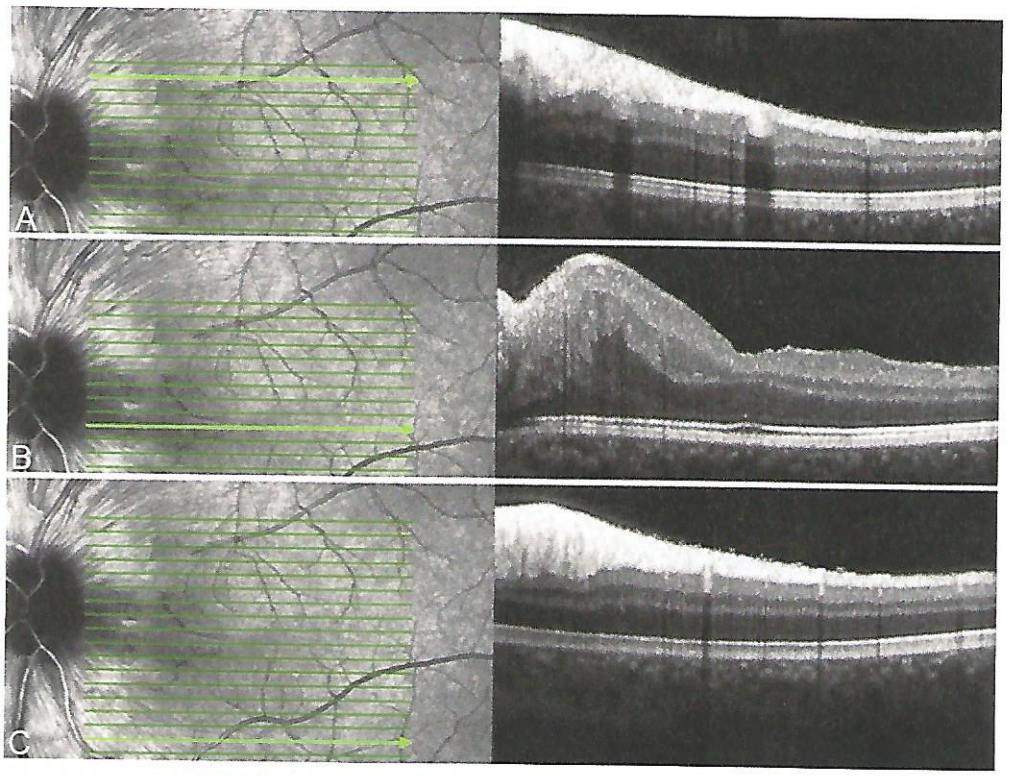

Fig. 3. Optical coherence tomography scans of left eye showing inner retinal thickening on the posterior pole that progresses toward the horizontal center of the papillomacular bundle forming the retinal crest (middle row).

retinitis pigmentosa, Leber hereditary optic neuropathy, and autosomal recessive spastic ataxia of Charlevoix–Saguenay (ARSACS). Important to note that most neurodegenerative conditions that manifest ataxia such as Friedreich ataxia, spinocerebellar ataxia, and cerebellar ataxia of unknown cause typically have normal or thin NFLs.

Both visual fields and color vision testing were in the normal range as was blood pressure. Peripheral retinal assessment was normal. OCT findings were

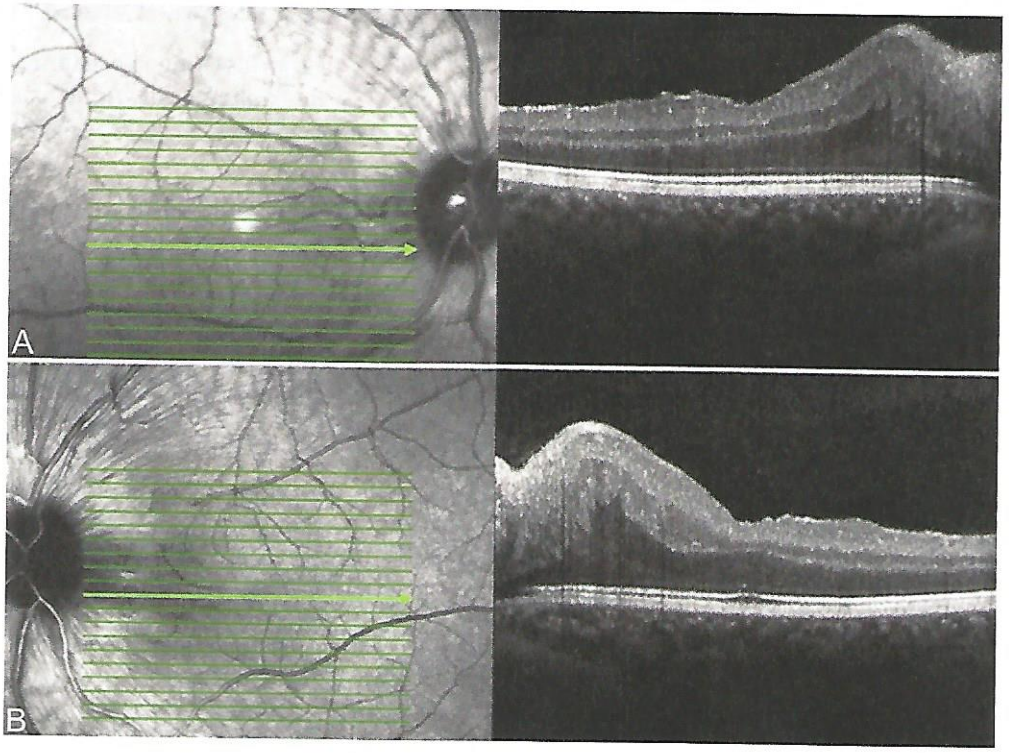

Fig. 4. Central OCT scan of both eyes presenting the dentate appearance demonstrating inner plexiform, inner nuclear, and outer plexiform layers.

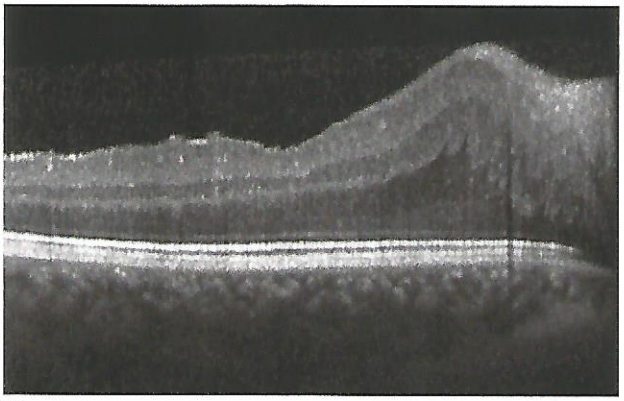

Fig. 5. Central OCT scan of the right eye in higher magnification showing the dentate appearance in details and the associated foveal pit hypoplasia.

symmetrical and included significant thickening of the inner retina. Inner retinal thickening progressed toward the horizontal raphe in the papillomacular bundle area forming the crest seen clinically in the fundus (Figure 3). Around this thicker area, the OCT demonstrated a peculiar dentate appearance of the inner plexiform, inner nuclear, and outer plexiform layers (Figure 4).

Question

What conditions can produce dentate changes to the retina as seen on OCT?

Response

Dentate appearance of the outer plexiform layer has been reported in carriers of X-linked retinitis pigmentosa and combined hamartoma of the retina and retinal pigment epithelium. Patients with ARSACS frequently demonstrate dentate changes to the inner retinal layers.

Question

What are the macular changes that can occur in patients with ARSACS?

Response

Microcysts and fovea plana as seen in Figure 5.

The patient was the child of consanguineous parents. Brain magnetic resonance imaging showed upper cerebellar vermis atrophy, linear pontine hypointensities in T2-weighted sequence, and thinning of the corpus callosum. Next generation sequencing of SACS gene was undertaken and identified homozygous pathogenic mutations confirming the diagnosis of ARSACS.

Discussion

The original description of the fundus abnormality in ARSACS mentioned retinal striations similar to the acute phase of Leber hereditary optic neuropathy.[1] Postmortem studies of the retinal changes observed in ARSACS are lacking, but early articles suggested that the increased visibility of RNFL could be secondary to persistence of myelinated fibers. Optical coherence tomography findings in ARSACS do not support this hypothesis because the expected blocking effect from opaque myelinated fibers on the outer retina does not occur.[2] Parkinson et al showed RNFL thickening was present in patients with ARSACS even when the fundus appeared normal on clinical examination. Their study have also demonstrated the diagnostic role of average RNFL thickness in OCT as a biomarker highly accurate in differentiating ARSACS from other types of hereditary ataxias, which do not exhibit significant retinal thickening.[3] Leavitt et al[4] also saw similar findings.

The dentate appearance affecting inner plexiform, inner nuclear, and outer plexiform layers is very unique and rarely seen in other diseases.[5] A similar sawtooth pattern in the outer plexiform layer has been described in cases of combined hamartoma of the retina and retinal pigment epithelium.[6] The images on the combined hamartoma of the retina and retinal pigment epithelium article suggest involvement of all the inner retinal layers, and the authors named it the omega sign after its resemblance to the Greek letter. The clinical appearance of combined hamartoma of the retina and retinal pigment epithelium with pigmentary changes as well as the bilateral and symmetrical OCT findings in ARSACS would help differentiate the two conditions. Henle fiber layer hemorrhage could also present a sawtooth pattern, but it is typically located below the outer plexiform layer in the outer retina.[7]

Autosomal recessive spastic ataxia of Charlevoix–Saguenay may be associated with *fovea plana*.[8] This case presents mild *fovea plana* corresponding to grade 1 in the grading scale proposed by Thomas et al[9] with absence of plexiform layers extrusion. Macular microcysts have also been described in ARSACS, but their pathological significance is yet to be determined.[5]

This case report illustrates the wide spectrum of OCT retinal findings in ARSACS. Retinal thickening is not restricted to RNFL and affects other layers of the inner retina as previously described.[10] The thickening is greater at the center of the papillomacular bundle usually in a linear shape with the aspect of a papillomacular fold or crest.[5] The dentate appearance affecting inner plexiform, inner nuclear, and outer plexiform layers is very unique and rarely seen in other diseases.[5]

Key words: autosomal recessive spastic ataxia of Charlevoix–Saguenay, optical coherence tomography, retinal nerve fiber layer, retinal thickening.

References

1. Bouchard JP, Barbeau A, Bouchard R, Bouchard RW. Electromyography and nerve conduction studies in Friedreich's ataxia and autosomal recessive spastic ataxia of Charlevoix-Saguenay (ARSACS). Can J Neurol Sci 1979;6:185–189.
2. Vingolo EM, Di Fabio R, Salvatore S, et al. Myelinated retinal fibers in autosomal recessive spastic ataxia of Charlevoix-Saguenay. Eur J Neurol 2011;18:1187–1190.
3. Parkinson MH, Bartmann AP, Clayton LMS, et al. Optical coherence tomography in autosomal recessive spastic ataxia of Charlevoix-Saguenay. Brain 2018;141:989–999.
4. Leavitt JA, Singer W, Brown WL, et al. Retinal and pontine striations: neurodiagnostic signs of autosomal recessive spastic ataxia of Charlevoix-Saguenay. J Neuroophthalmol 2014;34:369–371.
5. Rezende Filho FM, Parkinson MH, Pedroso JL, et al. Clinical, ophthalmological, imaging and genetic features in Brazilian patients with ARSACS. Parkinsonism Relat Disord 2019;62:148–155.
6. Chawla R, Kumar V, Tripathy K, et al. Combined hamartoma of the retina and retinal pigment epithelium: an optical coherence tomography-based reappraisal. Am J Ophthalmol 2017;181:88–96.
7. Baumal CR, Sarraf D, Bryant T, et al. Br J Ophthalmol 2020.
8. Borruat FX, Holder GE, Bremner F. Inner retinal dysfunction in the autosomal recessive spastic ataxia of Charlevoix-Saguenay. Front Neurol 2017;8:523.
9. Thomas MG, Kumar A, Mohammada S, et al. Structural grading of foveal hypoplasia using spectral-domain optical coherence tomography a predictor of visual acuity? Ophthalmology 2011;118:1653–1660.
10. Garcia-Martin E, Pablo LE, Gazulla J, et al. Retinal segmentation as noninvasive technique to demonstrate hyperplasia.in ataxia of Charlevoix-Saguenay. Invest Ophthalmol Vis Sci 2013;54:7137–7142.

MACULAR EDEMA IN A PECULIAR CASE OF PIGMENTARY MACULOPATHY

Sergio L. G. Pimentel, MD, PhD,* Lívia S. Conci, MD,* Luiz H. Lima, MD,†
Chandrakumar Balaratnasingam, MD,‡§ Lawrence A. Yannuzzi, MD,¶
Carol L. Shields, MD**

*From the *Department of Ophthalmology, University of São Paulo (USP), São Paulo, Brazil; †Department of Ophthalmology, Federal University of São Paulo (UNIFESP), São Paulo, Brazil; ‡Center for Ophthalmology and Visual Science, University of Western Australia, Perth, Australia; §Department of Ophthalmology, Sir Charles Gairdner Hospital, Western Australia, Australia; ¶Vitreous-Retina-Macula Consultants of New York, New York, New York; and **Wills Eye Hospital, Thomas Jefferson University, Philadelphia, Pennsylvania.*

A 16-year-old African male patient presented with a 4-year history of blurred vision in the right eye. His medical history was positive for jaundice at birth that was treated with phototherapy, congenital heart disease (due to the persistence of the *ductus arteriosus* and interatrial communication but without hemodynamic repercussion), supravalvular aortic stenosis, asthma, and allergic rhinitis. His current medication included a selective beta-blocker B1, atenolol, 50 mg/day. The family ocular history was unremarkable.

On ocular examination, his best-corrected visual acuity was 20/32 in the right eye (manifest refraction: $-1.00\ -2.50 \times 10°$) and 20/20 in the left eye (manifest refraction: $-2.25\ -1.00 \times 100°$). The anterior segment was unremarkable, without vitreous cells in either eye. The pupillary reflexes were normal; the intraocular pressure was 18 mmHg bilaterally. Fundus examination showed multiple, jet black, small nodular, and well-demarcated superficial retinal lesions in both eyes adjacent to the foveola (Figure 1). In the right eye, the five lesions were round and the largest basal diameters measured 60 μm (n = 2), 150 μm (n = 2), and 500 μm (n = 1). In the left eye, two lesions were round (170 and 190 μm) and one was linear (375 μm). The lesions were in the perifoveolar region, almost in a circular fashion, without crossing the foveola. They were clearly depicted in detail on fundus autofluorescence (FAF), presenting with a pronounced and homogeneous hypoautofluorescence and associated with a relative increased autofluorescence at the fovea (Figure 1). Ultrawide field showed a normal retina in the equator and periphery of both eyes, without similar peripheral lesions (Figure 2). The retina equator and periphery had normal autofluorescence (Figure 2).

Question

What is the differential diagnosis for this presentation?

Response

The pigmentary nature of the lesions suggests a degree of chronicity. In young patients, handheld laser pointer maculopathy must always be considered in the differential diagnosis. Retinal dystrophies such as Stargardt disease may also present similarly. An optical coherence tomography (OCT) assessment of the macula will be critical for further assessment of the macular phenotype and reconciling the diagnosis.

On OCT, the right eye demonstrated macular edema with cystoid changes of the outer plexiform layer and inner nuclear layer (Figure 3). The left eye had small cystoid changes at the outer plexiform layer (Figure 4). The outer retina bands and choroid appeared normal in both eyes. The central macular thicknesses were 346 and 237 μm in the right and left eyes, respectively. The subfoveal choroidal thicknesses were 360 and 355 μm in the right and left eyes, respectively.

Question

Do the cavitary abnormalities of macula assist in refining the diagnosis?

None of the authors has any financial/conflicting interests to disclose.

Reprint requests: Sergio L. G. Pimentel, MD, PhD, University of São Paulo (USP), Avenue Dr. Enéas Carvalho de Aguiar, 255, 6o Andar, Sala 6119, São Paulo, SP, 05403-900, Brazil; e-mail: sergiopimentel9@gmail.com

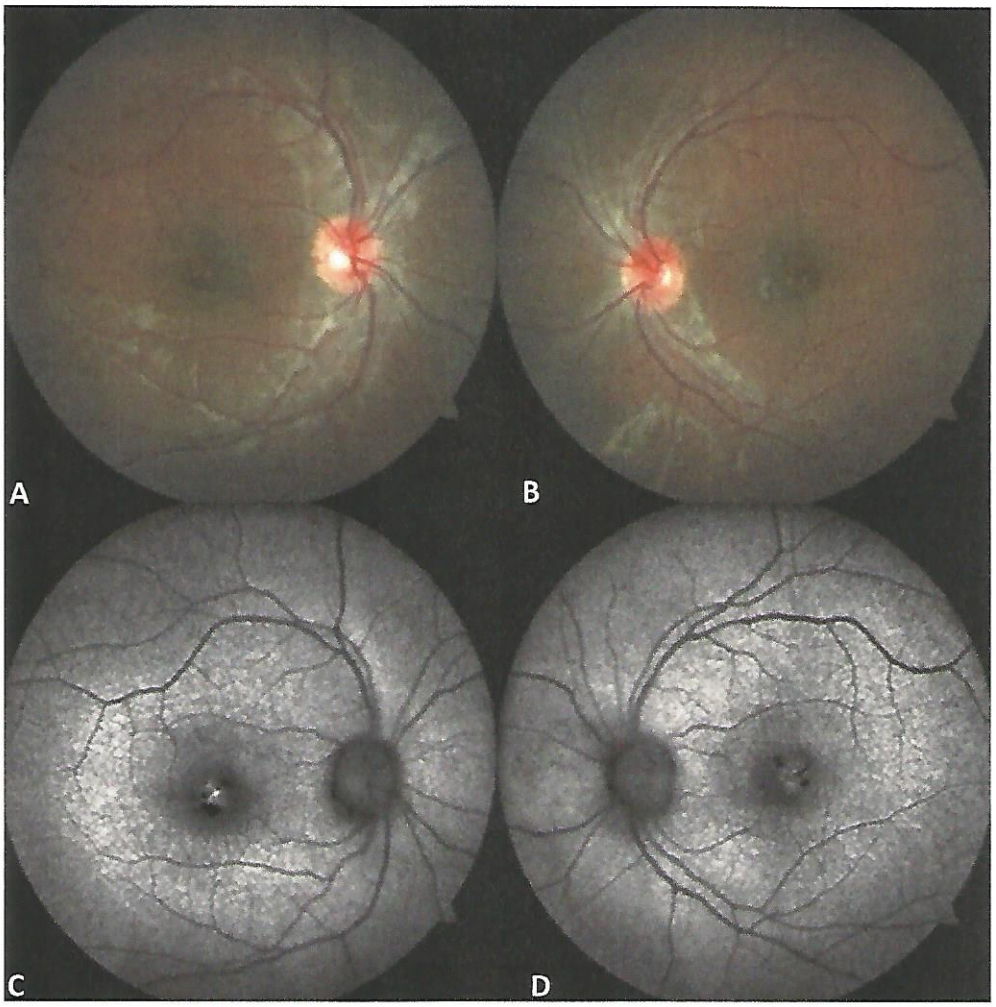

Fig. 1. A. Color fundus photograph of the right eye shows five black, small, round, and well-demarcated foveal lesions around the fovea measuring between 60 and 500 μm. **B.** Color fundus photograph of the left eye shows two round lesions (170 and 190 μm) and one linear lesion (375 μm) in a circular pattern in the perifoveolar region without crossing the foveola. **C** and **D.** Fundus autofluorescence of the right and left eyes, respectively, shows the lesions have intense and homogeneous hypoautofluorescence, with a relatively increased autofluorescence at the fovea.

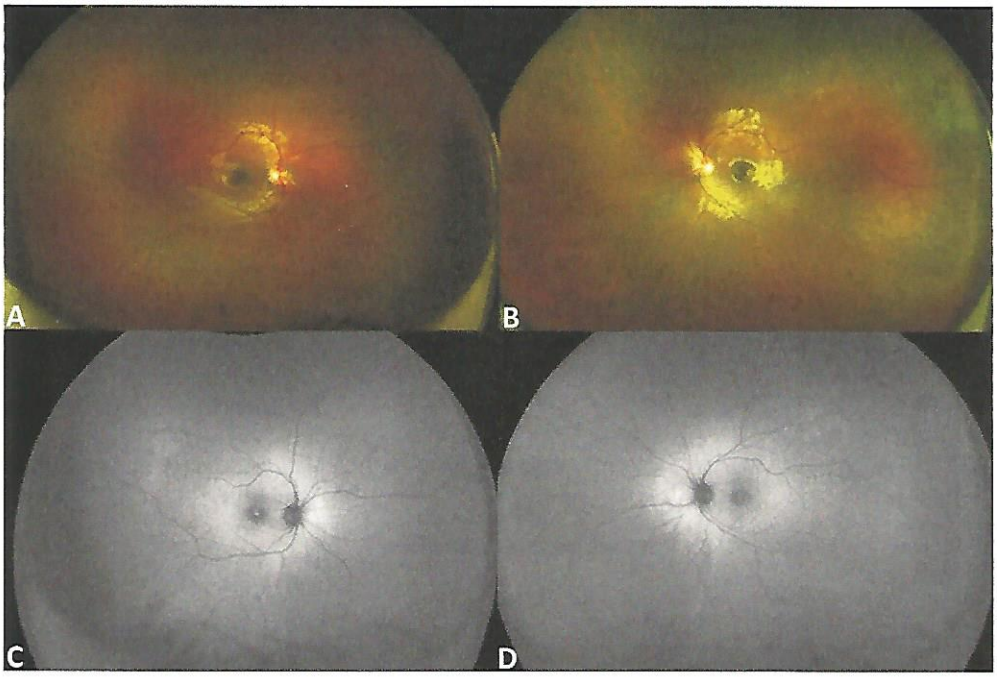

Fig. 2. A and **B.** Ultrawide field imaging shows that the lesions are confined to the fovea, with a normal equator and periphery in the right (**A**) and left (**B**) eyes. **C** and **D.** Ultrawide field FAF shows the equator and periphery have relatively normal autofluorescence patterns with no evidence of further lesions in the right (**C**) and left (**D**) eyes.

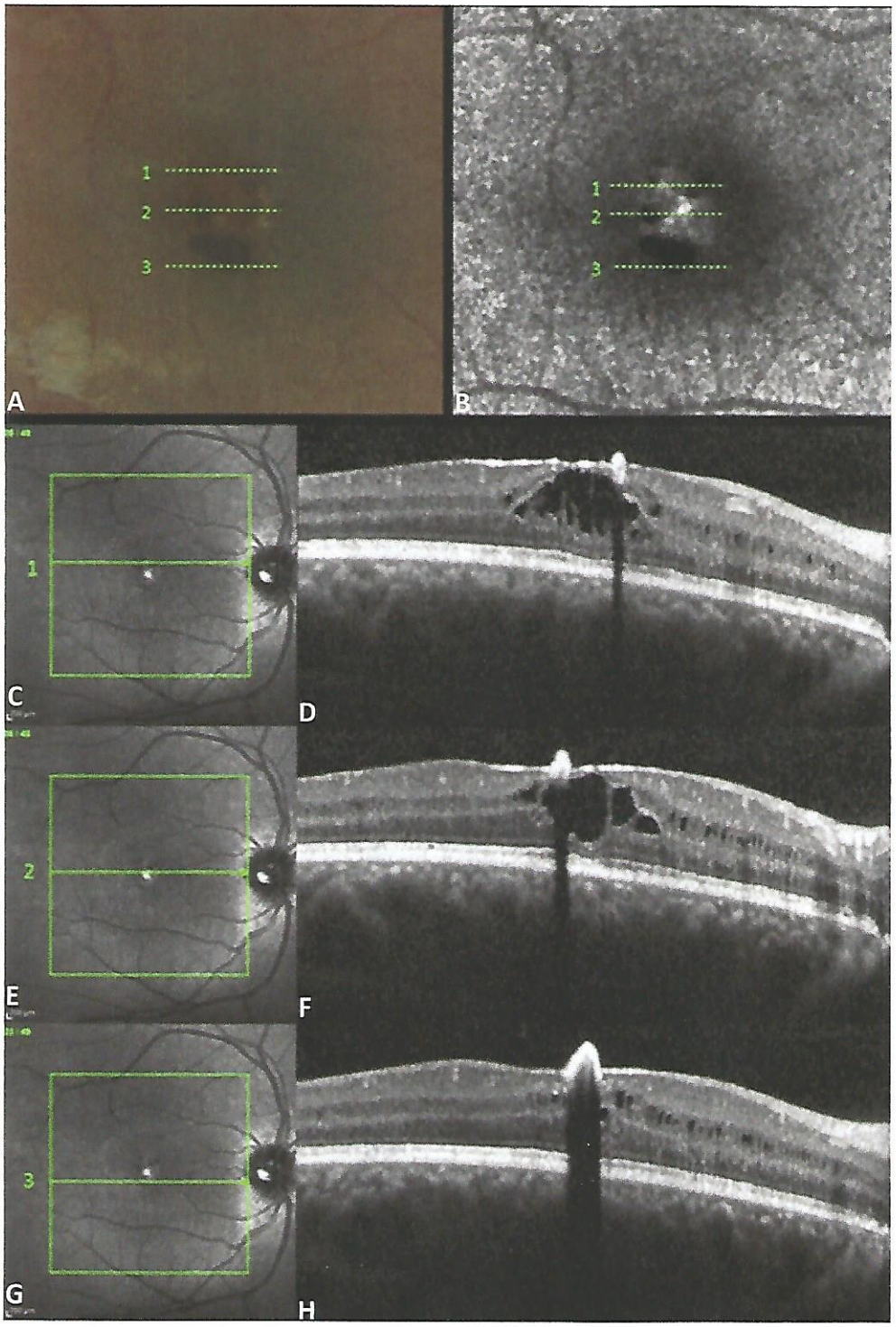

Fig. 3. Multimodal imaging of the right eye. **A.** Color fundus photograph. **B.** Fundus autofluorescence. **C–E.** Spectral-domain optical coherence tomography findings using three consecutive macular scans over different lesions corresponding to the dashed lines 1, 2, and 3 are shown in green in the Figures (**A** and **B**). **C–H.** Regardless of their size, small (dashed line 1), medium (dashed line 2), or relative large lesions (dashed line 3) show a similar pattern characterized by high reflectivity at the inner retina associated with intense underlying optical shadowing with distinct borders. The lesions have irregular surfaces and extend somewhat toward the attached vitreous. The larger the lesion, the larger the protrusion. Macular cystoid edema at the outer plexiform layer and inner nuclear layer was evident in all scans. The outer retina and choroid are normal. The central macular thickness is 346 μm.

Response

Very common causes of bilateral cystoid macular edema include diabetes mellitus and hypertension. Although this patient had a history of systemic hypertension, the blood pressure was well controlled with medications. Cavitary abnormalities of the macula are frequently seen in macula telangiectasia Type 2; however, this is unlikely to be the diagnosis because patients presenting with MacTel2 are typically of much greater age. Laser-induced injury to the macula can result in tissue destruction and retinal cavitations but typically are also associated with changes to the outer retina and retinal pigment epithelium (RPE). These features are not apparent in this case.

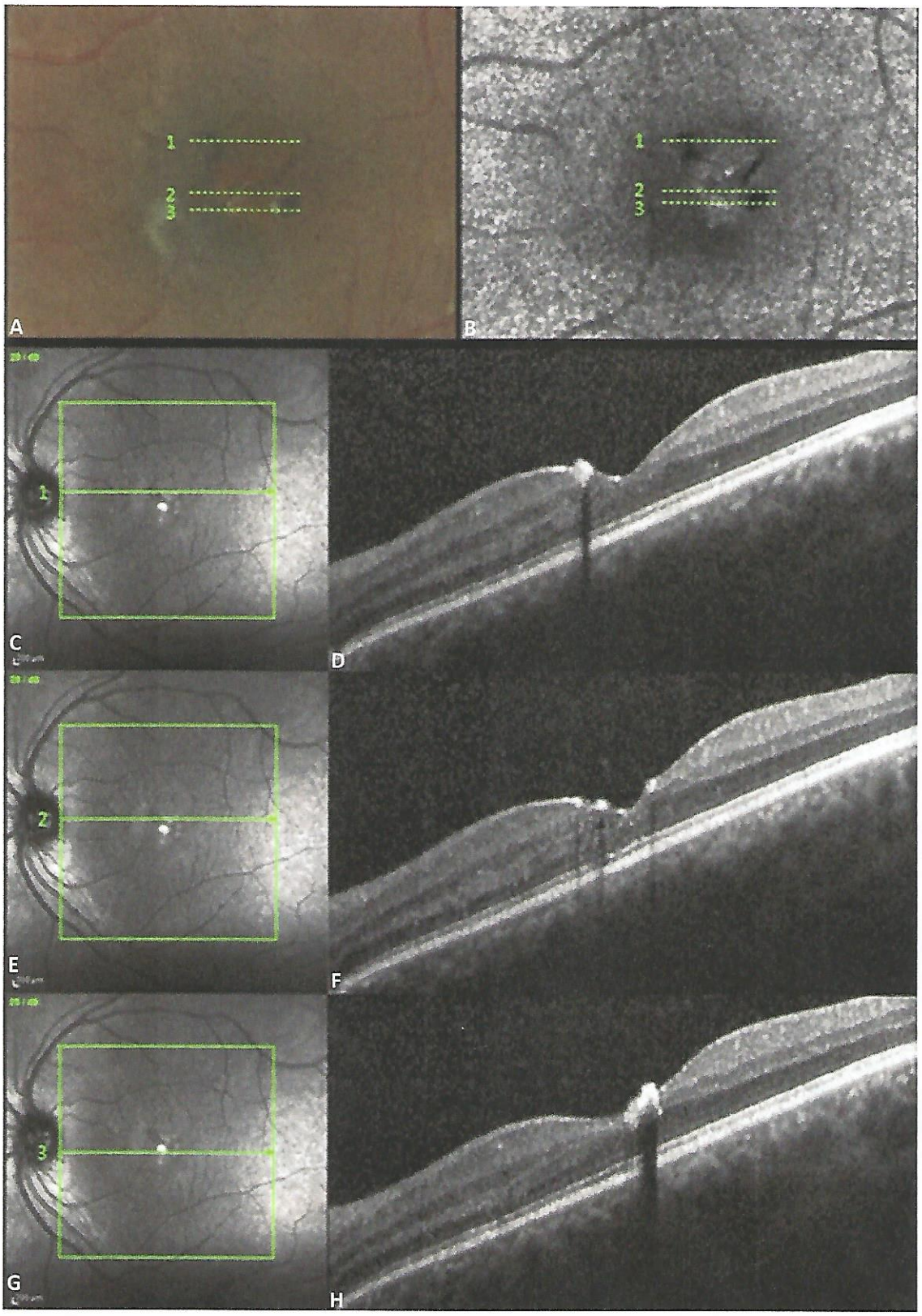

Fig. 4. Multimodal imaging of the left eye. **A.** Color fundus photograph. **B.** Fundus autofluorescence. **C–E.** Spectral-domain optical coherence tomography findings using three consecutive macular scans over different lesions that correspond to the dashed lines 1, 2, and 3 are displayed in green in Figures (**A** and **B**). **C–H.** All lesions have a similar pattern and are characterized by high reflectivity at the inner retina associated with intense underlying optical shadowing with distinct borders. **D** and **F.** Small cysts are seen at the outer plexiform layer, temporal to the fovea, and nasal to the fovea, respectively. The outer retina and choroid are normal. The central macular thickness is 237 μm.

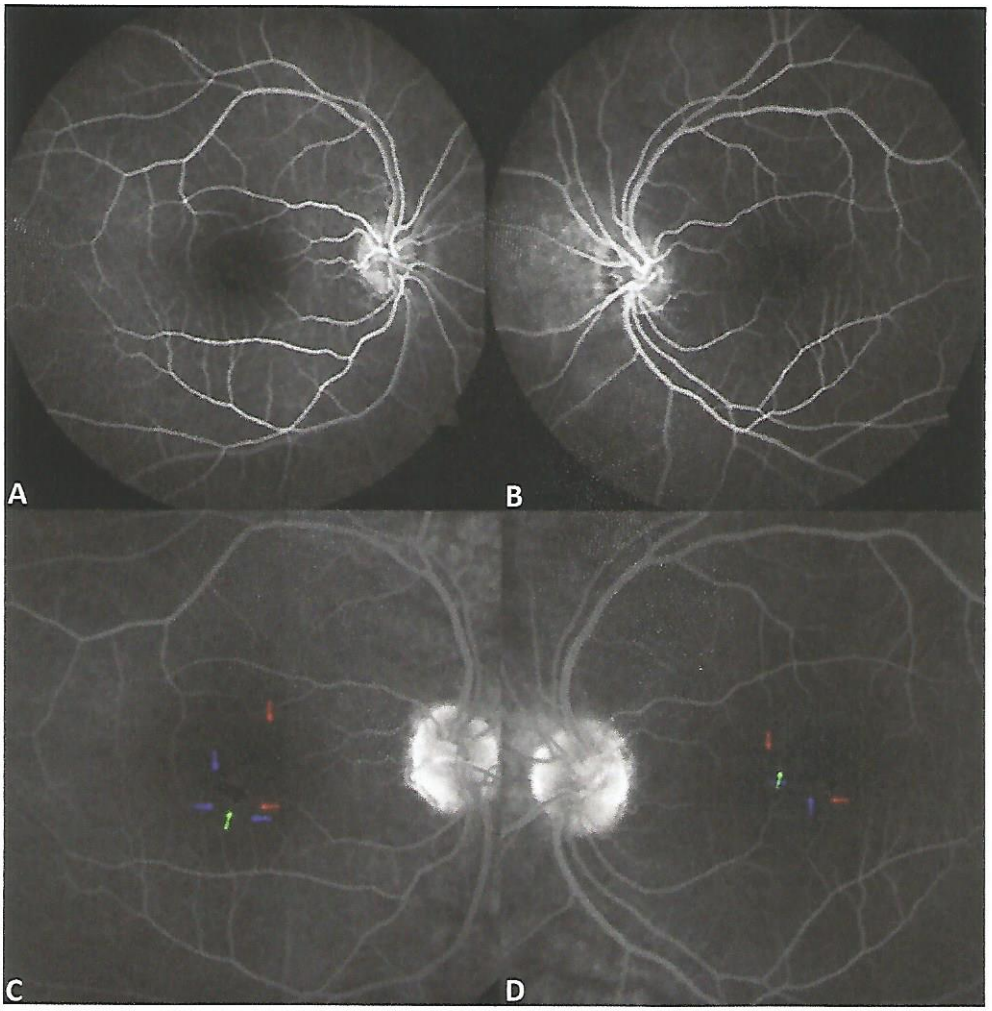

Fig. 5. A and **B.** Fluorescein angiography in the right and left eyes, respectively, shows multifocal early and persistent perifoveal hypofluorescence by the pigmented lesions. **C** and **D.** Discrete and focal late leakage around the larger lesions (green arrow) is supplied by arterial (red arrow) and venous (yellow blue arrow) feeder vessels.

Further analysis of OCT scans revealed distinct lesions of high reflectivity at the level of the inner retina associated with underlying optical shadowing (Figures 3 and 4). The lesions demonstrated anterior bowing toward the attached vitreous, with a characteristic that the larger the lesion, the larger the protrusion toward the vitreous.

Comment

The peculiar feature of this case is the localization of lesions to the inner retina. In most inherited and acquired lesions where pigmentary changes are seen in the macula, the lesions are typically localized to the outer retina and RPE.

Fluorescein angiography demonstrated subtle arterial and venous feeder vessels around the pigmented lesions. The fluorescein angiogram also revealed early and persistent hypofluorescence of the lesions and subtle and focal late leakage around the larger lesions in both eyes (Figure 5). Optical coherence tomography angiography (OCTA) images (6 × 6 mm) were captured using the Cirrus HD (Carl Zeiss Meditec) device. A cross-sectional analysis of vascular flow through the superficial capillary plexus (SCP) confirmed the feeder vessels seen on the fluorescein angiogram, with capillary rectification at the border of the larger inferior lesion in the right eye, and a discrete flow inside this lesion (Figure 6). In the left eye, flow was detected in all three lesions, at the level of the SCP (Figure 7). The deep capillary plexus, avascular retina, and choriocapillaris appeared to manifest normal flow signals in both eyes.

Question

What is the likely diagnosis?

Response

The location of pigmented lesions within the inner retina, the occurrence of cystoid macular changes, and

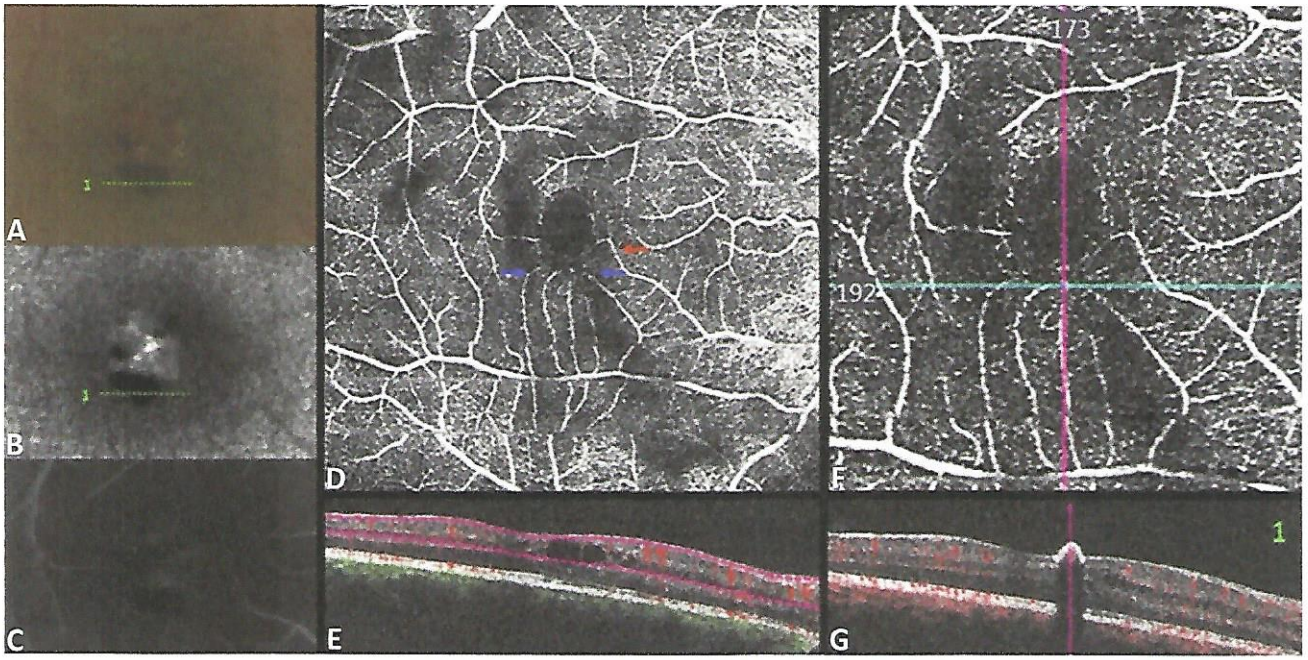

Fig. 6. Multimodal imaging of right eye. **A.** Color fundus photograph shows multiple and superficial retinal lesions within the macular area. The largest lesion (green dashed line) is observed just below to the fovea. **B.** Fundus autofluorescence demonstrates hypoautofluorescence (green dashed line) corresponding to the largest lesion observed on a color photograph. **C.** Fluorescein angiography depicts focal late leakage around the larger lesion. **D** and **F.** Magnified view: *En face* OCT at the SCP shows the feeder vessels seen on FA images (arterial flow outlined by the red arrow and venous flow by the blue arrows). **E** and **G.** Structural SD-OCT demonstrates flow at the topography of feeder vessels on *en face* OCT.

the presence of feeder vessels make congenital simple hamartoma of the retinal pigment epithelium (CSHRPE) a potential diagnosis.

Macular function analysis was obtained by microperimetric examination using the MP3 (Nidek Technologies, Padua, Italy). The parameters tested in the MP3 were 40

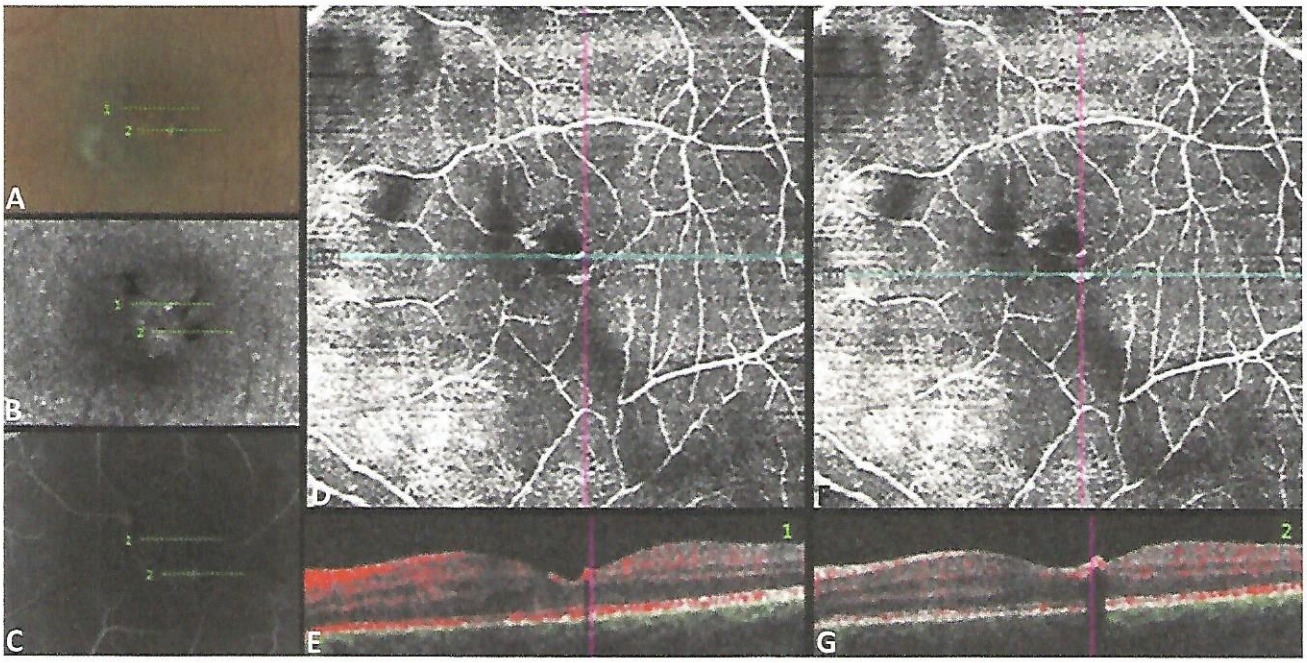

Fig. 7. Multimodal imaging in the left eye. **A.** Color fundus photograph. **B.** Fundus autofluorescence. **C.** Fluorescein angiography. **D** and **E.** *En face* OCTA shows the SCP with matching structural SD-OCT with flow, revealing the scan corresponding to the dashed line 1 (green) seen in **A–C**. Flow is detected inside the linear lesion in the *en face* and the matching structural SD-OCT. **F** and **G.** *En face* OCTA shows the SCP with matching structural SD-OCT with flow, revealing the scan corresponding to dashed line 2 (green) seen in **A–C**. The flow also is detected in the larger round lesion in the *en face* image and in the matching structural SD-OCT.

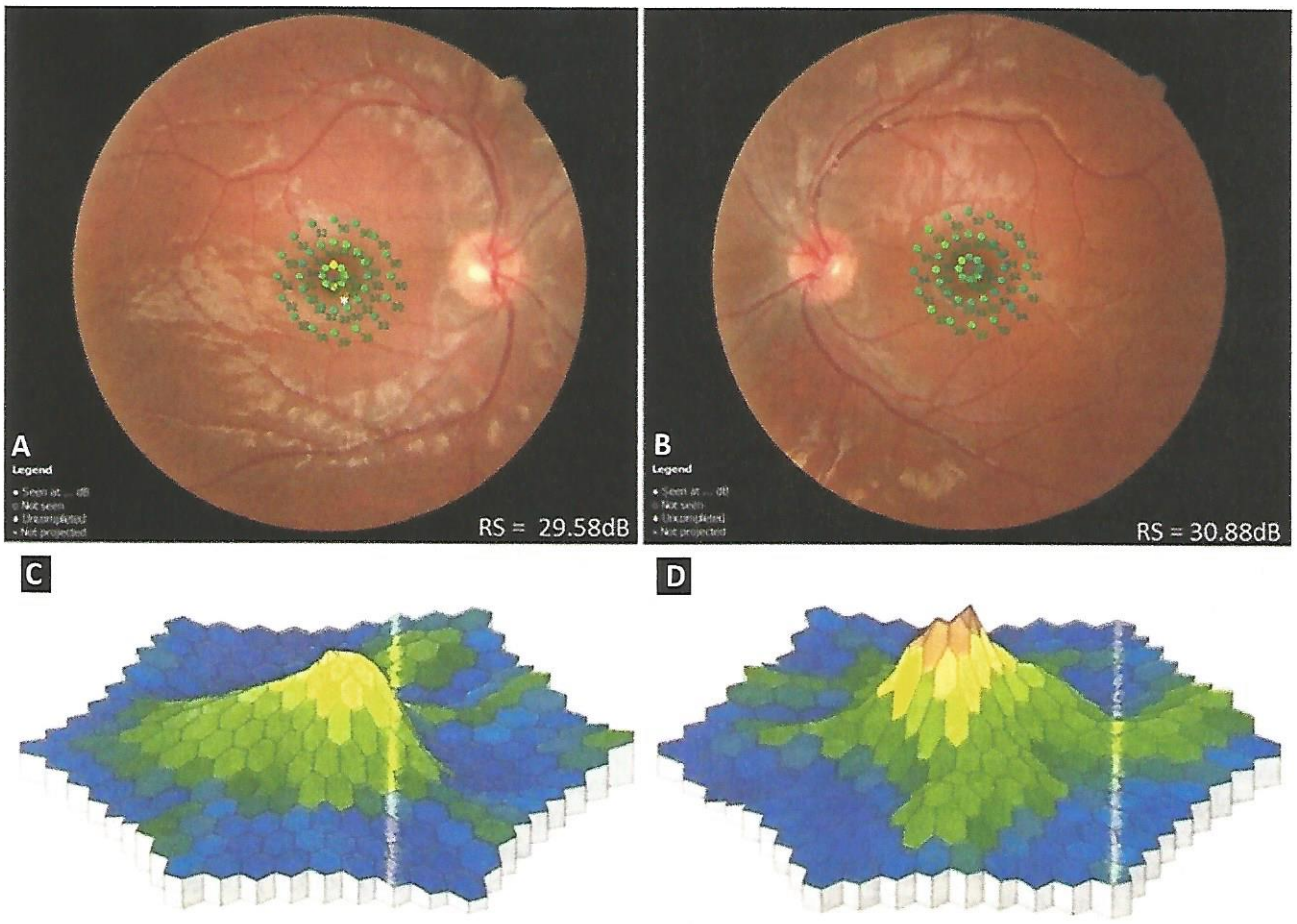

Fig. 8. A and **B.** Microperimetry (MP) of the right and left eye, respectively. A small and focal reduction in the RS is topographically correlated with the larger inferior juxtafoveal lesion in the right eye, with a mean RS of 29.58 dB. **C.** These reductions conform to the slight 10-degree amplitude reduction seen in the multifocal electroretinography of the right eye. **D.** In the left eye, the MP is virtually normal with no focal RS reduction and a mean RS of 30.88 dB. There is a similarity with the multifocal electroretinography results that are almost normal.

points, covering a total of 10 central degrees. The arithmetic means of the absolute thresholds in decibels (dB) measured at each point were calculated as the mean retinal sensitivity (RS) for each eye, which reached 29.58 and 30.88 dB in the right and left eyes, respectively (Figure 8, A and B). Microperimetry exhibited a small scotoma in the right eye that was topographically correlated with the larger inferior juxtafoveal lesion (Figure 8A).

Multifocal electroretinography (RETiscan System, Roland Consult, Brandenburg an der Havel, Germany) showed a slight 10-degree amplitude reduction in the right eye (Figure 8C) and almost normal results in the left eye (Figure 8D).

As the patient had good visual acuity, no treatment was administered for the macular edema.

Discussion

In 1981, Laqua[1] first reported CSHRPE in two eyes. In 1989, Gass published a review on focal congenital anomalies of the RPE, including 10 eyes with CSHRPE, and called these lesions "RPE hamartoma." They were not associated with alterations in the surrounding sensory retina, RPE, and choroid and were typically 0.5 to 1 disk diameter in size.[2] In 2003, Shields et al reviewed five eyes with CSHRPE and further detailed these lesions. The authors described patent feeder vessels in 100% of cases, surrounding retinal traction in 80%, retinal exudation in 20%, and a pattern of high internal reflectivity on ultrasound A-scans. The authors proposed that this condition was congenital because it was more commonly detected in children and the features were nonprogressive.[3] Shields et al first described the OCT findings in 2004,[4] and others did so later in addition to mentioning demarcated lesions with high reflectivity in the inner retina that were associated with posterior optical shadowing, irregular surfaces, and protrusion to the vitreous. After those four publications, 21 others characterized the clinical and multimodal imaging

features of CSHRPE.[5–26] In total, 42 patients have been described of age between 8 and 80 years. Of these cases, only a single case of bilateral disease has been reported in a patient with Down syndrome.[10] Furthermore, there have not been any previous reports of CSHRPE with multifocal lesions, as in the current case.

Congenital simple hamartoma of the retinal pigment epithelium typically presents as an isolated, black macular lesion with well-defined margins.[1–3] Multimodal imaging is required to make the precise diagnosis. The definitive diagnosis is frequently made using spectral-domain optical coherence tomography (SD-OCT), in which the lesion is well-demarcated with high reflectivity at the inner retina and marked shadowing of the underlying retina and choroid.[3] Several studies have described hypoautofluorescence of the lesions on FAF images and hypofluorescence in early-phase fluorescein angiography (FA) with/without discrete hyperfluorescence around the lesion in the late phase of the angiogram.[3,5–7] Fluorescein angiography may reveal feeder vessels related to the lesion. Similar to other studies,[5–9] the current case had intrinsic flow to the pigmented lesions at the SCP, seen bilaterally on OCTA and more evident in the left eye (Figures 6 and 7). The retinal vessels were oriented in apparent continuity with the lesion vasculature. In his original description, Gass[2] described the intrinsic vasculature as an element to characterize these tumors, sometimes masked by their inherent pigmentation.

In most cases, CSHRPE has been found incidentally, and the visual acuity is usually normal or slight affected, although some cases are significantly visually impaired.[2,3] In the 42 cases reported in the literature, 21 of 42 (50%) had a best-corrected visual acuity of 20/25 or better, 5 of 42 (12%) between 20/30 and 20/40, and 16 of 42 (38%) below 20/40.[3,5–26] The factors related to decreased visual acuity are macular edema,[11,13] amblyopia,[11] vitreomacular traction and surrounding foveal traction with an epiretinal membrane,[2,6,11] and tractional macular hole formation.[12,25] Interestingly, mild surrounding retinal traction is a common finding and may provide the pathophysiological basis for the development of foveal traction and macular holes.[3] In the current case, potential retinal function at the site of the pigmented lesions and surrounding margins was evaluated by microperimetry. Similar to Rodrigues et al,[8] we detected focally reduced RS among the corresponding areas of CSHRPE in the right eye (Figure 8A).

Macular edema has been described in two of 42 cases of CSHRPE. Barnes et al[11] described an eye with macular edema secondary to significant vitreomacular traction over the tumor. The tumor and traction were removed from the inner retina during pars plans vitrectomy. Postoperatively, the foveal anatomy was restored and the edema resolved, although with visual loss secondary to damage of the external limiting membrane, ellipsoid zone, and interdigitation zone at the fovea, but without RPE–Bruch membrane complex damage. Bach et al [13] also reported a presumed case of CSHRPE associated with macular edema and no vitreomacular traction. The authors attributed this finding to the tumor's vascular activity and administered one intravitreal application of bevacizumab (Avastin, Genentech Inc., South San Francisco, CA) with partial anatomic and visual improvement during the following 2 months. Arjmand et al[6] reported that macular edema could result from leakage from the intrinsic tumor vessels or vitreoretinal tractional forces, rather than microvascular ischemic disease.

Histopathological examination of CSHRPE was described initially by Holz et al[14] from a free-floating vitreous lesion. They described a tumor composed of angiomatous features and RPE hyperplasia. Barnes et al[11] reported the histopathological features of CSHRPE associated with vitreomacular traction and macular edema that was removed from the inner retina during pars plans vitrectomy. The lesion was characterized by nodular proliferation of hyperplastic RPE cells, with fibrous metaplasia, and attached peripheral gliotic retina and internal limiting membrane. There was no evidence of axons or vascular spaces in the lesion. Based on these findings, the authors presumed that the CSHRPE pathogenesis may be related to one or a group of RPE cells that migrate to the retinal surface during embryogenesis and proliferate as a hamartomatous lesion without involving the entire retinal thickness. They also hypothesized that another less plausible possibility would include RPE cell migration secondary to traction. Another recent theory related the etiology of CSHRPE to ectopic and incomplete differentiation of progenitor cells into RPE cells within the neural retina, with RPE hyperplasia and fibrosis.[27] Depending on the amount of cell rest, location, and density, the hyperplasia could be limited to the superficial or full-thickness retina[27] or, as in the current case, be multifocal, with diverse tumor sizes around the fovea.

The CSHRPE differential diagnosis includes other pigmented RPE lesions, that is, a combined hamartoma of the retina and RPE, congenital hypertrophy of the RPE, adenoma or adenocarcinoma of the RPE, and hyperplasia of the RPE. These conditions differ from CSHRPE in demographics, multimodal imaging presentation, and evolution.[3]

Comment

In this case, there is a juxtafoveal, bilateral, black, intraretinal lesion, with associated cystic changes within the retina and a barely detectable vitreous–retinal interface disturbance in each eye. The cystic changes in the retina are degenerative in nature (cystic macular degeneration or CMD), not permeable or cystoid macular edema. There was no perifoveal leakage on the fluorescein angiogram. The clinical interpretation is that of a bilateral simple hamartoma of the RPE as described by Gass[1] with a retinal feeder vessel and marked acoustical reflectance on B-scan ultrasonography. The consensus in the ophthalmic literature is that these lesions are congenital and generally stable through adulthood, usually with preservation of good visual function and without extension of the pathology to other contiguous layers of the anatomical macula. The alternative diagnoses include a combined hamartoma of the retina and retinal pigment epithelium, macular telangiectasia Type II, a toxic effect such as tamoxifen, and other ill-defined hereditary retinal disorders. The lesions in this case do not fit the phenotypical features of the known alternatives. However, there are exceptions. I have seen that macular telangiectasia Type II originates at the nasal juxtafoveal area; I have also seen it with intraretinal feeder vessels. I have seen bilateral combined hamartomas, but never quite so symmetric as in this case and never with such minimal preretinal or retinal fibrosis.

The one feature that is strikingly different from the usual solitary simple RPE hamartoma is the bilaterality. There has been only one previous case described as bilateral and that was in a patient with Down syndrome.[4] In addition, the localization of the RPE hyperplasia to the inner retina is unusual. In MacTel II, the pigment epithelial cells cluster in the deep retina, presumably from the angiomatous process that extends from the superficial retina posteriorly to the level of the RPE. In solitary simple hamartoma of the RPE, Barnes et al have suggested two possible mechanisms for the hamartoma to be in the inner retina: The first relates to the possibility of migrating RPE cells during embryogenesis to proliferate as an independent, focal mass without involvement of the rest of the retina. Another concept relates to the possibility of ectopic, incompletely differentiated progenitor cells forming a clustered RPE lesion within the retina. Greater experience with clinical pathological correlations is required before establishing a better understanding of the pathophysiological development of this perplexing lesion. In the meantime, management with observation is the recommended approach in the clinical setting.

Key words: congenital simple hamartoma of the retinal pigment epithelium, macular edema, multimodal imaging, pigmentary maculopathy.

References

1. Laqua H. Tumors and tumor-like lesions of the retinal pigment epithelium. Ophthalmologica 1981;183:34–38.
2. Gass JD. Focal congenital anomalies of the retinal pigment epithelium. Eye 1989;3:1–18.
3. Shields CL, Shields JA, Marr BP, et al. Congenital simple hamartoma of the retinal pigment epithelium: a study of five cases. Ophthalmology 2003;110:1005–1011.
4. Shields CL, Materin MA, Karatza EC, et al. Optical coherence tomography of congenital simple hamartoma of the retinal pigment epithelium. Retina 2004;24:327–328.
5. Zola M, Ambresin A, Zografos L. Optical coherence tomography angiography imaging of a congenital simple hamartoma of the retinal pigment epithelium. Retin Case Brief Rep 2018;12:1–5.
6. Arjmand P, Elimimian EB, Say EA, et al. Optical coherence tomography angiography of congenital simple hamartoma of the retinal pigment epithelium. Retin Case Brief Rep 2019;13:357–360.
7. Ito Y, Ohji M. Long-term follow-up of congenital simple hamartoma of the retinal pigment epithelium: a case report. Case Rep Ophthalmol 2018; 9:215–220.
8. Rodrigues MW, Cavallini DB, Dalloul C, et al. Retinal sensitivity and photoreceptor arrangement changes secondary to congenital simple hamartoma of retinal pigment epithelium. Int J Retina Vitreous 2019;5:1–8.
9. Pazzaglia GA. Multimodal imaging in congenital simple hamartoma of retinal pigment epithelium (CSHRPE): optical coherence tomography (OCT), autofluorescence and oct angiography, a review of the literature and case presentation. Adv Ophthalmol Vis Syst 2019;9:113–116.
10. Panagopoulos A, Chalioulias K, Murray AT. Bilateral congenital hamartomas of the retinal pigment epithelium in a patient with Down's syndrome. Eye 2008;22:735–736.
11. Barnes AC, Goldman DR, Laver NV, et al. Congenital simple hamartoma of the retinal pigment epithelium: clinical, optical coherence tomography, and histopathological correlation. Eye 2014;28:765–766.
12. Van de Moere A, Clark JB. Congenital simple hamartoma of the retinal pigment epithelium with a full-thickness macular hole. Retin Case Brief Rep 2009;3:80–82.
13. Bach A, Gold AS, Villegas VM. Simple hamartoma of the retinal pigment epithelium with macular edema. Optom Vis Sci 2015;92:S48–S50.
14. Holz FG, Alexandridis E, Volker HE, et al. Spontaneous incomplete avulsion of juxtafoveal retinal pigment epithelial hamartoma. Arch Ophthalmol 2001;119:903–907.
15. Shields CL, Materin MA, Ekaterini C, et al. Optical coherence tomography of congenital simple hamartoma of the retinal pigment epithelium. Retina 2004;24:327–328.
16. Shukla D, Ambatkar S, Jethani J, et al. Optical coherence tomography in presumed congenital simple hamartoma of retinal pigment epithelium. Am J Ophthalmol 2005;139:945–947.
17. Lopez JM, Guerrero P. Congenital simple hamartoma of the retinal pigment epithelium: optical coherence tomography and angiography features. Retina 2006;26: 704–706.

18. Gotoh M, Yoshikawa H, Kagimoto HT, et al. Congenital simple hamartoma of the retinal pigment epithelium in an Asian. Jpn J Ophthalmol 2008;52:144–145.
19. Madgula IM, Adatia FA, Sagoo MS, et al. Simple hamartoma of the retinal pigment epithelium in a man of African descent. Can J Ophthalmol 2009;44:e35–e36.
20. Kálmán Z, Tóth J. Two cases of congenital simple hamartoma of the retinal pigment epithelium. Retin Cases Brief Rep 2009;3:283–285.
21. Teke MY, Ozdal PÇ, Batioglu F, et al. Congenital simple hamartoma of retinal pigment epithelium: clinical and imaging findings. Case Rep Ophthalmol Med 2012;2012:654502.
22. Heo WJ, Park DH, Shin JP. A case of congenital simple hamartoma of the retinal pigment epithelium and Coats' disease in the same eye. Korean J Ophthalmol 2015;29:282–283.
23. Grant LW, Rajeev Seth RK. Congenital simple hamartoma of the retinal pigment epithelium. Sem Ophthalmol 2014;29:183–185.
24. Thorell MR, Kniggendorf VF, Arana LA, et al. Congenital simple hamartoma of the retinal pigment epithelium: a case report. Arq Bras Oftalmol 2014;77:114–115.
25. Stavrakas P, Vachtsevanos A, Karakosta E, et al. Full-thickness macular hole associated with congenital simple hamartoma of retinal pigment epithelium (CSHRPE). Int Ophthalmol 2018;38:2179–2182.
26. Souissi K, El Afrit MA, Kraiem A. Congenital retinal arterial macrovessel and congenital hamartoma of the retinal pigment epithelium. J Pediatr Ophthalmol Strabismus 2006;43:181–182.
27. Pujari A, Agarwal D, Chawla R, et al. Congenital simple hamartoma of the retinal pigment epithelium: what is the probable cause? Med Hypotheses 2019;123:79–80.

UNUSUAL CASE OF BILATERAL MACULAR DETACHMENT PRECEDING RENAL FAILURE

Carlos A. de Amorim Garcia Filho, MD,* Rodrigo A. de Oliveira, MD,† Rodrigo L. Meirelles, MD,‡ Luiz H. Lima, MD,‡ Chandrakumar Balaratnasingam, MD,§¶ Anita Agarwal, MD,** Carlos A. de Amorim Garcia, MD*

*From the Departments of *Ophthalmology, and †Nephrology, Federal University of Rio Grande do Norte, Natal, Brazil; ‡Department of Ophthalmology, Federal University of São Paulo, São Paulo, Brazil; §Center for Ophthalmology and Visual Science, University of Western Australia, Perth, Australia; ¶Department of Ophthalmology, Sir Charles Gairdner Hospital, Western Australia, Australia; and **West Coast Retina, San Francisco, California.*

A 58-year-old woman presented with a 4-month history of progressively decreasing visual acuity in both eyes and no other ophthalmic or systemic symptoms. Her medical history was relevant only for moderately controlled systemic hypertension.

Her best-corrected visual acuity was 20/100 and 20/200 in the right and left eyes, respectively. The intraocular pressures were normal and the anterior segments unremarkable bilaterally. Fundus examinations of both eyes revealed normal optic disks and multiple yellow, well-defined subretinal deposits in the macular and peripapillary regions (Figure 1). The subretinal lesions were hyperautofluorescent on fundus autofluorescence imaging, and more numerous than what was seen on color fundus imaging. On fluorescein angiography, the lesions were hypofluorescent with a masking effect. A few isolated focal areas of hyperfluorescence from leakage were seen between some of the lesions in both eyes (C arrows). Spectral-domain optical coherence tomography findings were similar in both eyes and showed multiple, round hyper-reflective subretinal deposits associated with submacular fluid and elongated outer segment structures. The choroid appeared thicker than normal in both eyes. Intraretinal fluid also was seen in the left eye (Figure 2).

Question—what is the differential diagnoses for this presentation?

Response—a number of conditions can lead to the deposition of bilateral hyperautofluorescent material within the macula. These include a range of inflammatory conditions such as acute exudative polymorphous vitelliform maculopathy, neoplastic conditions such as cloudy vitelliform maculopathy that is a precursor of vitreoretinal lymphoma, and paraneoplastic syndromes such as vitelliform maculopathy secondary to metastatic melanoma. Bilateral diffuse uveal melanocytic proliferation and idiopathic uveal effusion syndrome can also manifest hyperautofluorescent material associated with exudative retinal detachment in the posterior segment. Renal diseases such as immunoglobulin A nephropathy and glomerulonephritis can also lead to deposition of material beneath the retina. Vitelliform lesions can be the manifestation of drug toxicity, for example, desferrioxamine or mitogen-activated protein kinase inhibitors, or a feature of dystrophic and degenerative conditions of the macula such as pattern dystrophy, autosomal recessive bestrophinopathy, multifocal Best disease, and fundus flavimaculatus. However, a dystrophic or degenerative condition is unlikely given the subacute nature of vision loss in this patient.

Question—What is the next step in managing this case?

Response—a systemic malignancy must be excluded. Common sites of primary malignancy that are associated with a paraneoplastic syndrome include the chest, abdomen, and pelvis. These sites should be imaged, or the patient must be referred to an oncologist for appropriate investigations. Laboratory work-up including complete blood counts, renal function, liver function, and inflammatory markers

None of the authors has any financial/conflicting interests to disclose.

Reprint requests: Carlos A. de Amorim Garcia Filho, MD, Avenida Prudente de Morais 1044, AP 1302 Bloco Florença, Natal, Brazil, CEP 59020-510; e-mail: caagf@yahoo.com.br

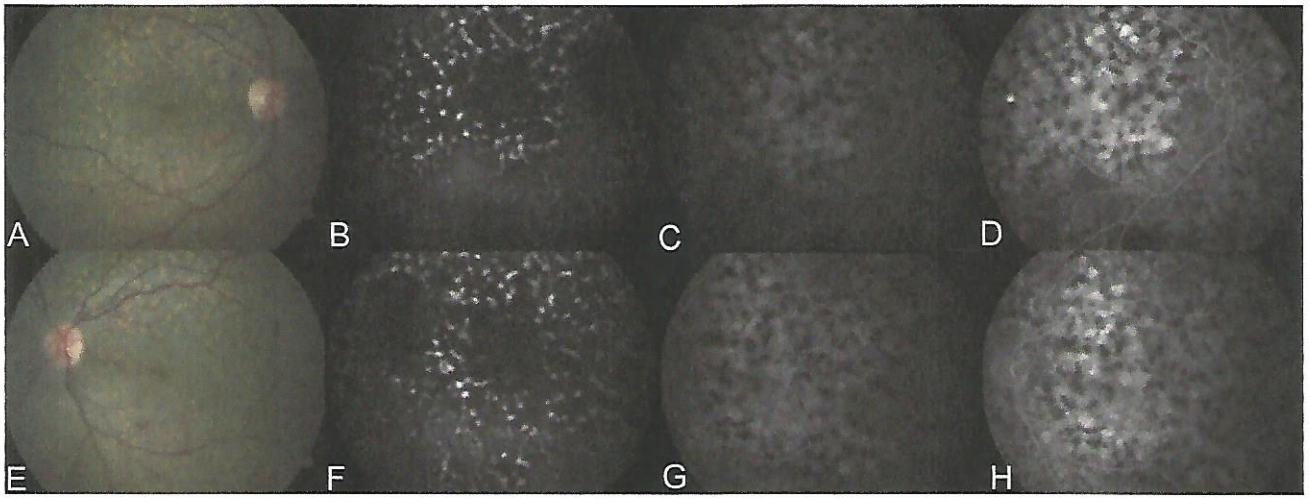

Fig. 1. A–H. Multimodal imaging of a 58-year-old woman with AL amyloidosis at presentation. **A** and **E.** Color fundus photographs of the right and left eyes, respectively, show the multiple yellowish, well-defined subretinal lesions in the macular and peripapillary regions. **B** and **F.** Fundus autofluorescence images of the right and left eye, respectively, demonstrate the alternating patterns of hypoautofluorescence and hyperautofluorescence, with subretinal deposits appearing hyperautofluorescent. Fluorescein angiography of the right eye (**C** and **D**) and the left eye (**G** and **H**) depict hypofluorescent lesions with a masking effect and some areas of hyperfluorescence with leakage.

must be performed to look for evidence of systemic inflammation. Masquerade syndromes including tuberculosis, syphilis, and sarcoidosis must also be excluded.

The hemato-oncology work-up was negative for any occult neoplasia in the abdomen, thorax, breast, uterus, digestive tract, or central nervous system. A systemic work-up was negative for infectious diseases including syphilis and tuberculosis. Laboratory examinations revealed low erythrocytes levels on a peripheral blood examination (hematocrit, 30%) and an elevated creatinine level (1.7 mg/dL).

Comment—normal hematocrit in women is 36%–48%. This patient has low hematocrit and raised creatinine implicating renal insufficiency in association with the retinal manifestations. Further investigations assessing renal structure and function are indicated. Importantly, urinalysis assessing protein content will allow differentiation between nephritic and nephrotic syndromes.

The patient developed a nephrotic syndrome with hypercreatinemia (2.76 mg/dL) and proteinuria. Urinary protein electrophoresis was normal, but immunofixation detected a monoclonal component of light-chain lambda protein. A kidney biopsy and Congo red stain showed amyloid deposition in the glomerular and interstitial compartment. Under polarized light, the classic apple–green birefringence was observed. Immunofluorescence was positive for lambda protein (Figure 3).

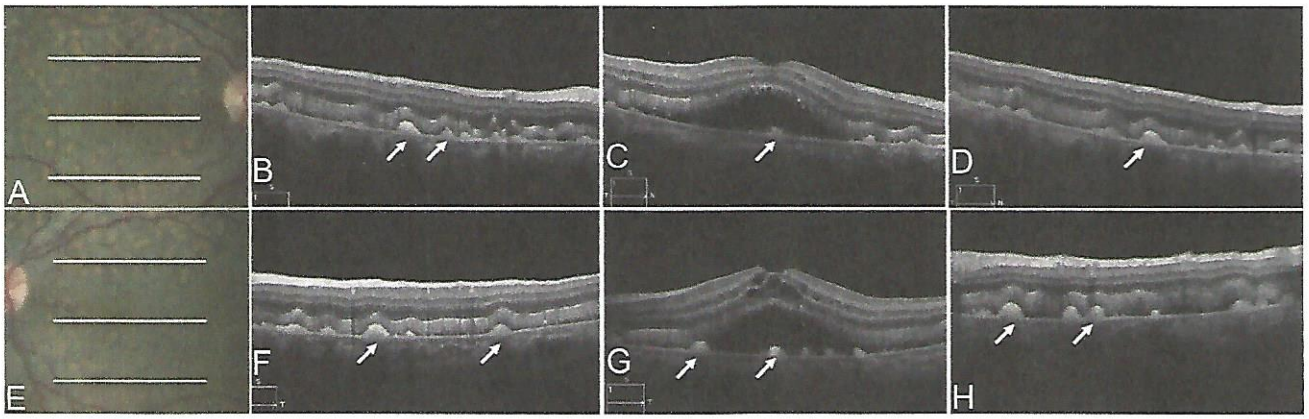

Fig. 2. Spectral-domain optical coherence tomography of a 58-year-old woman with AL amyloidosis at presentation. **A.** Color fundus photograph of the right eye with three lines representing the 6-mm B scan shown in the upper macula (**B**), fovea (**C**), and inferior macula (**D**). Multiple, round hyperreflective subretinal deposits (arrows) are associated with subretinal fluid. **E–H.** The left eye presents the same features as observed in the right eye but also has intraretinal fluid in the foveal area.

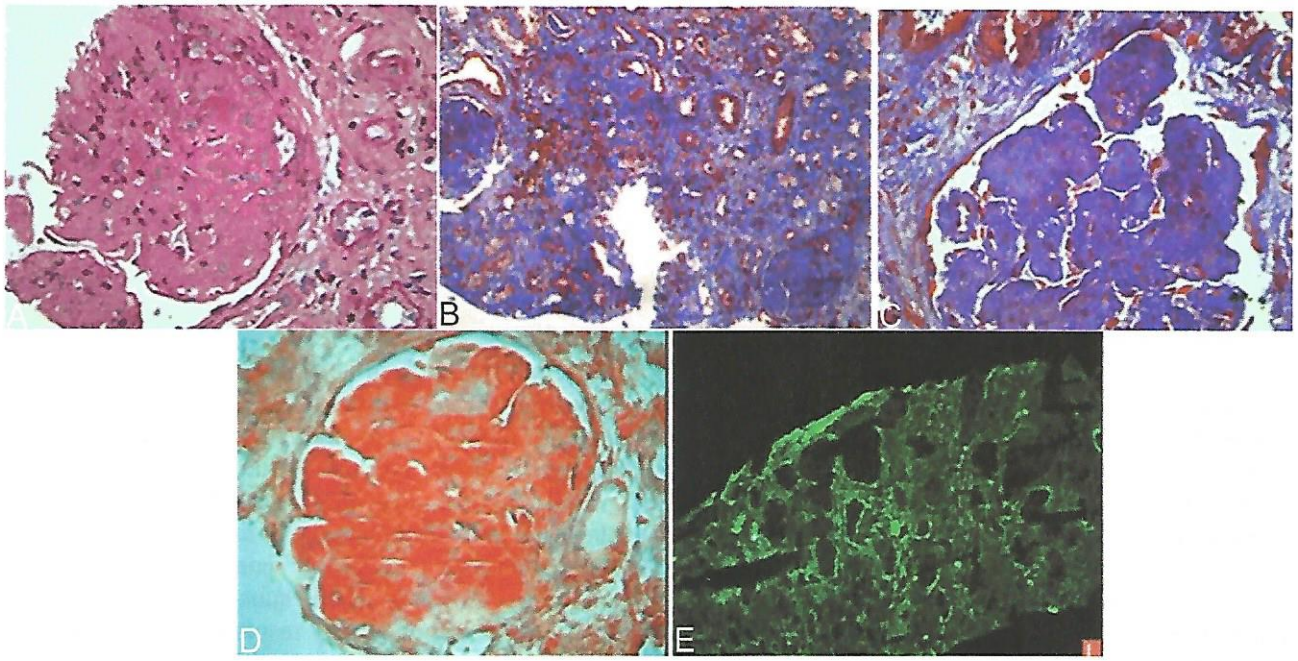

Fig. 3. Renal pathology findings of a 58-year-old woman with AL amyloidosis. **A.** Glomerular biopsy seen on light microscopy stained with hematoxylin and eosin. The amyloid material appears homogeneous, acellular, and amorphous. The interstitial compartment of the biopsy stained with Masson's trichrome (**B**), the glomerular portion stained with Masson's trichrome (**C**), and the glomerular compartment stained with Congo red shows the amyloid deposits (**D**). **E.** Immunofluorescence of the glomerulus is remarkable for monoclonal immunoglobulin lambda chain deposits.

Comment—the biopsy results are consistent with light-chain amyloidosis resulting from plasma cell dyscrasia. Investigations to assess the heart, bone marrow, and liver are prudent as light-chain amyloid can also deposit in these organs. Chemotherapy needs to be initiated.

The patient was started on systemic chemotherapy with cyclophosphamide, dexamethasone, and bortezomib. During the systemic treatment, she was also started on hemodialysis and, later, underwent a renal transplant. During follow-up, the best-corrected visual acuity improved in both eyes to 20/80 at 1 month, 20/50 at 6 months, and 20/30 at 2 years after chemotherapy and hemodialysis, followed by renal transplantation. As the best-corrected visual acuity improved, concomitant regression of most of the subretinal deposits and resolution of the subretinal fluid was seen (Figure 4).

Discussion

Light-chain (AL) amyloidosis is the most common form of systemic amyloidosis. It is a plasma cell

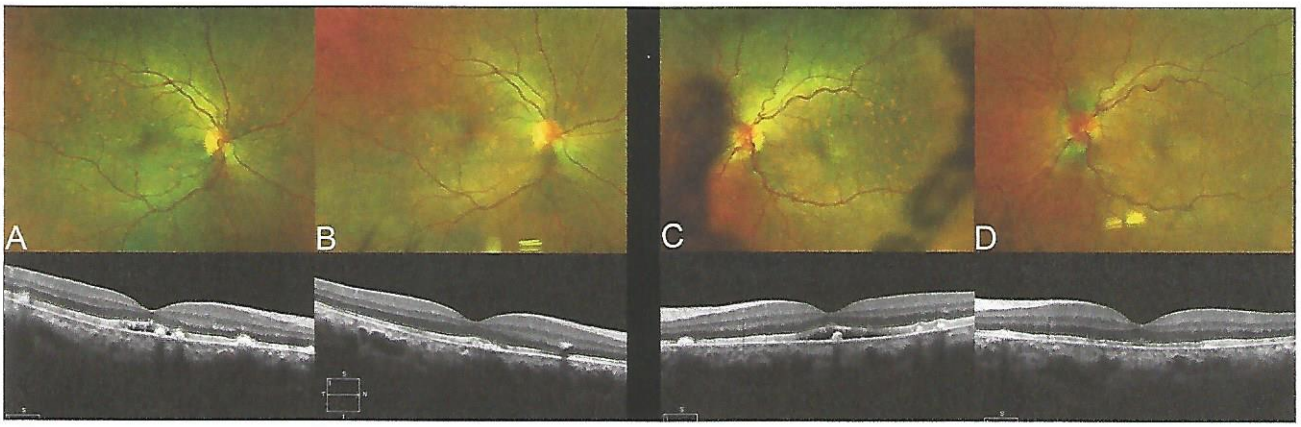

Fig. 4. Follow-up visits of the 58-year-old patient with AL amyloidosis. **A** and **B.** Color fundus photograph and spectral-domain optical coherence tomography B scan through the fovea of the right eye at 6 and 24 months, respectively, after treatment initiation. **C** and **D.** Color fundus photograph and spectral-domain optical coherence tomography B scan through the fovea of the left eye at 6 and 24 months, respectively, after treatment initiation. Regression of most of the subretinal deposits and resolution of the subretinal fluid are correlated with the improved bilateral best-corrected visual acuity from 20/100 and 20/200 in the right and left eye at baseline to 20/50 at 6 months and 20/30 in both eyes at the 24-month follow-up evaluation.

disorder in which immunoglobulin light-chain fragments (kappa or lambda) derived from a clonal population of plasma cells in the bone marrow are deposited in tissues.[1] All organs can be affected by the amyloid deposits, with the heart, kidney, and liver being the most commonly affected. The ophthalmic manifestations of systemic AL amyloidosis include deposits in the eyelid, conjunctiva, lacrimal gland, vitreous, extraocular muscles, temporal artery, retina, and choroid.[2]

Posterior segment involvement because of AL amyloidosis is rare.[3] In this case, multimodal imaging showed symmetric structural changes including hyperautofluorescent lesions in the posterior pole and peripapillary region. Spectral-domain optical coherence tomography analysis showed multiple hyperreflective deposits above the retinal pigment epithelium that corresponded to the hyperautofluorescent lesions. Whether the subretinal deposits observed in the color fundus images and spectral-domain optical coherence tomography images are true amyloid deposits, secondary to an inflammatory process or vitelliform deposits composed of lipofuscin, melano-lipofuscin granules, and extracellular material derived from shredded photoreceptor outer segment disks that accumulate in the subretinal space from retinal pigment epithelium dysfunction can only be determined after ocular biopsy and histologic study.[4]

Published reports of amyloidosis with ocular findings also have noted renal failure, which may be a marker for the severity of the systemic amyloid deposition.[5] The choroid and glomerulus share common histologic components and may be the common pathway of various related diseases involving abnormal protein deposition. Other renal diseases also may lead to drusen formation or drusenoid deposits such as dense deposit disease (membranoproliferative glomerulonephritis) and IgA nephropathy, but the deposits usually differ from those in the current case.

The nephrotic syndrome may also have a role in the choroidal changes and in the accumulation of subretinal fluid through modification of the oncotic pressure.[6,7] Fluorescein angiography showed leakage at the pigment epithelial level suggesting relative choriocapillaris ischemia affecting retinal pigment epithelium function, similar to the patient described by Carrera et al.[8] In addition, it is likely the choroidal vascular permeability change led to increased choroidal interstitial fluid that extended into the subretinal space. In contrast to the current patient, Augstburger et al[3] described a patient with AL amyloidosis with subretinal deposits that did not have leakage on fluorescein angiography despite the presence of a serous macular detachment. In addition, Dhrami-Gavazi et al[9] reported no leakage in a patient with kappa light-chain deposit disease and ocular findings similar to the current one, giving credence to passive accumulation of fluid from the choroidal permeability alterations.

The patient received hemodialysis initially and later underwent renal transplantation. During follow-up, marked regression of the subretinal deposits and resolution of the subretinal fluid with improvement in the visual acuity was seen. Restoration of the plasmatic protein balance and oncotic pressure with hemodialysis and later with renal transplant may be related to resorption of the subretinal fluid, whereas the systemic chemotherapy resulted in decreased production of the fibrillar proteins resulting in regression of the subretinal deposits.

Key words: light-chain amyloidosis, macular detachment, multimodal imaging, renal failure.

References

1. Van der Hilst JC, Simon A, Drenth JP. Molecular mechanisms of amyloidosis. N Engl J Med 2003;349:1872–1873.
2. Reynolds MM, Veverka KK, Gertz MA, et al. Ocular manifestation s of systemic amyloidosis. Retina 2018;38:1371–1376.
3. Augstburger E, Sahel JA, Audo I. Progressive chorioretinal involvement in a patient with light-chain (AL) amyloidosis: a case report. BMC Ophthalmol 2020;20:59.
4. Freund KB, Laud K, Lima LH, et al. Acquired vitelliform lesions: correlation of clinical findings and multiple imaging analysis. Retina 2011;31:13–25.
5. Roybal CN, Sanfilippo CJ, Nazari H, et al. Multimodal imaging of the retina and choroid in systemic amyloidosis. Retin Cases Brief Rep 2015;9:339–346.
6. D'Souza YB, Short CD. The eye: a window on the kidney. Nephrol Dial Transpl 2009;24:3582–3584.
7. Bilge AD, Yaylali SA, Yavuz S, et al. Bilateral serous macular detachment in a patient with nephrotic syndrome. Retin Cases Brief Rep 2018;12:260–262.
8. Carrera W, Rosco MG, Safo M, et al. Reactive AA amyloidosis in the setting of infective endocarditis manifesting as bilateral orbitopathy and choroidopathy. Retin Cases Brief Rep 2020. doi: 10.1097/ICB.0000000000001112. Epub ahead of print.
9. Dhrami-Gavazi E, Freund KB, Lee W, et al. Ocular manifestations of monoclonal immunoglobulin light chain deposition disease. Retin Cases Brief Rep 2017;11:310–315.

MYSTERY CASE: RETINAL PIGMENT EPITHELIAL DYSTROPHY IN A PATIENT WITH POLYNEUROPATHY

Sergio L. G. Pimentel, MD,* Mariana A. M. Misawa, MD,* Lívia S. Conci, MD,*
Beatriz S. Takahashi, MD,* Luiz H. Lima, MD,†
Chandrakumar Balaratnasingam, MD,‡§ Anita Agarwal, MD, PhD,¶
Eduardo Cunha de Souza, MD*

*From the *Department of Ophthalmology, University of São Paulo (USP), SP, Brazil; †Department of Ophthalmology, Federal University of São Paulo (UNIFESP), SP, Brazil; ‡Center for Ophthalmology and Visual Science, University of Western Australia, Perth, Australia; §Department of Ophthalmology, Sir Charles Gairdner Hospital, Western Australia, Australia; and ¶West Coast Retina, San Francisco, CA*

A 57-year-old Caucasian man with a longstanding history of progressive ataxia and peripheral neuropathy presented for ophthalmic evaluation. He was visually asymptomatic, but was found to have bilateral and symmetric mottling of the retinal pigment epithelium (RPE) in the macular area (Figure 1). Best-corrected visual acuity was 20/20 in both eyes.

Question

What is the significance of pigmentary maculopathy in a patient with ataxia and peripheral neuropathy?

Response

Such a presentation prompts the consideration of neurologic syndromes that also involve the retina. Hereditary spastic paraplegia or Kjellin syndrome, myotonic dystrophy, spinocerebellar atrophy, and mitochondrial diseases such as that associated with point mutation of mitochondrial DNA A3243G can lead to pigmentary maculopathies. The point mutation can result in a spectrum of overlapping syndromes including maternally inherited diabetes and deafness, mitochondrial myopathy, encephalopathy, lactic acidosis and stroke-like episodes, and myoclonic epilepsy with red ragged fibers. Progressive ataxia with peripheral neuropathy is not the usual history in patients with mitochondrial myopathy, encephalopathy, lactic acidosis and stroke-like episodes, ormyoclonic epilepsy with red ragged fibers. Refsum syndrome can also present with pigmentary retinopathy in the setting of cerebellar degeneration and peripheral neuropathy. A detailed family history and systemic enquiry for hearing difficulties and diabetes, can help reconcile the diagnosis of these patients.

On fundus autofluorescence, there was macular mottling with a linear branching pattern of hyperautofluorescence combined with a relative diffuse hypoautofluorescence in the macular area in both eyes (Figure 1). In addition, there was pronounced hypoautofluorescence in the nasal retina, starting close to the disk and spreading toward the midperiphery, associated with a reticular pattern of hyperautofluorescence that was symmetrical in both eyes (Figure 1). The temporal retina was affected in a similar pattern in both eyes. There was a sharp correspondence between fundus autofluorescence and fluorescein angiography changes. On fluorescein angiography, the reticular and branching hyperautofluorescence changes seen in the macula and around the equator appeared hypofluorescent on a diffuse background of transmission hyperfluorescence (Figure 1).

Comment

Fundus autofluorescence changes extending peripherally beyond the vascular arcades are uncommon in the spectrum of diseases due to mitochondrial DNA nucleotide A3243G point mutation. Spino cerebellar atrophy 7 and spinocerebellar atrophy 1 are not known to have macular RPE changes; they generally develop

None of the authors has any financial/conflicting interests to disclose.

Reprint requests: Sergio L. G. Pimentel, MD, University of São Paulo (USP), Av. Dr. Enéas Carvalho de Aguiar, 255, 6o andar, Sala 6119, São Paulo, SP 05403-900, Brazil; e-mail: sergiopimentel9@gmail.com

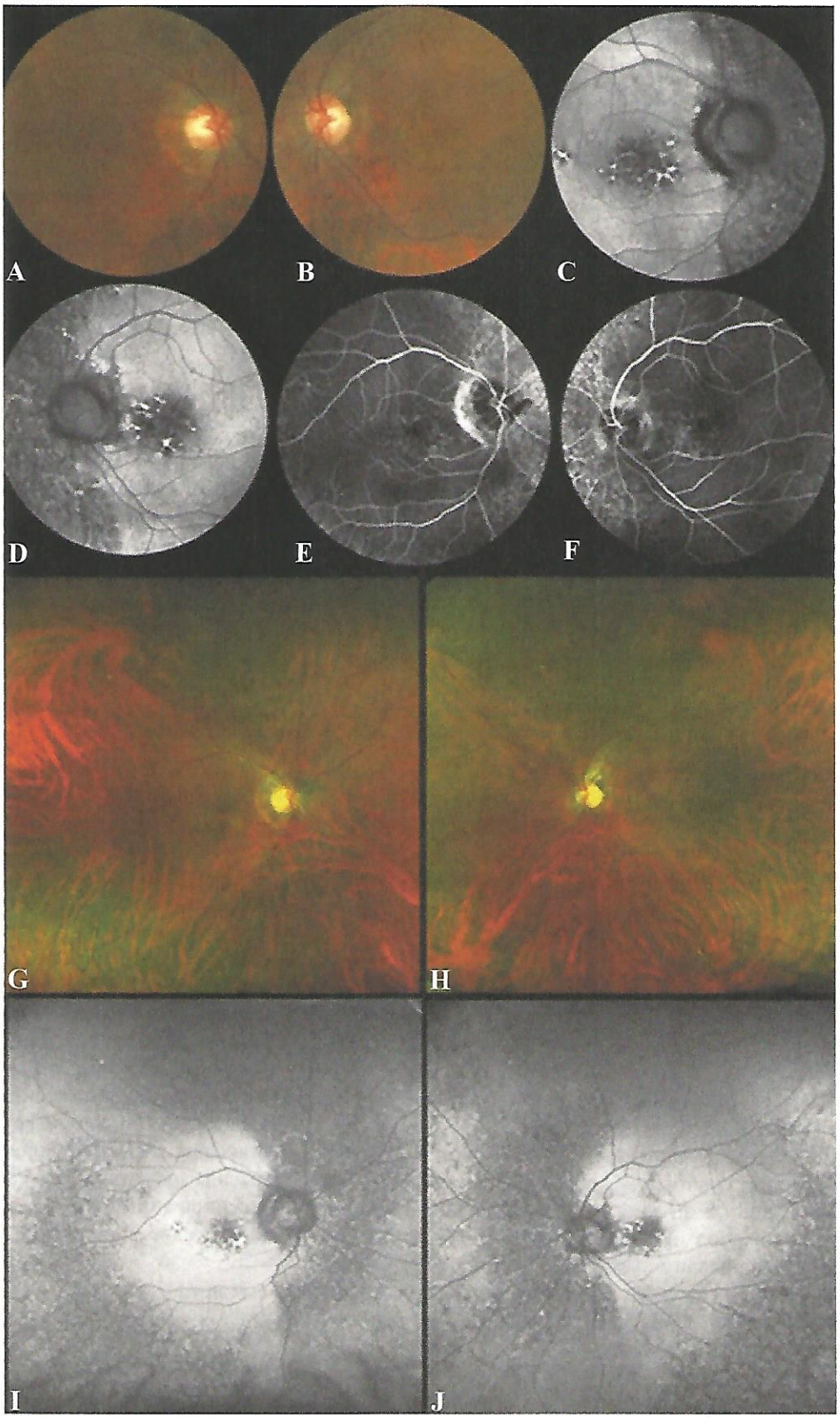

Fig. 1. Multimodal imaging of the both eyes. **A** and **B.** Color fundus photograph reveals mild mottling of the RPE in the macular area. **C** and **D.** FAF shows a branching pattern of hyperautofluorescence and a reduction in autofluorescence within the macula. **E** and **F.** Fluorescein angiography demonstrates early perifoveal blockage by the reticular lesions with hyperfluorescence due to transmission defects. **G** and **H.** Wide-field imaging shows extensive pigment rarefaction in the mid-peripheral retina. **I** and **J.** Wide-field autofluorescence imaging reveals pronounced hypoautofluorescence in the nasal hemiretina and middle-periphery region, associated with a reticular pattern of hyperautofluorescence. FAF, fundus autofluorescence.

macular thinning and atrophy of the foveal outer retina with no visible findings clinically. Kjellin syndrome and myotonic dystrophy have a very characteristic macular appearance of pattern dystrophy. The findings in this patient of central hypofluorescence with halo of hyperfluorescence and peripheral pigmentary alteration resembles Kjellin syndrome, although not completely typical of it. The peripheral pigmentary changes are also seen in Kjellin syndrome.

Neurologic examination revealed muscle atrophy (especially in the lower limbs), extremity deformities (*pes cavus*, hammer toes, and claw hands), and suppressed reflexes. There was no evidence of cerebellar disease. The electroneuromyography test demonstrated chronic mixed peripheral polyneuropathy on all four limbs, more severe on the distal lower limbs. Family history revealed that the patient's brother suffers from similar neurologic issues.

Comment

Based on the results of electroneuromyography and neurologic examination, the diagnosis is consistent with Charcot–Marie–Tooth (CMT) syndrome.

Question

What are the most common ocular manifestations of CMT syndrome?

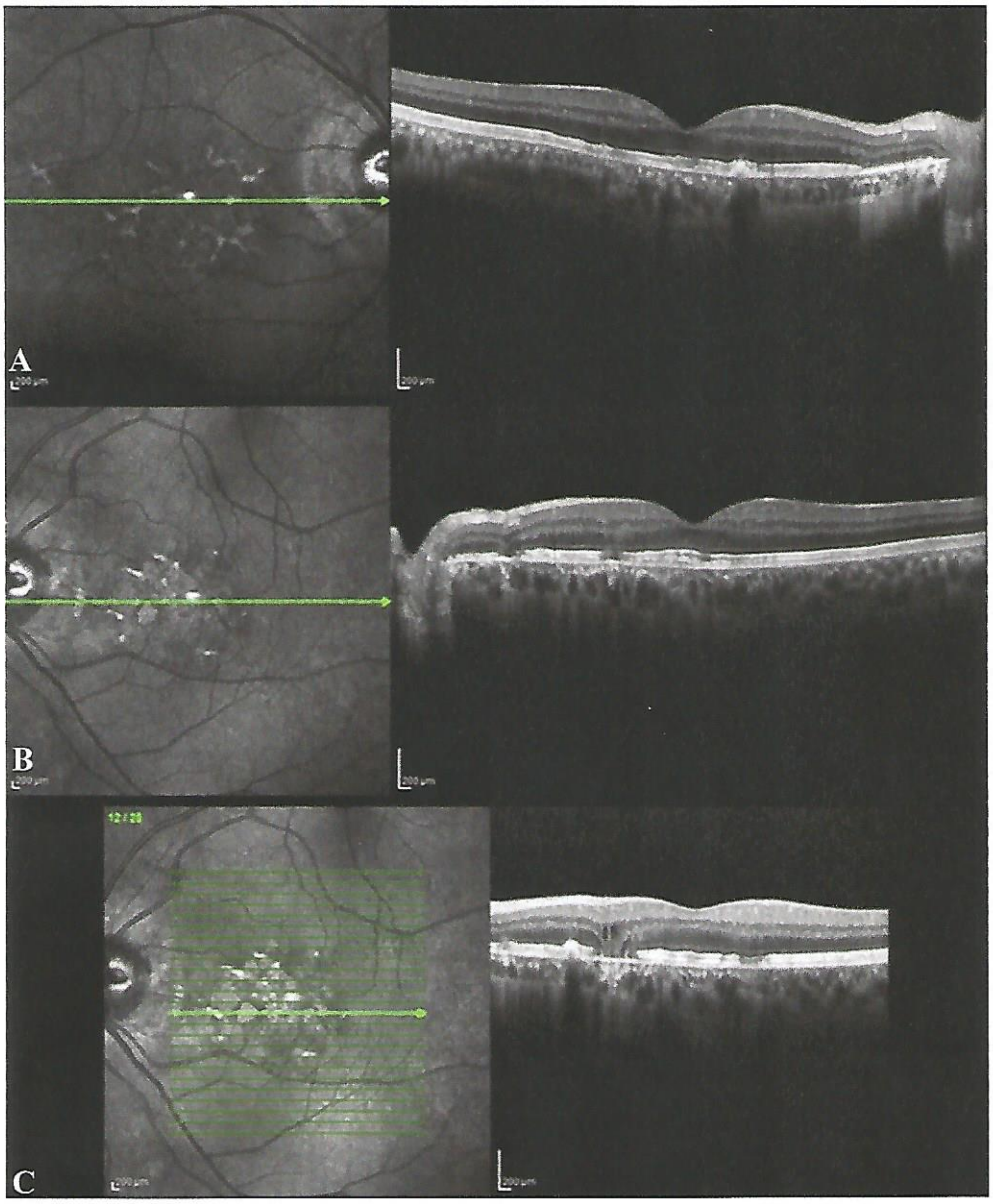

Fig. 2. Spectral-domain optical coherence tomography (SD-OCT) of both eyes. **A.** Cross-sectional SD-OCT image of the right macula shows focal thickening of RPE, with underlying shadowing. **B.** Cross-sectional SD-OCT image of the left macula demonstrates RPE irregularities associated with interruption of the inner segment/outer segment interface and a perifoveal area with absence of the RPE band, loss of photoreceptors and overlying outer retinal thinning. **C.** Cross-sectional SD-OCT image of the left eye shows focal thickening of RPE, with underlying shadowing, besides an area with absence of the RPE band, loss of photoreceptors and overlying outer retinal thinning with microcysts in the inner nuclear layer, and homogenous choroidal hypertransmission.

Response

The main ophthalmic manifestations include optic neuropathy, pupil abnormalities, and ophthalmoplegia. Pigmentary retinopathy is not a known manifestation of CMT syndrome. However, CMT disease is a heterogenous group of inherited peripheral neuropathies with several genetic defects that share clinical characteristics of progressive distal muscle weakness and atrophy, foot deformities, distal sensory loss, and diminished tendon reflexes. An overlap of features of axonal CMT and autosomal-recessive hereditary spastic paraplegia and amyotrophic lateral sclerosis is seen in patients with defects in the *ALS5/SPG11/KIAA1840* gene. Patients with *ALS5/SPG11/KIAA1840* gene defect have a pattern dystrophy of the macula resembling that seen in Kjellin syndrome. This patient's gene testing is pending, but is not clinically known to have features of *SPG11*. Patients with a myotonic dystrophy have a characteristic facial appearance, ptosis, early-onset male pattern baldness, and Christmas tree cataracts. A characteristic feature in such patients is the delay in relaxation of contracted muscles. For example, patients find it difficult to release their grip following a handshake.

The Panel 16 Quantitative Color Vision, Visual Contrast Test System and Pelli–Robson Contrast Sensitivity tests were within normal limits. The

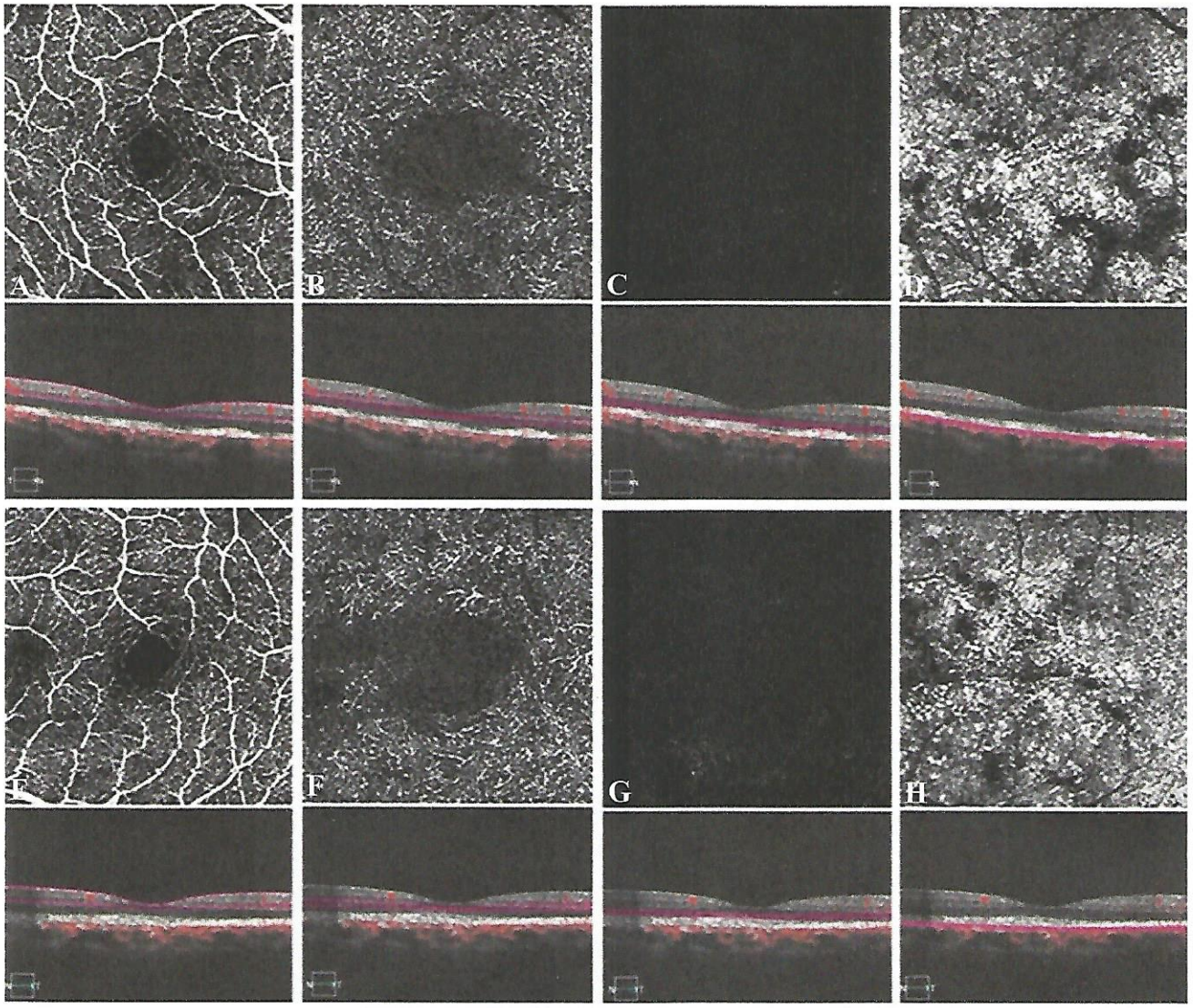

Fig. 3. OCT angiography (3 × 3 mm) of both eyes. **A** and **B.** Analysis of vascular flow through the superficial and deep plexuses reveals a normal capillary network in the right eye. **C.** Angiogram of the outer retina shows absence of vasculature in the right eye. **D.** Choriocapillaris angiogram appears heterogeneous, with black shadowing from retinal vessels in the right eye. **E** and **F.** Although there is a shadow artifact in the nasal portion of the slab, analysis of vascular flow through the superficial and deep plexuses reveals normal capillary network in the left eye. **G.** Angiogram of the outer retina shows absence of vasculature in the left eye. **H.** Choriocapillaris angiogram appears heterogeneous, with black shadowing from retinal vessels in the left eye.

anterior segment was unremarkable, no vitreous cells were noted, and pupillary reflexes were normal.

Optical coherence tomography (OCT) demonstrated focal fragmentation of the ellipsoid zone and interdigitation zone. There were also sites of external limiting membrane discontinuity and outer nuclear layer loss, sometimes with cysts at the inner nuclear layer and outer nuclear layer and RPE/Bruch layer damage, inducing choroidal hypertransmission in both eyes (Figure 2). Peripapillary retinal nerve fiber layer thickness was within normal limits in both eyes. Optical coherence tomography angiography (OCTA) of the superficial and deep plexuses were unremarkable however the OCT angiography revealed heterogeneous flow voids within the choriocapillaris (Figure 3).

Retinal function analysis was obtained by ocular electrophysiologic tests and microperimetry. Full-field electroretinogram (RETIport System, Roland Consult, Brandenburg an der Havel, Germany) was found to be in the normal range. Multifocal electroretinogram (RETIscan System, Roland Consult, Brandenburg an der Havel, Germany) group average waves were within normal limits. However, some traces presented decreased amplitude in both eyes, especially temporal to the fovea (Figure 4). Visual evoked potential (VEP, RETIport System, Roland Consult, Brandenburg an der Havel, Germany) was performed with large 1° stimuli and small 0.15° stimuli. In the right eye, both wave amplitude and latency of N75 and P100 were within the normal range. In the left eye, the wave amplitude was normal, but latency of N75 and P100 were increased by 15%. The parameters tested in the microperimetry examination from MP3 (Nidek Technologies, Padua, Italy) were 33 points, covering a total of 20 central degrees. The arithmetic means of the absolute thresholds in decibels (dB) measured at each point were calculated as the mean retinal sensitivity for each eye. It was 24.75 dB in OD and 25.75 dB in left eye. Microperimetry exhibited small areas of sensitivity reduction in OU, which were topographically correlated with posterior segment findings (Figure 5).

Discussion

CMT disease is defined as a group of inherited motor and sensory neuropathies resulting in distal limb weakness, sensory loss, feet deformities, and decreased deep tendon reflexes. Despite being the most common genetic neuromuscular disorder, it is a rare disease, with a prevalence around 1:2,500. CMT can be caused by a multitude of gene mutations and its clinical course is variable, because the same mutation may result in different phenotypes.[1,2]

CMT disease includes a very broad spectrum of neurologic phenotypes, because it can be caused by different gene mutations.[3–8] It is classified according to the characteristics of the polyneuropathy and its inheritance pattern (Table 1). Within each type of CMT, there are numerous subtypes depending on the gene mutation. Over 90% of patients with CMT have a mutation in the *PMP22*, *MFN2*, *MPZ*, or *GJB1* gene.[2] In the patient being presented, genetic testing is pending. However, a clinical diagnosis of CMT was made based on compatible neurologic manifestations associated with typical electroneuromyography findings (i.e., chronic mixed peripheral polyneuropathy on the

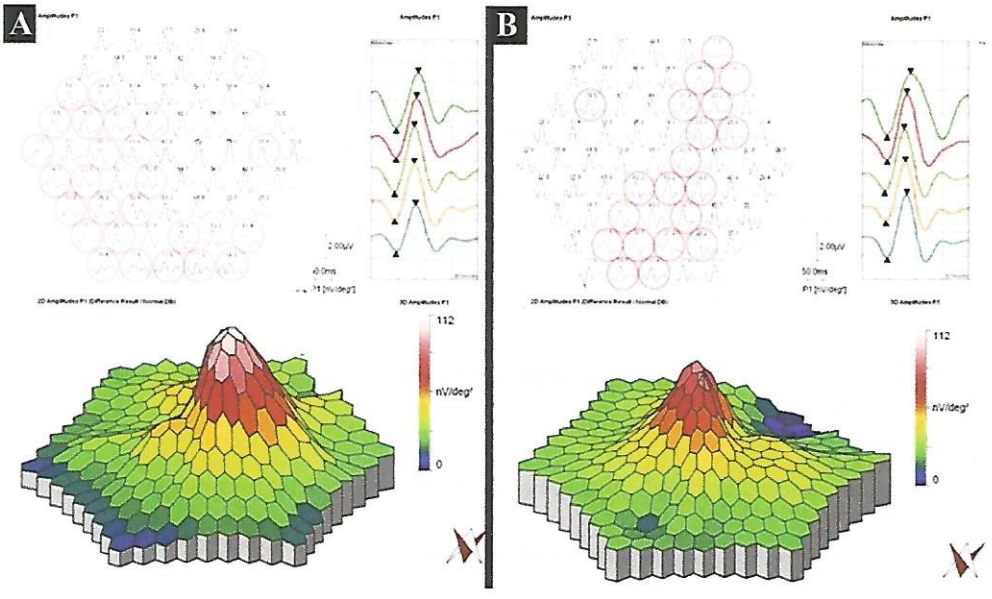

Fig. 4. Multifocal electroretinogram of both eyes. **A.** Right eye: group average waves within normality. Circled in red are the traces with decreased amplitude. **B.** Left eye: group average waves within normal range. Circled in red are the traces with decreased amplitude.

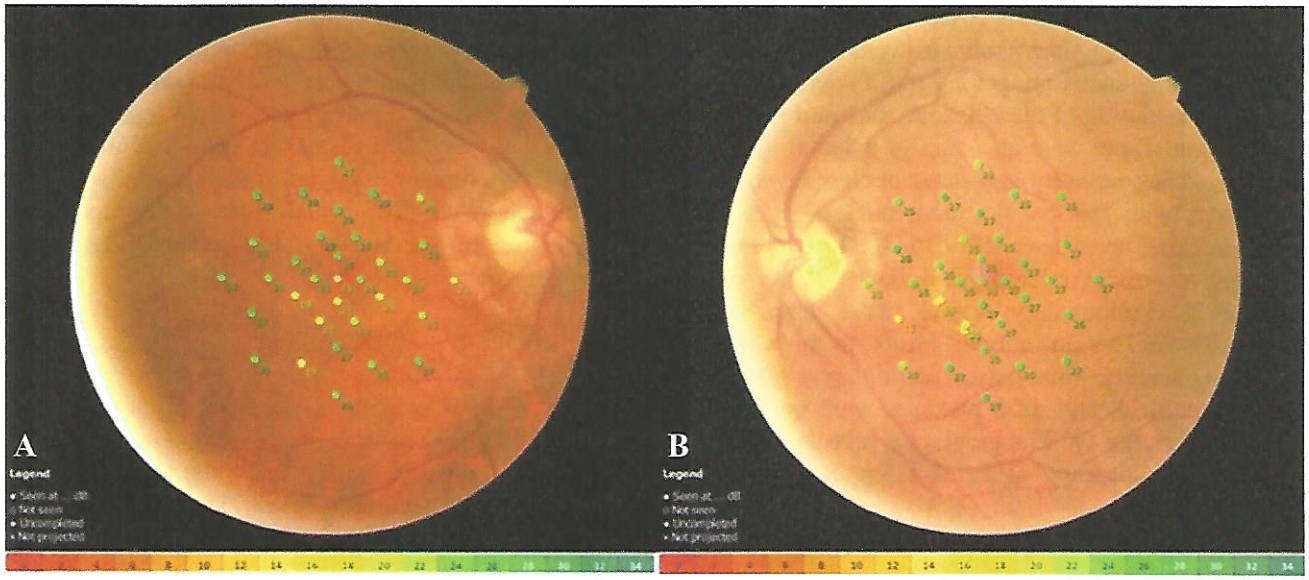

Fig. 5. **A** and **B.** Microperimetry (MP, 20 central degrees) of both eyes. MP exhibited focal reduced retinal sensitivity among corresponding areas of reticular changes in both eyes.

four limbs, more severe on the distal lower ones). It is likely that the patient had an intermediate form of autosomal-recessive CMT with PLEKHG5 deficiency.[9]

The spectrum of ophthalmic manifestations due to CMT is also broad. Gene mutations of known retinal dystrophies, such as mutation in the translation factor Histidyl-tRNA synthetase for Type IIIB Usher Syndrome, can be related to CMT.[10] However, the association between CMT and retinal dystrophies is not very common, and there are only a few cases reported.[11–13] Khoubesserian et al[11] evaluated a patient with CMT and *fundus flavimaculatus* retinal dystrophy. Ophthalmoscopy and fluorescein angiography showed central tapetoretinal degeneration with macular pigment changes and abnormal peripapillary vascular prominence. Reviewing those images, the findings seem to resemble idiopathic type 2 juxta foveolar telangiectasia or macular telangiectasia 2 (Mactel), which may have been a co-occurrence, rather than a real association. Photopic and scotopic electroretinographic recordings and electro-oculogram were normal. On the other hand, Stanescu-Segal and Michiels[12] studied 6 cases of heredotaxia, of which 3 were diagnosed with CMT. All of them had good VA, normal color vision and no perimetry defects. At ophthalmoscopy, two patients had discrete pigmentary changes in the macular area. All these patients, even those with normal fundus presentation, showed impairment on the electroretinogram. There are five other case reports of patients with CMT disease and pigmentary retinopathy evaluated by ophthalmoscopy.

Table 1.

Classification of Charcot–Marie–Tooth Disease

Type	Pathology/Phenotype
CMT1	Predominantly demyelinating polyneuropathy
CMT2	Predominantly axonal polyneuropathy
CMT3	Preferably known as Dejerine–Sottas, it includes a group of severely affected infants with CMT regardless of inheritance pattern or gene mutation
CMT4	Autosomal-recessive inheritance
CMTX	X-linked inheritance
DI-CMT	Dominant-intermediate form due to an intermediate-range slowing of conduction velocities in the arms
HSN	Hereditary sensory neuropathy
HMSN V	Associated with pyramidal involvement
HMSN VI	Associated with optic atrophy
dHMN	Pure motor forms characterized by sparing of sensory nerves on clinical, electrophysiologic, and pathologic examinations

HMSN, Hereditary Motor and Sensory Neuropathy; dHMN, Distal Hereditary Motor Neuropathy.

Although the full-field electroretinogram and multifocal group average waves were normal in this patient, there was mild alteration in some traces, and the visual evoked potential presented discrete increased latency, which could indicate early visual impairment. It is important to highlight that the patient's optic nerve examination was deemed to be within normal limits; and, despite delayed visual evoked potential being considered a hallmark of optic nerve disease, macular diseases can also be related to latency and amplitude changes in visual evoked potential.[14]

Key words: Charcot–Marie–Tooth syndrome, multimodal imaging, polyneuropathy, RPE dystrophy.

Acknowledgments

The authors thank Maria Kiyoko Oyamada MD PhD for performing and analysing electroretinogram exams. The authors thank Alex Haruo Higashi MD, Camila Sayuri Vicentini Otani MD, Daniel de Queiroz Omote MD, Eduardo Ferracioli Oda MD, and Rodrigo Hideharo Sato MD for helping document the case.

References

1. Montecchiani C, Pedace L, Lo Giudice T, et al. ALS5/SPG11/KIAA1840 mutations cause autosomal recessive axonal Charcot-Marie-Tooth disease. Brain 2016;139:73–85.
2. Ramchandren S. Charcot-Marie-Tooth disease and other genetic polyneuropathies. CONTINUUM: Lifelong Learn Neurol 2017;23:1360–1377.
3. Züchner S, De Jonghe P, Jordanova A, et al. Axonal neuropathy with optic atrophy is caused by mutations in mitofusin 2. Ann Neurol 2006;59:276–281.
4. Botsford B, Vuong LN, Hedges TR, III, Mendoza-Santiesteban CE. Characterization of Charcot-Marie-Tooth optic neuropathy. J Neurol 2017;264:2431–2435.
5. Houlden H, Reilly MM, Smith S. Pupil abnormalities in 131 cases of genetically defined inherited peripheral neuropathy. Eye 2008;23:966–974.
6. Kondo D, Shinoda K, Yamashita K, et al. A novel mutation in FGD4 causes Charcot-Marie-Tooth disease type 4H with cranial nerve involvement. Neuromuscul Disord 2017;27:959–961.
7. Pareyson D, Marchesi C. Diagnosis, natural history, and management of Charcot-Marie-Tooth disease. Lancet Neurol 2009;8:654–667.
8. Zerbib J, Querques G, Massamba N, et al. Reticular pattern dystrophy of the retina: a spectral-domain optical coherence tomography analysis. Am J Ophthalmol 2013;156:1228–1237.
9. Azzedine H, Zavadakova P, Planté-Bordeneuve V, et al. PLEKHG5 deficiency leads to an intermediate form of autosomal-recessive Charcot-Marie-Tooth disease. Hum Mol Genet 2013;22:4224–4232.
10. Abbott JA, Guth E, Kim C, et al. The Usher syndrome type IIIB Histidyl-tRNA synthetase mutation confers temperature sensitivity. Biochemistry 2017;56:3619–3631.
11. Khoubesserian P, van Regemorter N, Ohrn-Degueldre O, et al. Charcot-Marie-Tooth disease associated with retinal pigment dystrophy and protanopia. J Neurol 1979;222:1–10.
12. Stanescu-Segal B, Michiels J. Heredoataxia (Spinocerebellar Degeneration), ERG alterations, temporal aspects. Ophthalmologica 1979;178:267–272.
13. François J. Tapetoretinal degenerations in spinocerebellar degenerations (Heredoataxias). Acta Geneticae Medicae et Gemellologiae 1974;23:3–24.
14. Bass SJ, Sherman J, Bodis-Wollner I, Nath S. Visual evoked potentials in macular disease. Invest Ophthalmol Vis Sci 1985;26:1071–1074.

RETINAL HEMORRHAGES IN A PATIENT WITH ACUTE ATAXIA

Frederico Braga Pereira, MD,*†‡ Henrique Soares Dutra Oliveira, MD,‡ Vinícius C. Lima, MD,* Luiz H. Lima, MD,§ Chandrakumar Balaratnasingam, MD,¶** Jose S. Pulido, MD, MS, MPH, MBA,†† Eduardo Cunha de Souza, MD‡‡

*From the *Centro Oftalmológico de Minas Gerais, Belo Horizonte, Minas Gerais, Brazil; †Instituto de Olhos Ciências Médicas de Minas Gerais, Minas Gerais, Brazil; ‡Hospital Julia Kubitschek, Belo Horizonte, Minas Gerais, Brazil; §Department of Ophthalmology, Federal University of São Paulo, São Paulo, Brazil; ¶Center for Ophthalmology and Visual Science, University of Western Australia, Perth, Australia; **Department of Ophthalmology, Sir Charles Gairdner Hospital, Western Australia, Australia; ††Ocular Oncology Service, Wills Eye Hospital, Thomas Jefferson University, Philadelphia, Pennsylvania; and ‡‡Department of Ophthalmology, University of São Paulo, São Paulo, Brazil.*

A 19-year-old woman presented with a 3-day history of acute-onset blurred vision, nausea, vomiting, and hyporexia. Two weeks previously, she underwent a laparoscopic cholecystectomy due to biliary pancreatitis secondary to biliary sludge.

Her visual acuity was measured at count fingers at 2 m. Fundus examination showed bilateral symmetrical signs of diffuse arteriolar narrowing and peripapillary retinal nerve fiber layer (RNFL) thickening. Two large superficial hemorrhages were seen in the right eye along the temporal arcades. The optic disk margins were blurred bilaterally. Optical coherence tomography confirmed the increased thickness of the peripapillary RNFL bilaterally (Figure 1).

Question

What is a likely diagnosis for this presentation?

Response

Given the recent history of gall bladder surgery and pancreatitis, Purtscher-like retinopathy is a likely diagnosis. The retinal manifestations of Purtscher-like retinopathy include cotton wool spots, retinal hemorrhages, and optic disk edema.

She was promptly admitted to the intensive care unit because of severe hypokalemia and hypotension that was initially unresponsive to intravenous hydration. Neurological assessment revealed multidirectional torsional nystagmus and limb ataxia.

Comment

Ataxia and nystagmus are not associated with Purtscher-like retinopathy; therefore, an alternative diagnosis must be sought.

The patient is 18-week pregnant.

Question

How does this alter the management?

Response

Hyperemesis gravidarum is characterized by excessive nausea and vomiting during pregnancy. Although most common in first trimester, it can extend throughout the entire pregnancy in some women. Rarely, Wernicke encephalopathy, because of hyperemesis gravidarum, can result in the triad of signs including confusion, ocular abnormalities, and ataxia. Depleted thiamine levels need to be excluded.

Cranial computed tomography and computed tomography angiography were unremarkable. The cerebrospinal fluid was assessed after lumbar puncture and did not contain inflammatory cells. The cerebrospinal fluid opening pressure at the time of lumbar puncture was also normal. Serologic testing demonstrated reduced thiamine levels (1.3 μg/dL; normal range: 2.5–7.5 μg/dL). Prompt treatment with parenteral high doses of thiamine dramatically improved the bilateral visual acuity and systemic symptoms. Four weeks after treatment, the fundus signs recovered (Figure 2); the visual acuity levels were 20/25 in the right eye and 20/20 in the left eye.

None of the authors has any financial/conflicting interests to disclose.

Reprint requests: Frederico B. Pereira, MD, Rua Joaquim Linhares, 207, Apt. 1502, 30310-400 Belo Horizonte, Minas Gerais, Brazil; e-mail: retinafrederico@gmail.com

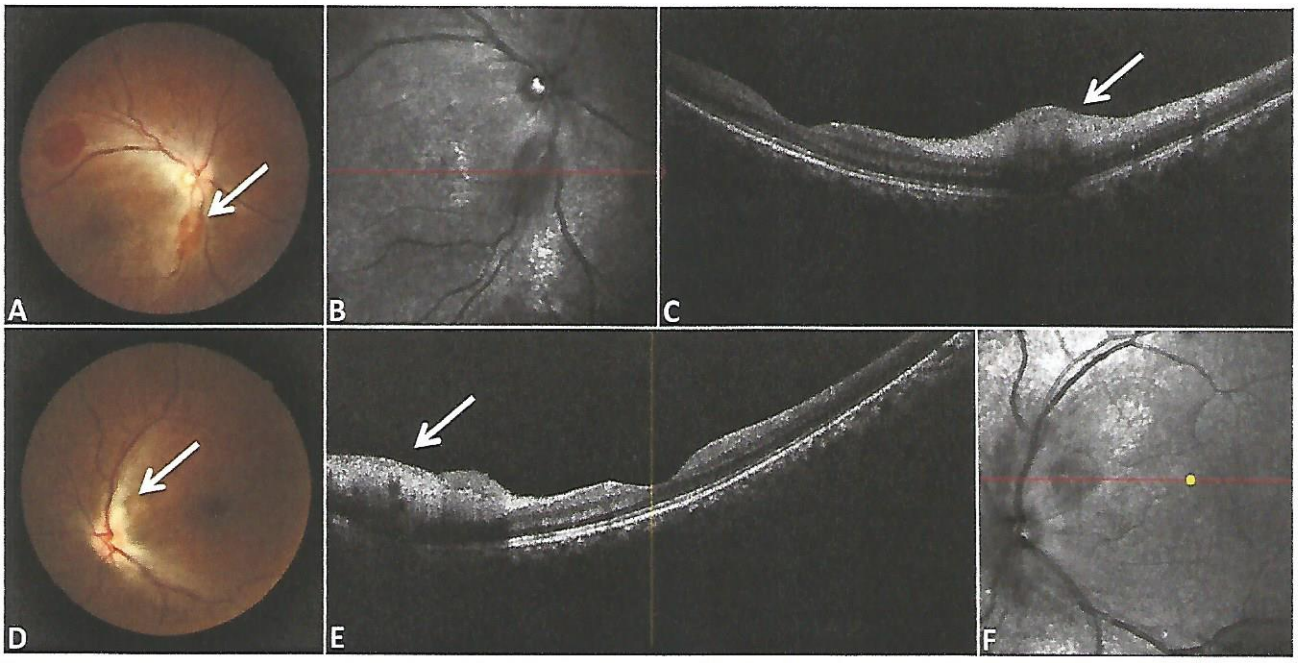

Fig. 1. A. Color photograph (right eye) shows the slightly blurred optic disk margins, diffuse arteriolar narrowing, a preretinal hemorrhage, and superficial hemorrhage adjacent to the optic disk (arrow). **B.** Infrared image shows an intraretinal hemorrhage. **C.** Optical coherence tomography (OCT) scan of the right eye shows an intraretinal hemorrhage (arrow) and thickening of the peripapillary retinal nerve fiber layer (RNFL). **D.** Color photograph (left eye) shows slightly blurred optic disk margins and RNFL thickening (arrow). **E.** Optical coherence tomography scan (left eye) shows thickening of the peripapillary RNFL (arrow) adjacent to the optic disk. **F.** Infrared image shows thickening of the peripapillary RNFL.

Discussion

Optic neuritis and retinal hemorrhages from thiamine deficiency is not in the usual differential list for retina specialists. This case is sobering because it is a treatable disease that might be easily missed.

Chiossi et al,[1] who reviewed 49 cases of Wernicke encephalopathy caused by hyperemesis gravidarum,

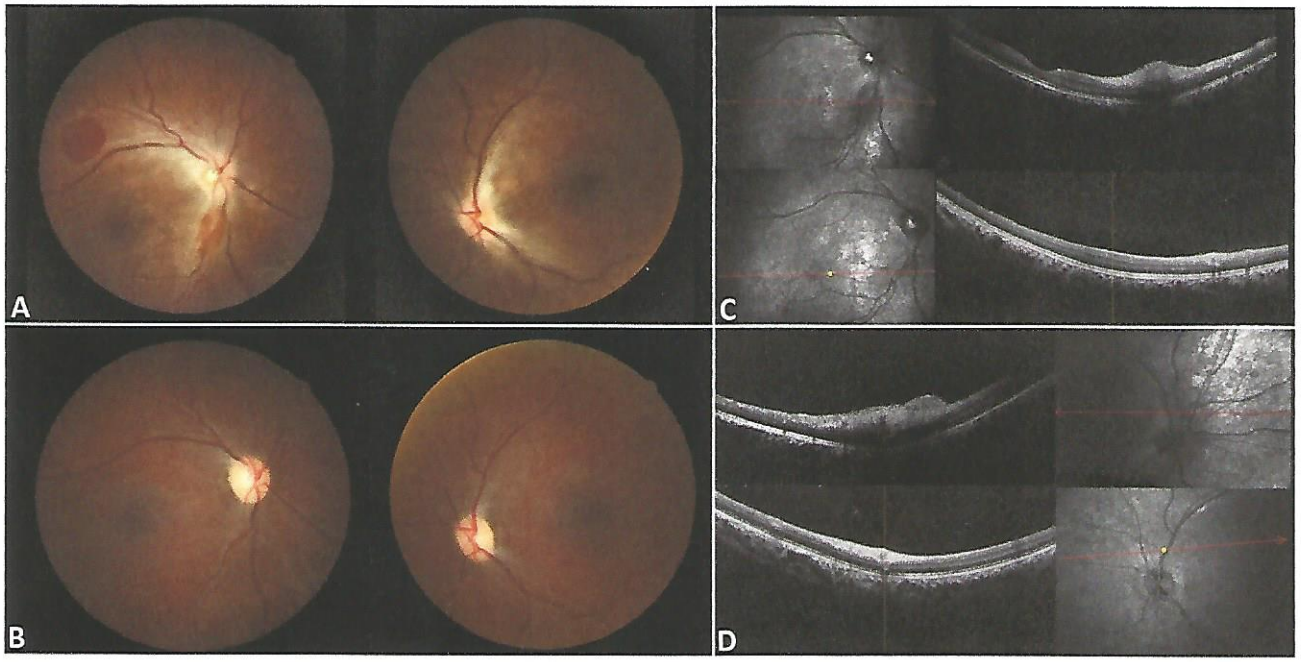

Fig. 2. A. Color photographs of both eyes before treatment. **B.** Color photographs of both eyes 4 weeks after treatment shows recovery of the fundus signs. **C.** Optical coherence tomography images of the right eye before treatment (top image) and 4 weeks after treatment (bottom image); recovery of both the intraretinal hemorrhages and the increased thickness of the peripapillary RNFL is seen. **D.** Optical coherence tomography images of the left eye before treatment (top image) and 4 weeks after treatment (bottom image) show recovery of the increased thickness of the peripapillary RNFL.

reported that Wernicke's classic triad (i.e., confusion, ocular abnormality, and ataxia) was present in only 46.9% of the patients. Those authors also reported a case of Wernicke encephalopathy secondary to severe hyperemesis gravidarum in which ophthalmoscopy revealed bilateral disk swelling and retinal hemorrhages.

Few reports have documented the funduscopic signs in Wernicke encephalopathy.[1–4] Optic disk edema is rare in this pathology, and retinal hemorrhages without optic disk edema occur more frequently.[4] The mechanism of the development of optic disk edema in this condition is poorly understood. In the current case, the optic disk margins were blurred and optical coherence tomography showed peripapillary RNFL thickening bilaterally, despite no objective evidence for increased intracranial pressure. Mumford[2] suggested that these findings might result from the occurrence of the typical neuropathological features of Wernicke encephalopathy, characterized by necrosis of nerve cells and subsequent edema within the optic nerve. Bohnsack and Patel[3] hypothesized that mitochondrial dysfunction first causes the swelling, telangiectasia, and hemorrhages of the RNFL, which was seen in the current case, and that optic disk swelling appears only if mitochondrial damage is severe and prolonged.

Left untreated, patients with Wernicke's encephalopathy can progress to neuronal death and permanent sequelae. There is no consensus on the optimal dose of thiamine, its form of preparation, treatment duration, or the number of daily doses.[5] A recommended regimen is 500 mg of thiamine intravenous infused over 30 minutes three times daily for 2 consecutive days and 250 mg intravenous or IM once daily for an additional 5 days, in combination with other B vitamins. It is mandatory that thiamine be given before or concomitantly with intravenous administration of glucose when a diagnosis of Wernicke encephalopathy is suspected because glucose alone can precipitate the disorder in thiamine-deficient individuals.[5] Parenteral thiamine administration is inexpensive, simple, effective, and generally safe, and adverse reactions, including anaphylaxis and bronchospasm, are reported but extremely rare.[5]

The current case is unusual in that visual impairment was the first symptom of an evolving thiamine deficiency secondary to severe hyperemesis gravidarum. Fundus signs were diffuse arteriolar narrowing, peripapillary RNFL thickening, superficial hemorrhages along the temporal arcades, and blurred optic disk margins bilaterally. Despite the scarce information in the literature, patients with suspicion of thiamine deficiency should undergo an emergent funduscopic examination independent of the presence of visual symptoms.

Key words: optical coherence tomography, retinal hemorrhages, retinal nerve fiber layer thickening, Wernicke encephalopathy.

References

1. Chiossi G, Neri I, Cavazzuti M, et al. Hyperemesis gravidarum complicated by Wernicke encephalopathy: background, case report, and review of the literature. Obstet Gynecol Surv 2006;61:255–268.
2. Mumford CJ. Papilloedema delaying diagnosis of Wernicke's encephalopathy in a comatose patient. Postgrad Med J 1989;65:371–373.
3. Bohnsack BL, Patel SS. Peripapillary nerve fiber layer thickening, telangiectasia, and retinal hemorrhages in Wernicke encephalopathy. J Neuroophthalmol 2010;30:54–58.
4. Cogan DG, Victor M. Ocular signs of Wernicke's disease. AMA Arch Ophthalmol 1954;51:204–211.
5. Galvin R, Bråthen G, Ivashynka A, et al. EFNS guidelines for diagnosis, therapy and prevention of Wernicke encephalopathy. Eur J Neurol 2010;17:1408–1418.

AN ASYMPTOMATIC CHILD WITH A JUXTAPAPILLARY LESION: DIAGNOSTIC CONUNDRUM

Carlos A. Moreira-Neto, MD, PhD,*† Carlos A. Moreira, Jr., MD, PhD,* Mario J. Nobrega, MD, PhD,‡ Luiz H. Lima, MD,§ Chandrakumar Balaratnasingam, MD,¶** Jose S. Pulido, MD, MS, MPH, MBA,†† Eduardo C. Souza, MD, PhD‡‡

*From the *Hospital de Olhos do Paraná, Curitiba, PR, Brazil; †Positivo University, Curitiba, PR, Brazil; ‡Hospital de Olhos Sadalla Amin Ghanem, Joinville, SC, Brazil; §Department of Ophthalmology, Federal University of São Paulo, São Paulo, Brazil; ¶Center for Ophthalmology and Visual Science, University of Western Australia, Perth, Australia; **Department of Ophthalmology, Sir Charles Gairdner Hospital, Western Australia, Australia; ††Wills Eye Hospital, Thomas Jefferson University, Philadelphia, Pennsylvania; and ‡‡Universidade de São Paulo, São Paulo, SP, Brazil.*

A 12-year-old female child was referred for a second opinion concerning a juxtapapillary lesion in the left eye. The presumptive diagnosis of the lesion by the referring physician was choroidal hemangioma and the patient, on presentation, had already received three treatments of intravitreal bevacizumab (Avastin, Genentech Inc, South San Francisco, CA) with no response. The lesion had also been treated with full-fluence photodynamic therapy with no response. The juxtapapillary lesion was incidentally detected by the referring physician upon routine eye assessment. The patient had no visual symptoms.

On presentation to our service, the visual acuity in the right eye was 20/20 with −4.00 diopters (D) of myopia and the visual acuity of the left eye was 20/30 with −5.00 D of myopia. Dilated examination of the right eye was unremarkable. Left retinal assessment revealed a flat, yellow, juxtapapillary lesion adjacent to the temporal and inferior margins of the optic disk (Figure 1A). Fluorescein angiography revealed early hyperfluorescence at the disk margin that increased in intensity toward the late frames (Figure 1, B and C). Ultrasound showed low reflectivity at the lesion site (Figure 2). Optical coherence tomography (OCT) through the optic disk did not identify an optic pit (Figure 3A). Optical coherence tomography through the lesion and the macula (Figure 3B) revealed intraretinal fluid in the central macula as well as absence of choroidal tissue. The boundaries of the optic disk, retinal pigment epithelium (RPE) tissue, choroidal tissue, and subretinal fluid within the juxtapapillary lesion are clarified in Figure 4, A and B. Figure 4, C and D shows a scan acquired below the inferior optic disk border where the area of choroidal tissue abnormality and subretinal fluid appears exaggerated. These features are also portrayed in three-dimension in Figure 4E. Optical coherence tomography angiography did not reveal choroidal flow signals within the juxtapapillary lesion (Figure 5).

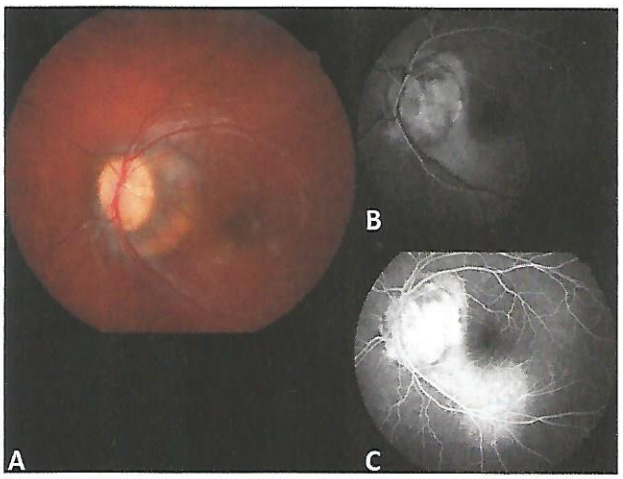

Fig. 1. A. Color fundus photograph of the left eye shows a large orange color lesion at the temporal and inferior edges of the optic disk. **B.** Fluorescein angiography of the left eye shows an early hyperfluorescent lesion in the vicinity of the optic disk. **C.** A hyperfluorescent window defect in the inferior temporal arcade region is evident in the later frames of the angiogram.

None of the authors has any financial/conflicting interests to disclose.

Reprint requests: Carlos A. Moreira-Neto, MD, PhD, Hospital de Olhos do Paraná, Rua Coronel Dulcício, 199, 3rd Floor, 80420-170 Curitiba, PR, Brazil; e-mail: camoreiraneto@gmail.com

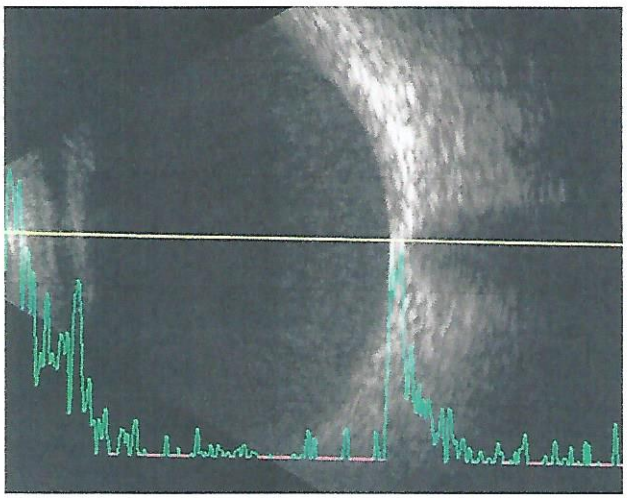

Fig. 2. Ultrasonography of the left eye shows low reflectivity at the topography of the lesion seen on color fundus photograph.

On the basis of the above imaging features, we felt that the juxtapapillary lesion was most likely within the spectrum of focal choroidal excavation and not a choroidal hemangioma. We elected to withhold further intravitreal therapy and photodynamic therapy. Over the course of 4 years, there has not been an appreciable change in the lesion size nor has the patient developed any new visual symptoms. We placed the patient on topical dorzolamide drops three times a day for 3 years to treat the cystic changes of the central macula with no effect.

Discussion

Focal choroidal excavation is a well-recognized entity that can be complicated by neovascular membranes, polyps, and less often by macular schisis or macular edema.[1–3] A focal choroidal excavation also can occur in isolation or be associated with some choroidal tumors, such as a choroidal osteoma or a sessile type of a retinal capillary hemangioblastoma.[4,5] In this case, B-scan ultrasonography and OCT did not demonstrate choroidal ossification, thereby excluding osteoma. Likewise, color imaging and fluorescein angiography were able to definitively exclude a capillary hemangioblastoma.

Few publications have reported an association between focal choroidal excavation and central serous chorioretinopathy.[6] Despite the presence of intraretinal and subretinal fluids on OCT images, the current patient did not show hyperfluorescent dots on fluorescein angiography, which ruled out central serous chorioretinopathy.

In 2013, Yeh et al described the features of peripapillary choroidal cavitation. Images in that report shared some features with our case as seen on color photography and OCT.[7] Similar to a choroidal excavation, a choroidal cavitation occurs more frequently in myopic patients. However, choroidal cavitations are typically found in an older age group. A study to emerge from Taiwan[3] revealed that the mean patient age with this entity was 47.9 ± 12.3 years.

The morphology and location of the RPE with respect to the choroid was an important distinguishing feature between our case and that of choroidal cavitation. Specifically, in our case, RPE tissue was separated from the photoreceptors and was seen to adhere to the inner part of the choroid even at sites where choroidal tissue was absent. By contrast, in choroidal cavitation, there is no separation between photoreceptors and the RPE as the abnormality lies within the choroid.

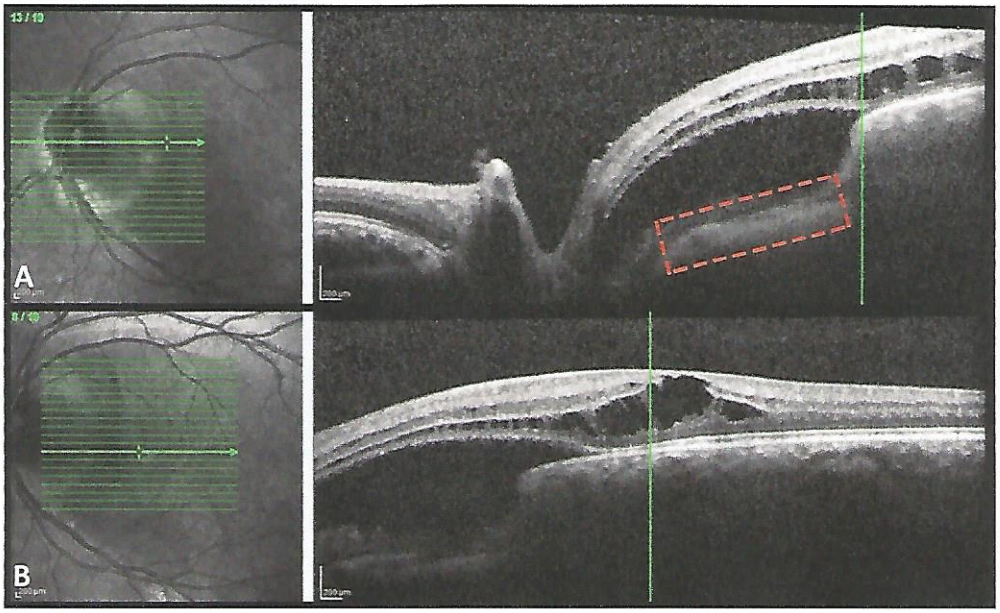

Fig. 3. A. B-scan OCT of the left eye through the optic disk and the lesion seen on *red-free* image does not show optic disk pit, but a hyperreflective line at the bottom that seems to represent the RPE (dashed red rectangle). **B.** B-scan OCT of the left eye within the macular area demonstrates the presence of intraretinal fluid, and absence of the choroid was observed at the topography of the lesion seen on *red-free* image.

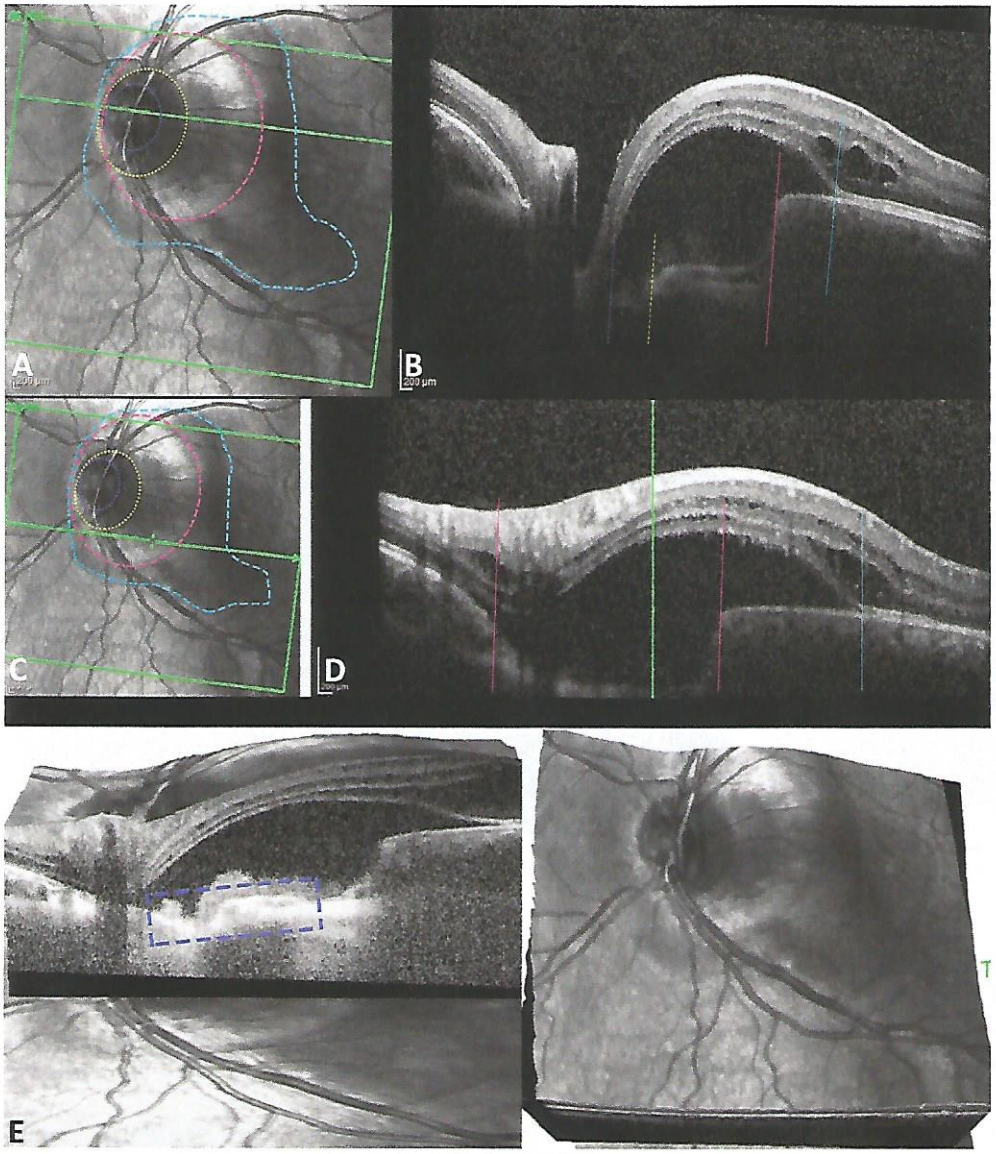

Fig. 4. A. Near-infrared image of the left eye. The red dashed ellipse represents the optic disk edges. The turquoise dashed ellipse indicates the area of the RPE absence. Choroidal excavation is defined by the area between turquoise ellipse and violet ellipse. The orange dashed line demonstrates the presence of subretinal fluid. The horizontal green line represents the B-scan OCT shown on (**B**). **B.** B-scan OCT of the left eye. The red dashed line represents optic disk temporal edge. The area between the red and turquoise vertical dashed lines does not show RPE. A possible area of choroidal excavation is observed the between turquoise and violet dashed lines. The orange dashed line depicts the extension of the subretinal fluid. **C.** Near-infrared image of the left eye highlights a different area of interest as shown in panel. **D.** The area of choroidal excavation is limited by two violet dashed lines and is noted to be greater in this region. **E.** Three-dimensional OCT image of the left eye shows that the RPE (dashed rectangle) follows the choroidal malformation.

We also considered the diagnosis of an optic disk pit; however, OCT did not reveal any observable malformations within the optic disk nor did it identify a communication between the subretinal space and vitreous. We also considered a diagnosis of choroidal coloboma; however, that congenital abnormality typically involves the inferior and not the temporal portions of the optic disk.

Commentary From Dr. Pulido

The authors present a case of a juxtapapillary hypolucent area on OCT. They have a broad differential, which included a choroidal coloboma but excluded that because colobomas typically are present at the 6 o'clock position where the embryologic fissure meets. Although this is true, their anomaly looks like the RPE stops abruptly and does not extend to the disk by photography clockwise from 1,230 to 7. The next question that arises is where is the edge of the optic nerve? From the color photographs, it looks like the nerve is ovoid and larger temporally than nasally. Closer examination of the fundus photographs shows that the "pink" part of the temporal disk is actually quite small and what one is really seeing is bare sclera without overlying RPE or choroid. This observation is further justified by Figure 1B, where the RPE edge is well seen temporally as an edge that has blocking fluorescence and some staining. Between that and the disk, there are some deep choroidal vessels seen at one o'clock. Now, one can see the staining of the actual temporal edge of the optic nerve. On OCT, one can see the temporal edge of the RPE that correlates and confirms the fundus appearance that the RPE is quite temporal to the disk. The RPE is needed for choroidal development and thus the choroid

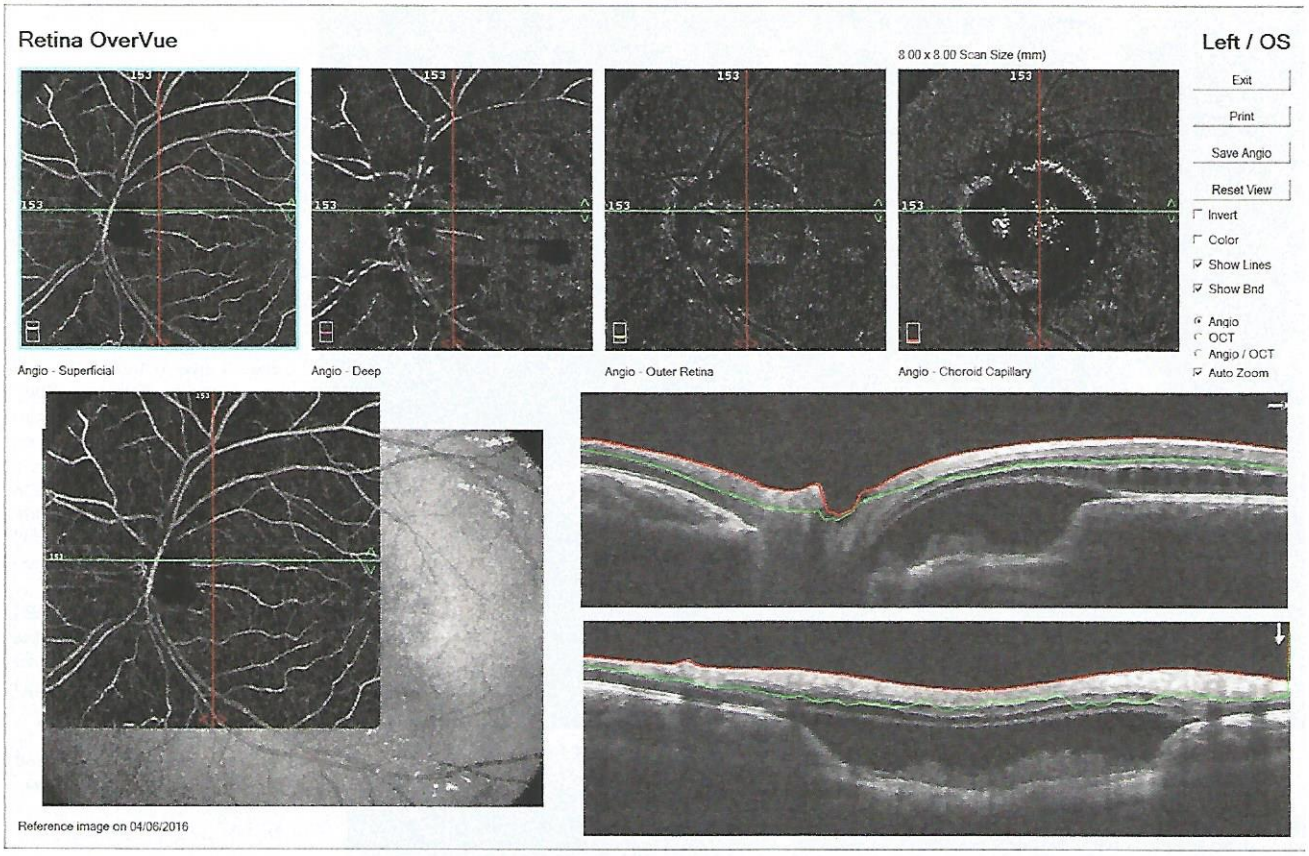

Fig. 5. Optical coherence tomography angiography of the left eye with segmentation slabs. Flow signals are not observed at within the area of juxtapapillary abnormality.

is just an anlage nasal to the RPE. Furthermore, the disk is quite attenuated temporally. Furthermore, the OCT looks exactly like the OCT described in previous atypical cases of coloboma.[8,9] So, in summary, I think that this is a congenital malformation of the RPE and underlying choroid. It is probably in the spectrum of colobomatous changes of the optic nerve.

Key words: choroidal coloboma, choroidal excavation, multimodal imaging, optical coherence tomography angiography.

References

1. Margolis R, Mukkamala SK, Jampol LM, et al. The expanded spectrum of focal choroidal excavation. Arch Ophthalmol 2011;129:1320–1325.
2. Chowdhury M, Rishi P. Juxtapillary choroidal excavation with polypoidal choroidal vasculopathy: an unusual association. Indian J Ophthalmol 2019;67:401–403.
3. Hsu CK, Liu CC, Chen JT, Chang YH. Foveoschisis with focal choroidal excavation. Taiwan J Ophthalmol 2014;4:189–190.
4. Pierro L, Marchese A, Gagliardi M, et al. Choroidal excavation in choroidal osteoma complicated by choroidal neovascularization. Eye 2017;31:1740–1743.
5. Kase S, Ishida S. Photocoagulation for juxtapapillary retinal hemangioma in a young girl: a case report. Mol Clin Oncol 2019;10:521–523.
6. Ellabban AA, Tsujikawa A, Ooto S, et al. Focal choroidal excavation in eyes with central serous chorioretinopathy. Am J Ophthalmol 2013;156:673–683.
7. Yeh SI, Chang WC, Wu CH, et al. Characteristics of peripapillary choroidal cavitation detected by optical coherence tomography. Ophthalmology 2013;120:544–552.
8. Nakano Y, Miki A, Honda S, Nakamura M. Polypoidal choroidal vasculopathy associated with optic disc coloboma. Case Rep Ophthalmol 2018;9:92–95.
9. Chen Y, Ma X, Hua R. Multi-modality imaging findings of huge intrachoroidal cavitation and myopic peripapillary sinkhole. BMC Ophthalmol 2018;18:24.

CRYSTALLINE RETINOPATHY IN A MAN WITH PERIPHERAL NERVE SHEATH TUMORS

Luiz F. Teixeira, MD,*† Eliana M. M. Caran, MD,† Monique K. Mangeon, MD,†
Luiz H. Lima, MD,* Chandrakumar Balaratnasingam, MD,‡§ David Sarraf, MD, PhD,¶
Rodrigo L. Meirelles, MD*

*From the *Department of Ophthalmology, Federal University of São Paulo (UNIFESP), São Paulo, Brazil; †Pediatric Oncology Institute Federal University of São Paulo, São Paulo, Brazil; ‡Center for Ophthalmology and Visual Science, University of Western Australia, Perth, Australia; §Department of Ophthalmology, Sir Charles Gairdner Hospital, Western Australia, Australia; and ¶Stein Eye Institute, University of California, Los Angeles, Los Angeles, CA.*

A 27-years-old male presented with bilateral blurred vision over the course of 1 month. The best-corrected visual acuity was 20/30 in the right eye and 20/50 in the left eye. Fundus examination showed peri-macular intraretinal crystalline lesions in both eyes (Figure 1). The patient's medical history was positive for longstanding peripheral nerve sheath tumors.

Question—What is the differential diagnoses for this presentation?

Response—The differential diagnosis of crystalline retinopathy is broad. One of the common causes of this presentation includes macular telangiectasia Type 2. Drug-related toxicity due to tamoxifen, canthaxanthine, nitrofurantoin, talc, and methoxyflurane can also produce this clinical picture. Systemic disease can also manifest crystalline retinopathy and these include Sjogren–Larsson syndrome, cystinosis, and primary hyperoxaluria. Excessive intake of Kola nuts may or may not be associated with West African crystalline maculopathy and this refractile disorder occurs only in patients of West African descent and is not typically associated with vision loss.

Peripheral retinal examination demonstrated crystal deposits in the peripheral retina of the right eye (Figure 2).

Question—Does peripheral retina involvement aid in the differential diagnosis of this case?

Response—Rarely, crystalline maculopathies can be associated with peripheral retinal crystals. Tamoxifen retinopathy is one of the unique disorders in which crystalline retinal deposits can be identified both in the posterior pole and in the far periphery.

Hyperreflective lesions in the inner and outer retinal layers were noted on spectral-domain optical coherence tomography in both eyes (Figure 3).

Question—Do the location of crystals within the retina vary between retina diseases?

Response—The location of crystals within retina layers can aid in the diagnosis. Tamoxifen maculopathy is remarkable for a deposition of crystals, in a donut-ring around the fovea, more commonly at the level of the nerve fiber layer and inner plexiform layer. Although canthaxanthine maculopathy can also be associated with inner retinal crystals, the ring of deposition is usually wider with a predilection for the papillomacular bundle. Cystinosis and oxalosis demonstrate deposition of crystals in all retinal layers, whereas talc retinopathy is associated with exclusively intravascular deposits. In macular telangiectasia Type 2, the crystals are predominantly identified as a small cluster in the inner retina within the foveal region.

The patient's past medical history was remarkable for NF1 (sporadic mutation) diagnosed 12 years before presentation. During this period, the patient developed hundreds of peripheral nerve sheath tumors throughout the body (Figure 4). High-dose tamoxifen therapy (150 mg/day) was prescribed for an extended period to

None of the authors has any financial/conflicting interests to disclose.

Reprint requests: Luiz F. Teixeira, MD, Federal University of São Paulo (UNIFESP), Rua Botucatu, 821, Vila Clementino, São Paulo, Brazil, 04023-062; e-mail: luizfteixeira@hotmail.com

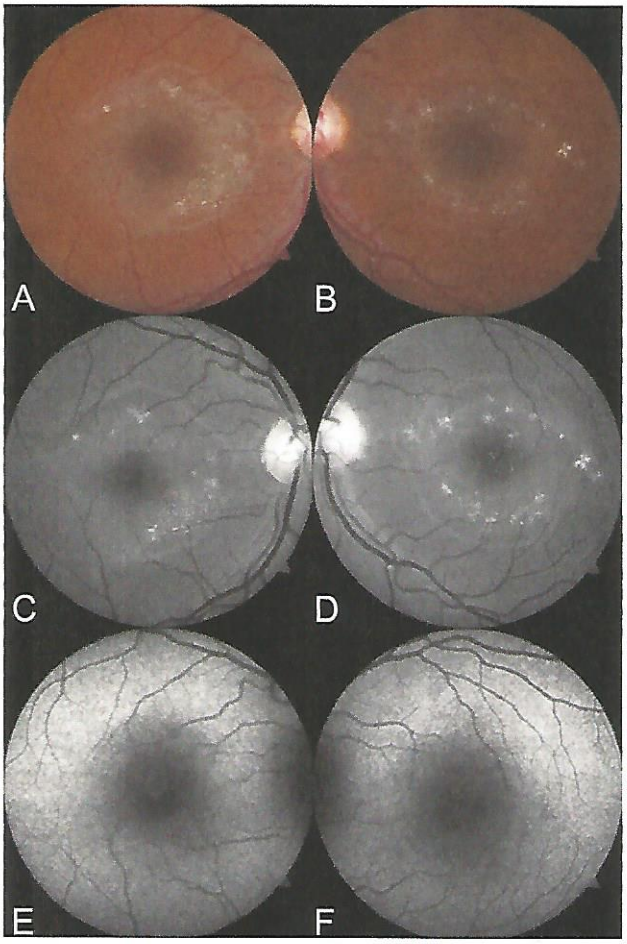

Fig. 1. A and **B.** Color fundus photographs show perimacular yellowish refractile deposits in both eyes. **C** and **D.** Red-free fundus photographs illustrate bilateral perimacular crystalline deposits in both eyes. **E** and **F.** Fundus autofluorescence of both eyes shows increased macular hypoautofluorescence.

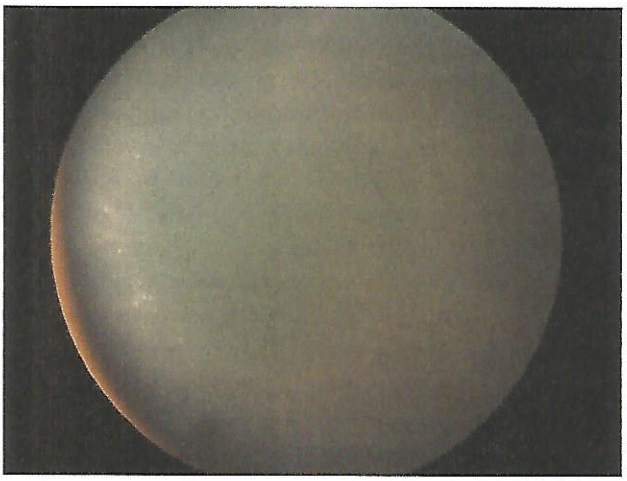

Fig. 2. Color photography of the right eye demonstrates the same refractile deposits in the temporal periphery.

control tumor growth and development. The patient had received a cumulative dose of 122 g of tamoxifen when he presented with visual complaints.

Comment

Tamoxifen toxicity can involve other ocular structures resulting in keratopathy, cataract, and optic neuritis. cystoid macular edema, with petaloid leakage with fluorescein angiography, can be noted in very severe cases. These complications also need to be excluded in patients with tamoxifen retinopathy.

In this case, tamoxifen was discontinued and 6 months later the visual acuity improved to 20/25 in the right eye and to 20/40 in the left eye. The crystalline lesions remained stable in both eyes in the macular area and in the peripheral retina in the right eye. No macular edema, retinal atrophy, or foveal cavitation developed during the follow-up period.

Discussion

Kaiser–Kupfer and Lippman[1] in 1978 first described retinal toxicity from tamoxifen. Studies have reported prevalence rates between 1.5% and 11.8% in patients with breast cancer adjuvantly treated with tamoxifen.[2] Tamoxifen crystalline retinopathy is generally encountered in patients receiving high daily and cumulative doses of the drug or treatment for a long period of time however the threshold at which retina toxicity occurs remains to be determined. The pathophysiology of tamoxifen retinopathy is not completely clear but axonal degeneration after formation of retinal deposits and lipid drug complexes has been proposed.[3] Tamoxifen is known to be toxic to Muller cells and the pathophysiology of crystalline retinal deposition may be similar to Mac Tel 2.[3]

The retinopathy due to tamoxifen can be unilateral or bilateral with a broad spectrum of disease severity. Macular refractile deposits associated with cystoid macular edema typically develops in patients exposed to very high cumulative chemotherapeutic doses of tamoxifen with daily dosages between 100 and 200 mg daily.[4] Cystic foveal cavitation associated with focal ellipsoid zone loss, similar to Mac Tel 2 and in the absence of marked crystalline deposition, is very rare and is associated with low daily dosages of tamoxifen, typically 20 mg daily, used for adjuvant breast cancer therapy.[5,6]

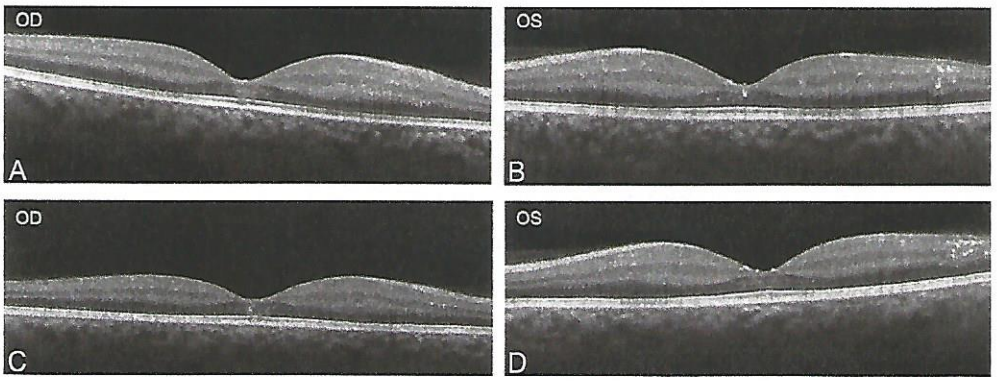

Fig. 3. A and **B.** Spectral-domain optical coherence tomography of both eyes shows hyperreflective lesions at all levels of the sensory retina, which is more remarkable in left eye. Follow-up Spectral-domain optical coherence tomography 6 months after the tamoxifen was discontinued illustrates stable lesions in the right (**C**) and left (**D**) eyes.

Fig. 4. Total body magnetic resonance imaging depicts hundreds of superficial and deep peripheral nerve sheath tumors throughout the body.

Key words: crystalline retinopathy, neurofibromatosis, optical coherence tomography, tamoxifen.

References

1. Kaiser-Kupfer MI, Lippman ME. Tamoxifen retinopathy. Cancer Treat Rep 1978;62:315–320.
2. Noureddin BN, Seoud M, Bashshur Z, et al. Ocular toxicity in low-dose tamoxifen: a prospective study. Eye (Lond) 1999;13:729–733.
3. Kovach JL, Isildak H, Sarraf D. Crystalline retinopathy: unifying pathogenic pathways of disease. Surv Ophthalmol 2019;64:1–29.
4. Rahimy E, Sarraf D. Bevacizumab therapy for tamoxifen-induced crystalline retinopathy and severe cystoid macular edema. Arch Ophthalmol 2012;130:931–932.
5. Bourla DH, Sarraf D, Schwartz SD. Peripheral retinopathy and maculopathy in high-dose tamoxifen therapy. Am J Ophthalmol 2007;144:126–128.
6. Lee S, Kim HA, Yoon YH. OCT angiography findings of tamoxifen retinopathy: similarity with macular telangiectasia type 2. Ophthalmol Retina 2019;3:681–689.

VITREOUS HEMORRHAGE IN A PATIENT WITH POLYNEUROPATHY

Annelise N. Gonçalves, MD,* Luiz H. Lima, MD,†
Chandrakumar Balaratnasingam, MD,‡§ Anita Agarwal, MD,¶ Rodrigo Jorge, MD*

*From the *Department of Ophthalmology, Ribeirão Preto School of Medicine, University of São Paulo, Ribeirão Preto/São Paulo, Brazil; †Department of Ophthalmology, Federal University of São Paulo, São Paulo, Brazil; ‡Center for Ophthalmology and Visual Science, University of Western Australia, Perth, Australia; §Department of Ophthalmology, Sir Charles Gairdner Hospital, Western Australia, Australia; and ¶West Coast Retina, San Francisco, California.*

A 77-year-old white man with a long-standing history of paresthesias and hypesthesias involving the upper and lower limbs presented with an 8-month history of floaters in both eyes. His ophthalmic history was positive for cataract surgery in both eyes. At presentation, his best-corrected visual acuity was 20/20 in his right eye and 20/30 in his left eye. Intraocular pressures were normal. Slit-lamp biomicroscopy was unremarkable with no evidence of anterior segment neovascularization (NVE). Posterior segment examination revealed peripheral retinal microangiopathy with multiple microaneurysms, dot hemorrhages and vitreous opacities in both eyes. Left eye fundus examination revealed vitreous hemorrhage. Fluorescein angiography showed large areas of nonperfusion in the periphery with multiple microaneurysms, capillary telangiectasias, small NVEs elsewhere, and patchy hypofluorescence from blockage from vitreous opacities and blood (Figure 1).

Question—What are the likely causes for this presentation?

Response—The most common causes of bilateral microangiopathy and vitreous hemorrhage include systemic diseases such as diabetes mellitus, systemic hypertension, sickle cell disease, possibly Eales disease or other retinal vasculitis such as systemic lupus erythematosus. Retinal vein occlusion(s), ocular ischemic syndrome, and less commonly anemic retinopathy, hypercoagulable/hyperviscosity states, and radiation retinopathy can also present with a similar picture.

A diagnostic work-up for the above and infectious conditions was negative. Spectral domain optical coherence tomography revealed needle-shaped deposits perpendicular to the vitreoretinal interface in the fovea of the left eye and irregular retinal atrophy temporal to the macula in both eyes (Figure 2).

Question—Do the OCT findings aid the diagnosis?

Response—Vertically oriented, hyper-reflective needle-shaped deposits at the level of the vitreoretinal interface on OCT imaging is a characteristic feature of vitreous amyloidosis. Vertical hyper-reflective lesions as seen on OCT have also been reported in vitreoretinal lymphoma; however, in lymphoma there are other features typically seen on OCT such as changes beneath the retinal pigment epithelium, the subretinal space, and outer retina.

The patient's medical history was positive for systemic arterial hypertension, psoriatic arthritis and prostate cancer, for which he underwent prostatectomy 12 years prior. He was currently being monitored by neurology for familial amyloidotic polyneuropathy because of a positive family history. The diagnosis was confirmed at 62 years old after sequencing of the Transthyretin (TTR) gene confirmed the presence of the amyloidogenic mutation Val30Met (V30M). He was receiving treatment with tafamidis, an antiamyloid therapy, gabapentin, and duloxetine for symptomatic polyneuropathy, atenolol for systemic arterial hypertension and adalimumab for arthritis.

Question—What are the ocular manifestations of familial amyloidosis?

Response—Familial amyloidosis more frequently results in anterior segment manifestations including abnormal conjunctival vessels, scalloped iris and

None of the authors has any financial/conflicting interests to disclose.

Reprint requests: Rodrigo Jorge, MD, Ribeirão Preto School of Medicine, Bandeirantes 3900, Ribeirão Preto, São Paulo 14049-900, Brazil; e-mail: retinausp@gmail.com

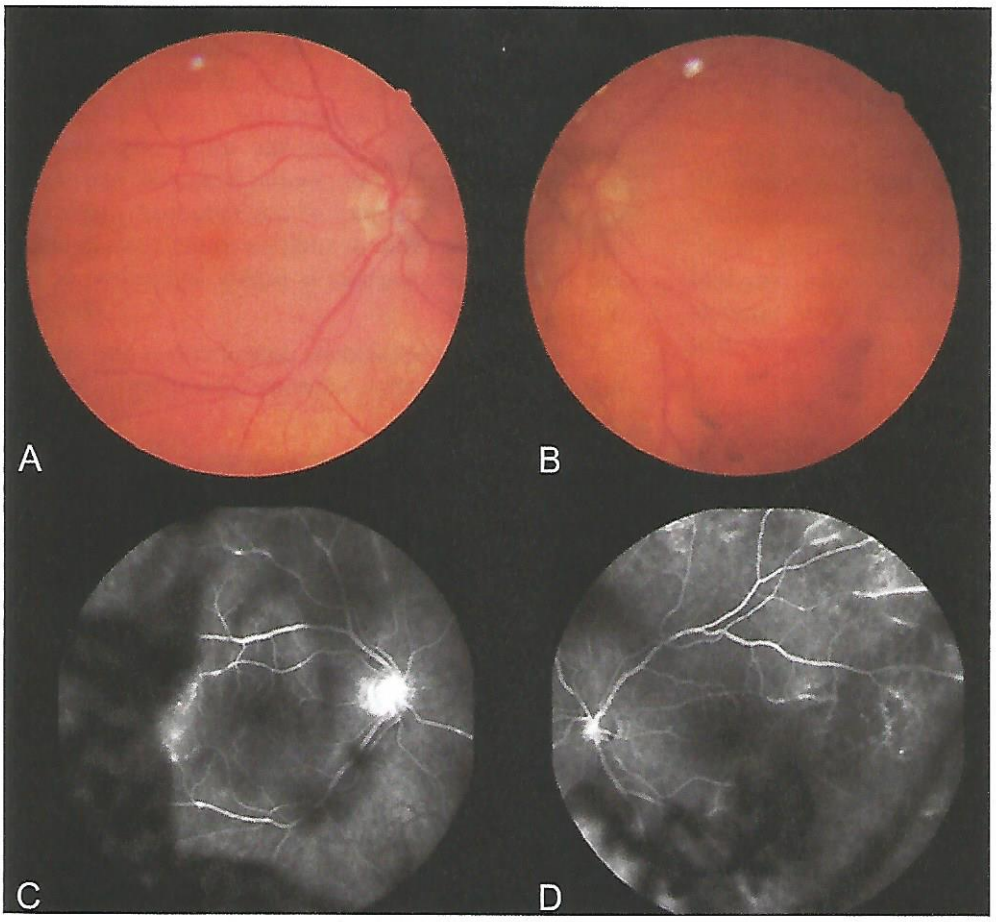

Fig. 1. A. Color fundus photograph of the right eye shows microaneurysms and few dot hemorrhages temporal to the macula. **B.** Vitreous hemorrhage in the left eye. **C.** Mid-phase fluorescein angiography of the right eye highlights microaneurysms temporal do the macula and optic disk new vessels. **D.** Optic disk neovascularization and peripheral retinal nonperfusion in the left eye.

deposition of amyloid on the iris and lens capsule. The intraocular pressures may be elevated. Posterior segment manifestations of familial amyloidosis include vitreous amyloidosis and retinal angiopathy. Patients that are treated for familial amyloidosis with liver transplantation have an increased prevalence of vitreous amyloidosis. Often, a family history may not be evident and the first diagnosis of familial amyloidosis can be made in patients even in their 70's.

There was reduced capillary density in the deep capillary plexus on SD-OCT angiography (SD-OCTA) (Figure 2). The patient was treated with laser photocoagulation targeting the regions of ischemic retina in both eyes. One month after laser treatment, the patient maintained good visual acuity with best-corrected visual acuity of 20/20 in the right eye and 20/25 on the left eye, and no further episodes of vitreous hemorrhage occurred in the period of 10-month follow-up.

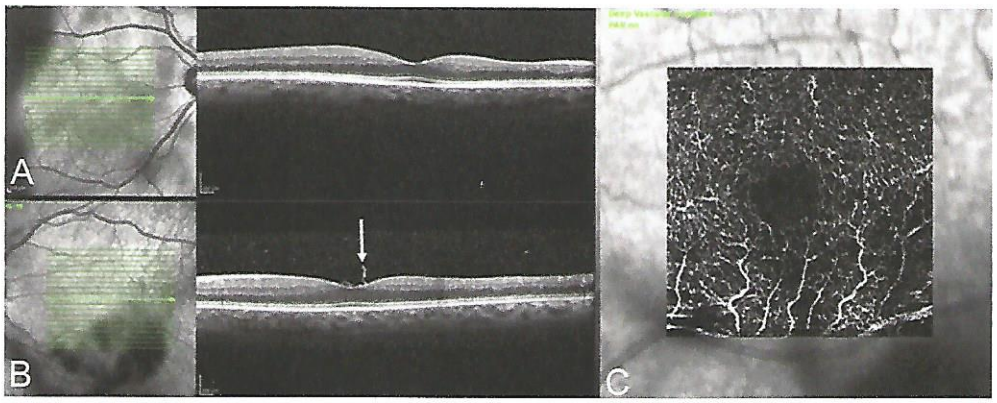

Fig. 2. A. Spectral domain optical coherence tomography of the right eye shows discrete amyloid deposits on the foveal vitreoretinal interface, and irregular thickness of the inner retina. **B.** Spectral domain optical coherence tomography of the left eye reveals typical needle-shaped amyloid deposits perpendicular to the foveal vitreoretinal interface (arrow). **C.** 6- × 6-mm OCT angiography picture of the deep capillary complex illustrates reduced macular capillary density.

Discussion

Familial transthyretin amyloidosis (TTR V30M) may lead to various retinal and vitreous findings, including strand-like, or more widespread vitreous opacities, retinal amyloid angiopathy resulting in microaneurysms, retinal hemorrhages and capillary drop out, secondary retinal and optic disk NVE, subretinal, choriocapillaris, and choroidal amyloid deposition.[1,2] This patient presented with vitreous hemorrhage, an uncommon presenting feature that has only been reported in three previous papers by Sandhu et al, O'Hearn et al and Chen et al.[3–5]

The fundus features in this case are consistent with ocular fundus and fluorescein angiography changes described previously in familial amyloidosis patients. Although Savage et al[6] first described some arteriolar changes associated with peripheral retinal NVE in 1982, the presence of typical retinal microangiopathy with retinal hemorrhages and microaneurysms on fluorescein angiography was originally described by Kojima et al.[2] Zou et al later documented peripheral capillary nonperfusion and, more recently, Rousseau et al described the occurrence of optic disk NVE similar to the findings in this patient.[7,8]

The etiology of retinal amyloid angiopathy is poorly understood. Wong and McFarlin[1] proposed that circulating amyloid may deposit in the endothelial cells, with progressive impairment of these cells and consequent retinal nonperfusion. Liver is the largest source of abnormal amyloid production. The retinal pigment epithelial cells are known to produce TTR amyloid locally in the eye and are the likely source for amyloid deposition in the choroid and around the choriocapillaris in some eyes. Whether some of this reaches the retinal endothelium is not clearly understood. The peripheral nonperfusion may lead to vaso-endothelial growth factor production and consequently optic disk and retinal NVE. Increased vaso endothelial growth factor levels in vitreous has been recorded in patients with familial amyloidosis subjected to pars plana vitrectomy for dense vitreous deposits.[4,7]

The presence of needle-shaped hyperreflective images perpendicular to the retinal surface on OCT as seen in this patient are quite characteristic, and was first described by Hattori et al.[9] They probably represent early deposits of amyloid material on the vitreoretinal interface. Optical coherence tomography angiography also showed decreased capillary density in the deep capillary plexus, suggesting that the macular circulation is also affected by the amyloid microangiopathy, as previously demonstrated by Tei et al.[10]

In summary, familial amyloidosis may lead to a typical retinal microangiopathy, which may affect the central and peripheral retina, and should be considered in the differential diagnosis of retinal NVE and vitreous hemorrhage, where the usual suspects such as diabetes, hypertension, ocular ischemia, and radiation are absent. A history of polyneuropathy,r peripheral and/or autonomic in addition to the vasculopathy, and the vitreous opacities is highly suggestive of the diagnosis.

Key words: amyloidosis, optical coherence tomography, polyneuropathy, vitreous hemorrhage.

Acknowledgments

The authors thank the Brazilian Retina and Vitreous Society for the support regarding this publication.

References

1. Wong VG, McFarlin DE. Primary familial amyloidosis. Arch Ophthalmol 1967 78:208–213.
2. Kojima A, Ohno-Matsui K, Mitsuhashi T, et al. Choroidal vascular lesions identified by ICG angiography in a case of familial amyloidotic polyneuropathy. Jpn J Ophthalmol 2003;47:97–101.
3. Sandhu R, Westcott M, Pavesio C, et al. Retinal microangiopathy as an initial manifestation of familial amyloid cardiomyopathy associated with transthyretin e89k mutation. Retin Cases Brief Rep 2013;7:271–275.
4. O'Hearn TM, Fawzi A, He S, et al. Early onset vitreous amyloidosis in familial amyloidotic polyneuropathy with a transthyretin Glu54Gly mutation is associated with elevated vitreous VEGF. Br J Ophthalmol 2007;91:1607–1609.
5. Chen JJ, Kalevar A, Vora RA, et al. Transthyretin v30m familial amyloidosis presenting as isolated retinal angiopathy. Retin Cases Brief Rep 2018;12:S76–S80.
6. Savage DJ, Mango CA, Streeten BW. Amyloidosis of the vitreous. Fluorescein angiographic findings and association with neovascularization. Arch Ophthalmol 1982;100:1776–1779.
7. Zou X, Dong F, Zhang S, et al. Transthyretin AL36Pro mutation in a Chinese pedigree of familial transthyretin amyloidosis with elevated vitreous and serum vascular endothelial growth factor. Exp Eye Res 2013;110:44–49.
8. Rousseau A, Terrada C, Touhami S, et al. Angiographic signatures of the predominant form of familial transthyretin amyloidosis (Val30Met mutation). Am J Ophthalmol 2018;192:169–177.
9. Hattori T, Shimada H, Yuzawa M, et al. Needle-shaped deposits on retinal surface in a case of ocular amyloidosis. Eur J Ophthalmol 2008;18:473–475.
10. Tei M, Maruko I, Uchimura E, Iida T. Retinal and choroidal circulation determined by optical coherence tomography angiography in patient with amyloidosis. BMJ Case Rep 2019;12:e228479.

MULTIPLE EVANESCENT WHITE DOT SYNDROME MASQUERADER

Remo T. Moraes, MD,* Ana L. Peixoto, MD,* Lucas S. Moraes, MD,† Luiz H. Lima, MD,‡ Chandrakumar Balaratnasingam, MD,§¶ David Sarraf, MD, PhD,** Raul N. G. Vianna, MD, PhD††

*From the *Instituto Brasileiro de Oftalmologia (IBOL), Rio de Janeiro, Brazil; †Department of Ophthalmology, Hospital da Gamboa, Rio de Janeiro, Brazil; ‡Department of Ophthalmology, Federal University of São Paulo (UNIFESP), São Paulo, Brazil; §Center for Ophthalmology and Visual Science, University of Western Australia, Perth, Australia; ¶Department of Ophthalmology, Sir Charles Gairdner Hospital, Western Australia, Australia; **Jules Stein Eye Institute, University of California, Los Angeles, California; and ††Department of Ophthalmology, Universidade Federal Fluminense, Niterói, Brazil.*

A 31-year-old healthy White man presented with a 3-day history of blurred vision and photopsias in the right eye. The best-corrected visual acuity of the right and left eyes was, respectively, 20/40 (−1.50 sphere) and 20/20 (−1.75 sphere). There were no cells in the anterior chamber or vitreous. Funduscopic retinal examination was remarkable for foveal granularity associated with multiple deep gray–white dots scattered in the posterior pole (Figure 1, A and B) of each eye. Optical coherence tomography (OCT) disclosed focal areas of ellipsoid zone (EZ) disruption (Figure 1, C and D) in each eye.

Question

What is the most likely diagnosis?

Response

The patient's age and the subacute nature of visual symptoms are a presentation consistent with a diagnosis of multiple evanescent white dot syndrome (MEWDS). This is supported by the imaging findings that include foveal granularity with fundus photography and multifocal areas of outer retinal disruption with OCT. However, MEWDS is rarely bilateral and is commonly associated with a viral prodromal illness. Given the atypical features of this case, other inflammatory diseases must be considered, such as idiopathic multifocal choroiditis. The masquerade syndromes including syphilis, sarcoidosis, and tuberculosis must always be considered in this age group, especially with bilateral presentations. Vitreoretinal lymphoma could present with a similar clinical picture but would be extremely unlikely given the patient age.

Patient did not attend his scheduled appointments but instead returned after 6 months complaining of further visual deterioration. Visual acuities were recorded as 20/40 and 20/60 in the right and left eyes, respectively.

Question

Is MEWDS still a likely diagnosis?

Response

No. The natural course of MEWDS is typically very favorable and is characterized by resolution of clinical signs and symptoms within 3 months in most cases. Progression of symptoms and reduction in visual acuity over 6 months implicate an alternative diagnosis.

Funduscopy showed a yellowish outer retinal placoid lesion in the macula of the right eye and white spots in both eyes (Figure 2, A and B). Fundus autofluorescence showed hyperautofluorescent spots in the posterior poles bilaterally and an area of hypoautofluorescence inferonasal in the macula of the right eye (Figure 2, C and D). Fluorescein angiography disclosed progressive hyperfluorescence in the macula, punctate hypofluorescent and hyperfluorescent spots in the midperiphery, hot optic disks in both eyes (Figure 2, E and F), and peripheral retinal vessel staining. Optical coherence tomography of the macula showed diffuse EZ disruption in both eyes (Figure 2, G and H) and cystoid macular edema in the left eye (Figure 2H). Optical coherence tomography angiography (OCTA) showed multiple areas of decreased choriocapillaris flow (Figure 3).

None of the authors has any financial/conflicting interests to disclose.

Reprint requests: Remo T. Moraes, MD, Instituto Brasileiro de Oftalmologia (IBOL), Praia de Botafogo, 206, Botafogo, Rio de Janeiro, Brazil 22250-040; e-mail: remo@globo.com

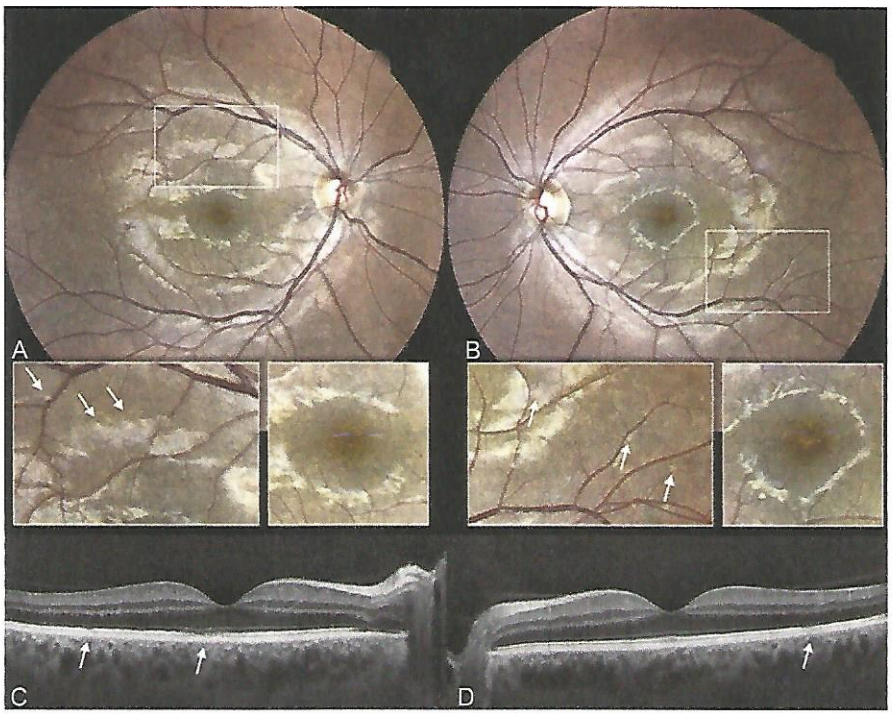

Fig. 1. **A** and **B.** Color fundus photograph shows bilateral foveal granularity with multiple gray–white dots at the level of the outer retina scattered in the posterior pole (arrows). **C** and **D.** Spectral-domain optical coherence tomography shows focal areas of EZ disruption (arrows).

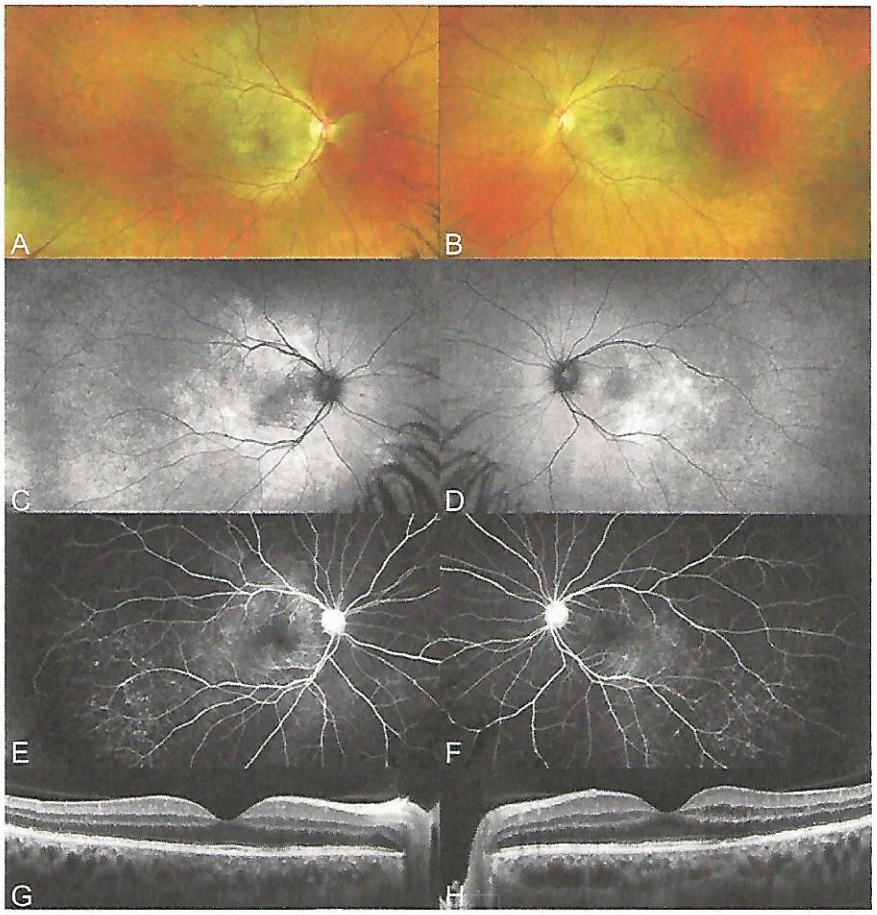

Fig. 2. **A–H.** Multimodal imaging 6 months after the initial presentation. **A** and **B.** Ultra-widefield color fundus photograph demonstrates a yellowish outer retinal placoid lesion in the macula of the right eye. **C** and **D.** Fundus autofluorescence shows hyperautofluorescence in the posterior poles bilaterally and an area of hypoautofluorescence with punctate hyperautofluorescent spots in the inferonasal macula of the right eye. **E** and **F.** Fluorescein angiography depicts progressive hyperfluorescence in the macula and punctate hypofluorescent and hyperfluorescent spots in the midperiphery of both eyes. **G** and **H.** Spectral-domain OCT shows diffuse disruption of the EZ of both eyes and cystoid macular edema in the left eye (**H**).

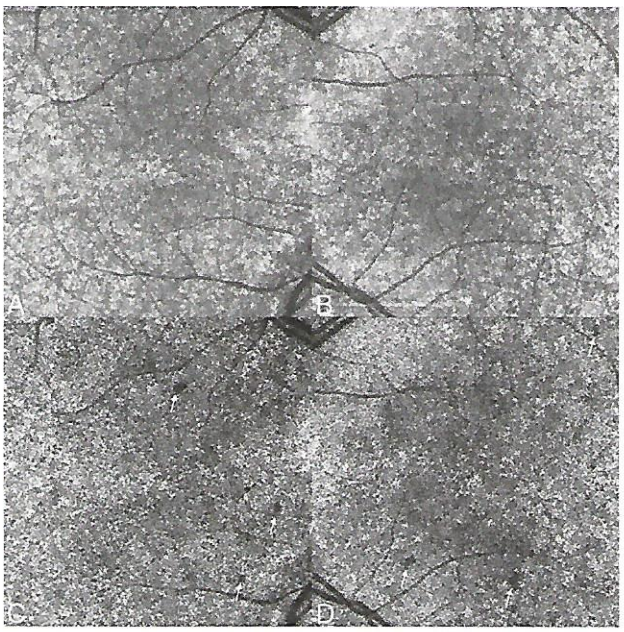

Fig. 3. *En face* OCT (**A** and **B**) and OCTA (**C** and **D**) segmented at the choriocapillaris level. Multiple areas of decreased choriocapillaris flow are illustrated (arrows).

Question

What is the most likely diagnosis?

Response

Placoid lesions of the retina associated with disruption of the outer retinal bands on OCT can be consistent with a diagnosis of acute syphilitic posterior placoid chorioretinitis. The fluorescein angiogram also demonstrated an inflammatory process in the posterior segment given the hot optic disk and staining of retinal vessels. It is important to note that tuberculosis and sarcoidosis can present with a similar clinical picture. Flow voids within the choriocapillaris, as noted with OCTA, is not specific to syphilis and may be associated with other outer retinal diseases including acute posterior multifocal placoid pigment epitheliopathy.

Systemic tests were performed and a positive result for syphilis (the fluorescent treponemal antibody absorption test and venereal disease research laboratory test with a titer of 1/512). The result from Tuberculosis testing was negative.

Question

What is the management of this case?

Response

The patient was treated with aqueous crystalline penicillin G 18 million units daily for 14 days followed by benzathine penicillin G 2.4 million units once weekly for 3 weeks. One week after finishing the treatment, the patient was asymptomatic and visual acuity recovered to 20/20 in each eye, although some outer retinal irregularities persisted (Figure 4). The result from HIV testing was positive, and the patient was commenced on antiretroviral therapy.

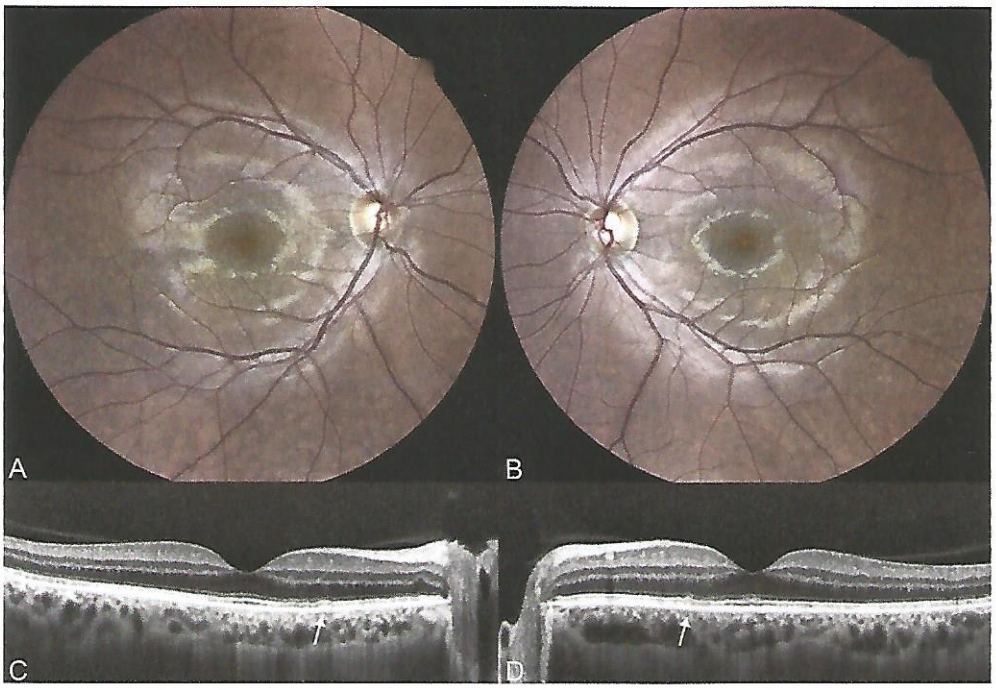

Fig. 4. Color fundus photograph (**A** and **B**) and OCT (**C** and **D**) after treatment. Outer retinal dots and foveal granularity have resolved in each eye with fundus photography. On OCT, EZ has predominantly recovered with some mild persistent irregularities (arrows).

Discussion

Russell et al[1] recently described a series of patients with initial clinical findings compatible with a diagnosis of MEWDS but with an underlying inflammatory, infectious, or neoplastic disease that was later uncovered with more extensive investigation and longer follow-up. The investigators emphasized the importance of identifying atypical features of so-called "MEWDS masquerade" syndromes, as a treatable disease was often encountered. In the current patient, treponemal and nontreponemal serologic tests established the diagnosis of syphilis and systemic penicillin therapy led to recovery of vision and reversal of macular disease.

The ocular manifestations of syphilis can develop at any stage of the disease, but most frequently, present in the secondary and tertiary stages. Ocular syphilis is colloquially known as "the great masquerader" because of its broad range of clinical manifestations and the propensity to mimic different ocular diseases.[2,3] As a result, establishing the diagnosis can be challenging. The most frequent posterior segment manifestation of syphilis is acute syphilitic posterior placoid chorioretinitis,[4] as noted in the current patient, which is a distinctive retinal manifestation of ocular syphilis first described by de Souza et al[5] and later more clearly defined by Gass et al.[6] The overlap with MEWDS has only recently been reported.[1,7] Syphilitic outer retinitis is a less common manifestation in which EZ loss is identified with OCT imaging in the absence of placoid retinitis.[8]

Pichi et al[8] failed to detect any evidence of choroidal abnormalities in their OCT study of acute syphilitic posterior placoid chorioretinitis; however, OCTA studies have shown choriocapillaris voids in patients with syphilitic placoid lesions, although no inner choroidal flow abnormalities have been noted in eyes with MEWDS with OCTA analysis. In our case, OCTA identified presumed areas of reduced choriocapillaris flow. The disrupted choriocapillaris flow in acute syphilitic posterior placoid chorioretinitis in conjunction with the hyperreflective dots observed in the outer retina corroborates the mechanism proposed by Gass et al,[6] which includes an inflammatory reaction at the level of the choriocapillaris–retinal pigment epithelium–photoreceptor complex.

Ocular syphilis is generally treated with a neurosyphilitic regimen of IV crystalline penicillin G. After treatment, the current patient was asymptomatic, and his visual acuity recovered completely. Although significant EZ recovery was noted, some persistent defects were detected. Pichi et al[9] noted that 90% of cases of acute syphilitic posterior placoid chorioretinitis showed complete EZ recovery after systemic penicillin therapy.

Key words: acute syphilitic posterior placoid chorioretinitis, ellipsoid zone, multiple evanescent white dot syndrome, optical coherence tomography angiography.

References

1. Russell JF, Pichi F, Scott NL, et al. Masqueraders of multiple evanescent white dot syndrome (MEWDS). Int Ophthalmol 2020;40:627–638.
2. Lima LH, de Andrade GC, Vianello S, et al. Multimodal imaging analyses of hyperreflective dot-like lesions in acute syphilitic posterior placoid chorioretinopathy. J Ophthalmic Inflamm Infect 2017;7:1.
3. Zett C, Lima LH, Vianello S, et al. En-face optical coherence tomography of acute syphilitic posterior placoid chorioretinopathy. Ocul Immunol Inflamm 2018;26:1264–1270.
4. Pichi F, Neri P. Multimodal imaging patterns of posterior syphilitic uveitis: a review of the literature, laboratory evaluation and treatment. Int Ophthalmol 2020;40:1319–1329.
5. de Souza EC, Jalkh AE, Trempe CL, et al. Unusual central chorioretinitis as the first manifestation of early secondary syphilis. Am J Ophthalmol 1988;105:271–276.
6. Gass JD, Braunstein RA, Chenoweth RG. Acute syphilitic posterior placoid chorioretinitis. Ophthalmology 1990;97:1288–1297.
7. Hussnain SA, Gal-Or O, Daccache A, et al. Multimodal imaging of atypical acute syphilitic posterior placoid chorioretinitis mimicking a white dot syndrome. Ophthalmic Surg Lasers Imaging Retina 2019;50:e52–e55.
8. Pichi F, Sarraf D, Arepalli S, et al. The application of optical coherence tomography angiography in uveitis and inflammatory eye diseases. Prog Retin Eye Res 2017;59:178–201.
9. Pichi F, Ciardella AP, Cunningham ET Jr, et al. Spectral domain optical coherence tomography findings in patients with acute syphilitic posterior placoid chorioretinopathy. Retina 2014;34:373–384.

Ovid®

The world's most trusted medical research platform.

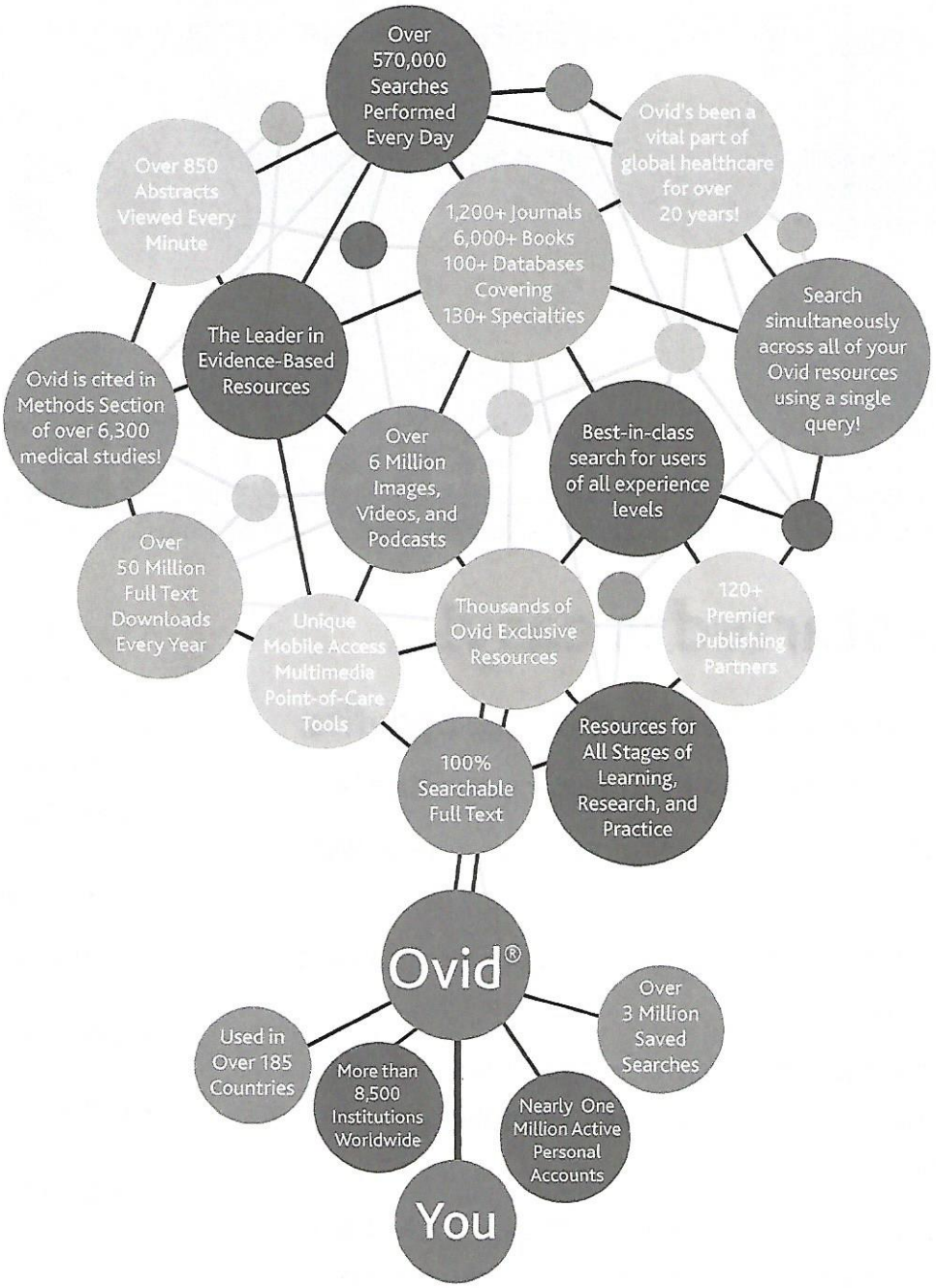

Make Ovid the source for all of your medical, nursing, and healthcare research needs.

VISIT YOUR LIBRARY - ASK A LIBRARIAN - EXPLORE OVID

ovid.com

Wolters Kluwer

6-V170

Registration has its benefits.

Getting started is easy!

To enjoy these and other journal site benefits:

1. Visit the journal website and click **Register** in the login box.
2. Choose a username and password, enter your email address and click continue.
3. At the next screen, complete your personal information and click continue again.
4. Next, enter the requested information about your practice, taking note of any required fields. Click **Complete Registration**.
5. After you receive email confirmation, just click on the link in the email within 48 hours to automatically activate your journal benefits.

Register one time only and you can enjoy valuable benefits from all your favorite Lippincott Williams & Wilkins published journals!

- Customize your options
- Create personal article collections
- Email articles to colleagues
- Save your searches
- Download podcasts
- Sign up for eTOCs

journals.lww.com

See what you might be missing.

Wolters Kluwer

5-Q356

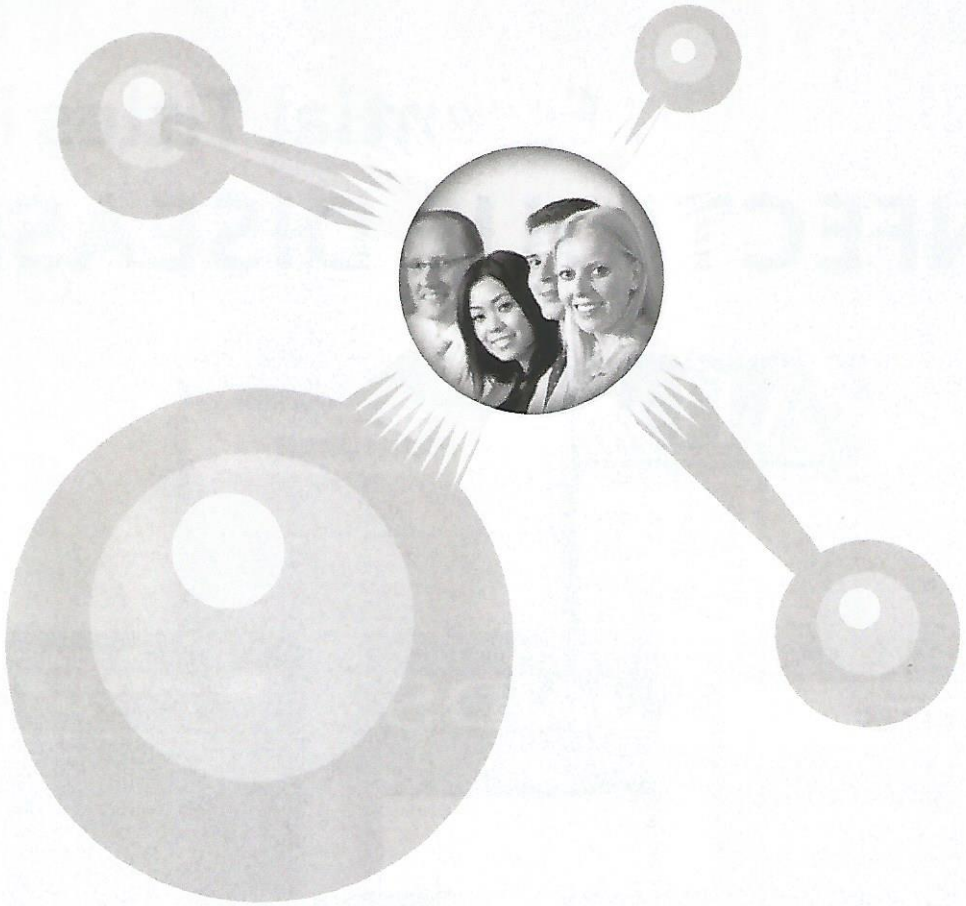

As a health professional, you're in demand.

Explore your numerous career options at HealthProfessionsJobsPlus.com today. You'll be able to:

- Post your resume
- Sign up for job alerts
- Search our selective job listings
- Apply today! Find a job that provides the respect and advancement you've been looking for.
- Experience a site from a name you know and trust, **Lippincott Williams & Wilkins**

Plus, the site is easy to use and features comprehensive information for each listing. Visit **HealthProfessionsJobsPlus.com** and begin exploring your options today.

Join other career-minded health professionals who visit **HealthProfessionsJobsPlus.com** each month!

HealthProfessions JOBSPLUS
Lippincott Williams & Wilkins
The Health Career Authority

Wolters Kluwer Health | Lippincott Williams & Wilkins

1-K299

Essential Titles in
INFECTIOUS DISEASE

Search articles, register for eAlerts, view abstracts, and SUBSCRIBE online at **journals.lww.com**.

Wolters Kluwer

8-R174